UNIVERSITY OF CALIFORNIA,
IRVINE

8-Week Inhalation of Ambient Particulate Matter with Distinct Chemical Signatures Differentially Alters Murine Cardiac Electrophysiology

DISSERTATION

submitted in partial satisfaction of the requirements
for the degree of

DOCTOR OF PHILOSOPHY

in Environmental Health Sciences

by

David Alexander Herman

Dissertation Committee:
Professor Robert F. Phalen, Chair
Professor Michael T. Kleinman
Professor Stephen C. Bondy

2020

DEDICATION

To

my wife, Katy, and my family.

TABLE OF CONTENTS

LIST OF FIGURES

LIST OF TABLES

LIST OF EQUATIONS

LIST OF ABBREVIATIONS

• OH:	hydroxyl radical
AAALAC:	Association for Assessment and Accreditation of Laboratory Animal Care
AED (D_P):	aerodynamic equivalent diameter
Al:	aluminum
AMS:	aerosol mass spectrometer
ANOVA:	analysis of variance
ANS:	autonomic nervous system
AP:	action potential
apoE$^{-/-}$ mice:	hyperlipidemic mice lacking the apoE gene; prone to atherosclerosis
AQS:	air quality station
ATP:	adenosine triphosphate
AV:	atrioventricular
AVN:	atrioventricular node
BALF:	bronchioalveolar lavage fluid
BAX:	BLC2-associated X protein
BCL2:	B-cell lymphoma 2
BP:	blood pressure
Ca^{2+}:	calcium
CalEPA:	California Environmental Protection Agency
CAPs + O_3:	concentrated ambient particles mixed with 200 ppb O_3
CAPs:	concentrated ambient particles
CO:	carbon monoxide
CPC:	condensation particle counter
CPZ:	capsazepine
CRP:	C-reactive protein
Cu/ZnSOD:	copper/zinc superoxide dismutase
Cu:	copper
CV:	cardiovascular disease
DeCAPs + $O_{3:}$	denuded concentrated ambient particles mixed with 200 ppb O_3
DeCAPs:	denuded concentrated ambient particles
DEP:	diesel exhaust particles
DFCH:	dichlorofluorescein
DNA:	deoxyribonucleic acid
DTT:	dithiothreitol
EC:	elemental carbon
ECG:	electrocardiogram
EDTA:	ethylene diamine tetra-acetic acid
E_m:	membrane potential
EPA:	Environmental Protection Agency
EPR:	electron spin resonance
Fe:	iron
FID:	flame ionization detector
GHK:	Goldman-Hodgkin-Katz
GLM-MANOVA:	general linear model-multivariate analysis of variance
GM-CSF:	granulocyte macrophage colony-stimulating factor
GPx:	glutathione peroxidase
GR:	glutathione reductase
GSH:	reduced glutathione
GSSG:	oxidized glutathione disulfide
H:C	hydrogen to carbon ratio
H_2O_2:	hydrogen peroxide
HEPA:	high-efficiency particle-free air
HF HRV:	high frequency HRV

HRV:	heart rate variability
IACUC:	Institutional Animal Care and Use Committee
IARC:	International Agency for Research on Cancer
$I_{Ca,L:}$	L-type Calcium Channels
I_{CaT}:	T-type Calcium Channels
ICP-MS:	inductively coupled plasma mass spectrometer
I_f:	"Funny" pacemaker current
$I_{K,ACh}$:	Acetylcholine-activated Potassium Channels
$I_{K,ATP}$:	ATP-Inhibited Potassium Channels
I_{k1}:	inward rectifier current
I_{Kr}:	rapid delayed rectifier current
I_{Ks}:	slow delayed rectifier current
I_{Kur}:	ultra-rapid delayed-rectifier current
IL:	interleukin
I_{Na}:	fast sodium channel
INF:	interferon
I_{NKA}:	Na^+-K^+ ATPase current
IP:	intraperitoneal
IP_3:	inositol triphosphate
Ir:	Iridium
$I_{to,f}$:	fast transient outward current
$I_{to,s}$:	slow transient outward current
I_{to}:	transient outward current
JNK:	c-Jun NH2-terminal kinase
K^+:	potassium
LDL:	low-density lipoprotein
LF HRV:	low frequency HRV
LPM:	liters per minute
MAPK:	mitogen activated protein kinase
MCP:	monocyte chemoattractant protein
MIP:	macrophage inflammatory protein
Mn:	manganese
MnSOD	manganese superoxide dismutase
Na^+:	sodium
NAAQS:	National Ambient Air Quality Standards
NADPH:	nicotinamide adenine dinucleotide phosphate
NCX:	sodium calcium exchanger
NF-κB:	Nuclear Factor kappa-light-chain-enhancer of activated B cells
NIST:	National Institute of Standards and Technology
NO_2	nitrogen dioxide
NOAA:	National Oceanic and Atmospheric Administration
NOX:	nicotinamide adenine dinucleotide phosphate oxidase
NOx:	nitric oxides
Nrf2:	nuclear factor (erythroid-derived 2)-like
O:C	oxygen to carbon ratio
O_2:	superoxide
O_3:	ozone
OC:	organic carbon
Ox stress:	oxidative stress
PAH:	polycyclic aromatic hydrocarbon
PCA:	photochemically active
PCB:	polychlorinated biphenyl
PM:	particulate matter
PM_{10}:	particulate matter with an aerodynamic diameter ≤ 10 μm
$PM_{2.5}$:	particulate matter with an aerodynamic diameter ≤ 2.5 μm
PMN:	polymorphonuclear leukocytes

ppb:	parts per billion
ppm:	parts per million
PTFE:	polytetrafluoroethylene
QTcM:	Mitchell's heart rate corrected QT interval
Q-UFPM:	particulate matter with an aerodynamic diameter ≤ 0.18 μm
RMP:	resting membrane potential
RMSS:	root mean square of successive differences in the R-R interval
ROS:	reactive oxygen species
RPM:	revolutions per minute
RyRs:	ryanodine receptor
SAN:	sinoatrial node
SCAQMD:	South Coast Air Quality Management District
SDNN:	standard deviation of the averaged N-N values
SEM:	standard error of the means
SERCA:	SR Ca^{2+}-ATPase
Si:	silicon
SO_4^{2-}:	sulphate
SOA:	secondary organic aerosol
SOD:	superoxide dismutase
SR:	sarcoplasmic reticulum
SRM:	standard reference material
SVOC:	semi-volatile organic compounds
Tc:	Technetium
Ti:	titanium
TNF:	tumor necrosis factor
TOT:	thermal evolution/optical transmittance
TRP:	transient receptor potential
TRPA1:	transient receptor potential ankyrin 1
TRPVI:	transient receptor potential vanilloid 1
UCI:	University of California, Irvine
UFPM:	particulate matter with an aerodynamic diameter ≤ 0.1 μm
UV:	Ultraviolet
VACES:	versatile aerosol concentration enrichment system
VPR:	volume pressure recording
Zn:	zinc
HMOX1:	heme oxygenase
NQO1:	NAD(P)H dehydrogenase quinone 1
CAT:	catalase
CPZ:	Capsazepine
ROFA:	residual oil fly ash
MDA:	Malondialdehyde
ET:	Endothelin

ACKNOWLEDGMENTS

I would like to acknowledge my advisor, Dr. Kleinman for his help and support throughout my time as an undergraduate and graduate researcher. His broad expertise has provided me with the tools and skills necessary for a successful career as a scientist. I would like to thank Dr. Phalen for providing an unconventional take on topics discussed during my time in the Environmental Health Sciences program. I would also like to acknowledge Dr. Lisa Wingen who has provided invaluable guidance, support, and collaboration throughout this project. Many thanks to my cherished colleagues in the lab, especially Andrew Keebaugh, Samantha Renusch, and Rebecca Arechavala who have supported my antics over the years, but also Irene Hasen, Jessica Monterrosa-Mena, Amanda Ting, and Bishop Bliss. Lastly, my sincere appreciation to all the faculty, staff, and students in the Environmental Health Sciences program for never hesitating to provide assistance, either personal or professional, at a moment's notice.

Personally, I owe a great deal to my wife Katy Rupp as she has been a critical supporter of this endeavor from the beginning. I also must thank my family and parents for their unwavering encouragement. Finally, I would like to thank my dog Sadie for always being a smelly source of comfort during stressful situations…and there were many.

CURRICULUM VITAE

EDUCATION

University of California, Irvine 04/2020 (expected)
Center for Occupational and Environmental Health
Doctor of Philosophy, Environmental Health Sciences; Emphasis in Exposure Sciences
Research Advisor: Dr. Michael T. Kleinman, PhD

University of California, Irvine, School of Biological Sciences 06/2014
Bachelor of Sciences, Ecology and Evolutionary Biology
Minor in Education

RESEARCH EXPERIENCE

Air Pollution and Health Effects Laboratory 2014-present
University of California, Irvine, School of Medicine
Research Advisor: Michael Kleinman
PhD Candidate/Graduate Student Researcher

Air Pollution and Health Effects Laboratory 2012-2014
University of California, Irvine, School of Medicine
Research Advisor: Michael Kleinman
Undergraduate Researcher

TEACHING EXPERIENCE

University of California, Irvine 2017-2019 (3 quarters)
Teaching Assistant: Biological Sciences: From Organisms to Ecosystems

University of California, Irvine 04/2017-06/2017
Assistant Course Coordinator*:* Principles of Toxicology

AWARDS

- Air & Waste Management Association 2019 Annual Conference
  2nd Place (of 6), Doctoral Student Poster Competition
- Southern California Regional Chapter, Society of Toxicology 2018 Annual Conference
  2nd Place (of 11), Student Presentation
- Southern California Regional Chapter, Society of Toxicology 2017 Annual Conference
  3rd Place (of 4), Student Presentation
- Air & Waste Management Association 2017 Annual Conference
  1st Place (of 7), Doctoral Student Poster Competition
- Southern California Regional Chapter, Society of Toxicology 2016 Annual Conference

2nd Place (of 10), Student Presentation

FELLOWSHIPS AND CERTIFICATES

The Loh Down on Science 2016-2018
Science Communication Fellow
Managing Editor (2017-2018)
Science Script Writer (2016-2017)

LEADERSHIP/SERVICE

Young Leadership Advisory Council 2017-Present
South Coast Air Quality Management District
Member

School of Medicine Student Advisory Council 2015-present
University of California, Irvine
Member

PROFESSIONAL AFFILIATES

Society of Toxicology 2015-present
Member

- Cardiovascular Toxicology Specialty Section 2016-present
- Inhalation and Respiratory Toxicology Specialty Section 2015-present
- Southern California Regional Chapter 2015-present

Air and Waste Management Association 2014-present
Member

PUBLICATIONS

(* indicates invited publication)

D. A. Herman, L. M. Wingen, A. J. Keebaugh, S. R. Renusch, I. Hasen, R. M. Johnson, and M. T. Kleinman. *Seasonal Effects of Ambient PM2.5 on the Cardiovascular System of Hyperlipidemic Mice.* Under final review to the Journal of Air & Waste Management Association.

V. Perraud, M. J. Lawler, K. T. Malecha, R. M. Johnson, **D. Herman**, N. Staimer, M. T. Kleinman, S. A. Nizkorodov & J. N. Smith. *Chemical Characterization of Nanoparticles and Volatiles Present in Mainstream Hookah Smoke,* Aerosol Science and Technology, 2019

* M. T. Kleinman, L. M. Wingen, **D. A. Herman**, R. Johnson, and A. Keebaugh. *Can Reactions between Ozone and Organic Constituents of Ambient Particulate Matter Influence Effects on the Cardiovascular System?* Multiphase Environmental Chemistry in the Atmosphere. January 2018, 439-458

***D. A. Herman,** L. Wingen, M. T. Kleinman**.** *Seasonal Effects of PM2.5 on the Cardiovascular System in Hyperlipidemic Mice*. West Coast Air & Waste Management Association Webinar. February 2019.

L. Owens, A. MacMillan, **D. A. Herman,** R. F. Phalen. 2014 Advances in Aerosol Dosimetry Research Conference Proceedings.

D. A. Herman, A. Keebaugh, M. T. Kleinman. *Electrocardiogram Changes in ApoE-/- Mice Following Exposure to the Semi-Volatile Fraction of Ultrafine Concentrated Ambient Particulate Matter.* Undergraduate Research Opportunities Program Journal, University of California, Irvine, 2014.

PRESENTATIONS

(* indicates invited presentation, # indicates award winner)

#**D. A. Herman**, V. Tanwar, R. Johnson, S. R. Renusch, I. Hasen, N. Schwieterman, L. E. Wold, U. Luderer, M. T. Kleinman. *The Cardiovascular Effects of Ovarian Hormone Removal in ApoE-/- Mice Chronically Exposed to Concentrated Ambient PM2.5*. Air & Waste Management Association Annual Conference, Quebec City, July 2019.

D. A. Herman, R. Johnson, M. T. Kleinman. *The Use and Efficacy of Rodent Nose-Only Exposure Systems in Nicotine Inhalation Studies*.

- Air & Waste Management Association Annual Conference, Quebec City, July 2019
- Society of Toxicology Annual Conference, Baltimore, March 2019

D.A. Herman. *Blowin' in the Wind: Hazards Associated with Gas-Powered Leaf-Blowers.* University of California, Irvine's Environmental Health Seminar Series. November 2018

D. A. Herman, R. Johnson, S. R. Renusch, A. J. Keebaugh, S. C. Chen, L. M. Wingen, M. T. Kleinman. *Seasonal Effects of PM2.5 on the Cardiovascular System in Hyperlipidemic Mice*. Air & Waste Management Association Annual Conference, Hartford, July 2018

D. A. Herman, R. Johnson, I. Hasen, U. Luderer, M. T. Kleinman. A Comparison of *Cardiovascular Responses in Male and Female ApoE-/- Mice exposed to Concentrated Ambient PM2.5*.

- Air & Waste Management Association Annual Conference, Hartford, July 2018
- Society of Toxicology Annual Conference, San Antonio, March 2018

D.A. Herman. *Little Plastics, Big World: Toxicological Implications form Exposure to Micro- and Nano-Plastics*. University of California, Irvine's Environmental Health Seminar Series. February 2018

[#]**D. A. Herman**, A. Keebaugh, L. M. Wingen, R. Johnson, K. Malott, M. T. Kleinman. *How Does Co-Exposing ApoE-/- Mice with Various Forms of Concentrated Ambient PM2.5 and Ozone Affect Normal Electrocardiogram Measurements?*

- Southern California Regional Chapter of the Society of Toxicology Annual Conference, San Diego, October 2017
- Air & Waste Management Association Annual Conference, Pittsburgh, June 2017
- Society of Toxicology Annual Conference, Baltimore, March 2017

D. A. Herman and L. M. Wingen. 2017. *Shot through the Heart, and Particles are to Blame!* Science and Societal Impacts of Air Quality and Climate Issues: Past, Present and Future. University of California, Irvine, April 2017.

D.A. Herman. *A Million Little Spears: The Toxicological Effects of High Aspect Ratio Particles*. University of California, Irvine's Environmental Health Seminar Series. April 2017

D. A. Herman, A. Keebaugh, M. T. Kleinman. *Electrocardiogram Effects of a Co-Exposure with Concentrated Ambient PM2.5 and Ozone in ApoE-/- Mice.* Southern California Regional Chapter of the Society of Toxicology Annual Conference, Irvine, October 2016.

D. A. Herman, A. Keebaugh, S. R. Renusch, M. T. Kleinman. *Influences of the semi-volatile organic fraction of ultrafine concentrated ambient particulate matter on electrocardiogram measurements in ApoE-/- mice.* Society of Toxicology Annual Conference, New Orleans, March 2016.

D.A. Herman. *Houston, We've Had a Problem: A Toxicological Look at the Rocket Fuel Hydrazine*. University of California, Irvine's Environmental Health Seminar Series. April 2016

D. A. Herman. *Carbon Nanofibers (CNFs) and Nanotubes (CNTs): A Growing Industry with Growing Potential Risks*. University of California, Irvine's Environmental Health Seminar Series. April 2015

D. A. Herman, A. Keebaugh, M. T. Kleinman. *Electrocardiogram changes in ApoE -/- mice following exposure to thermally denuded ultrafine concentrated ambient particulate matter*. Air and Waste Management Annual Conference, Long Beach, June 2014

D. A. Herman, A. Keebaugh, M. T. Kleinman. *Electrocardiogram changes in ApoE -/- mice following exposure to the semi-volatile organic fraction of quasi-ultrafine concentrated ambient particulate matter.* Undergraduate Research Opportunities Program Annual Symposium, University of California, Irvine, May 2014

ABSTRACT OF THE DISSERTATION

8-Week Inhalation of Ambient Particulate Matter with Distinct Chemical Signatures Differentially Alters Murine Cardiac Electrophysiology

By

David Alexander Herman

Doctor of Philosophy in Environmental Health Sciences

University of California, Irvine, 2020

Professor Robert. F. Phalen, Chair

Introduction: Chronic exposure to particulate matter (PM) has been associated with increased risks for several cardiovascular (CV) diseases which can culminate in higher morbidity and mortality. This research will test the effects of particle chemistry on the mouse electrocardiogram (ECG) by investigating adverse cardiac outcomes following exposures 1) during different seasons (winter/summer), and 2) to whole concentrated ambient particle (CAPs; containing organic species) or denuded CAPs (DeCAPs; PM thermally stripped of organic species) with/without the addition of ozone (O_3), a ubiquitous environmental pollutant.

Methods: A Versatile Aerosol Concentration Enrichment System (VACES) was used to concentrated PM atmospheres. Hyperlipidemic mice ($apoE^{-/-}$) were exposed via whole body inhalation chambers for 5 hrs./day, 4 days/wk. All ECG parameters were acquired from freely moving, conscious mice and assessed at the same time every evening. An aerosol mass spectrometer (AMS) provided single-particle size and chemical composition as well as cumulative size-classified mass concentrations in real-time for non-refractory sub-micron aerosol

particles. The oxidative potential of different types of PM was analyzed using the antioxidant enzymes glutathione peroxidase (GPx) and glutathione reductase (GR).

Results: Electrocardiogram (ECG) anomalies were exacerbated during periods with high ambient O_3 levels suggesting that increased atmospheric interaction with O_3 and other atmospheric pollutants generates more biologically active PM. CAPs exposure was found to be more cardiotoxic than DeCAPs exposure. Adding O_3 to either CAPs or DeCAPs failed to elicit more severe adverse health effects compared to single pollutant exposures. Particles containing semi-volatile organic compounds (SVOCs) produced dissimilar inhibitory responses in GPx and GR suggesting that oxidative stress could be altered via GSH accumulation. Levels of enzymatic impairment were similar in response to PM+O_3 mixtures regardless of PM-bound SVOCs present suggesting that O3 is reacting with a more stable PM-bound constituents.

Conclusion: This report describes how inhaled ambient PM is linked to alterations in cardiac electrophysiology and provides useful insight into particle characterization and cardiac dysfunction in relation to specific PM fractions and/or PM+O_3 mixtures. Information about particle oxidative stress would be a valued addition to air quality legislation which currently relies on particle size as a main toxicological risk factor.

CHAPTER 1: GENERAL INTRODUCTION

Exposure to elevated concentrations of particulate matter (PM) and ozone (O_3) in polluted ambient air is a major public health issue that is associated with over 4 million premature deaths worldwide. [1-3] Chronic exposure to PM has been associated with increased risks for a number of cardiovascular (CV) risk factors including cardiac arrhythmias, myocardial infarctions, and chronic obstructive pulmonary disorder which can culminate in higher morbidity and mortality.[4-12] Despite vigorous regulatory efforts in the U.S. residents of many communities are exposed to elevated concentrations of PM. For example, several southern California counties have reported average ambient pollutant levels in excess of National Ambient Air Quality Standards (NAAQS) or CalEPA standards, exposing roughly 18 million residents to $PM_{2.5}$ (PM with diameters ≤ 2.5 μm) and O_3 at concentrations that might cause or exacerbate lung and heart diseases. Additionally, chronic exposure to PM leads to changes in disease biomarkers such as altering heart rate variability (HRV), changes in vascular tone, increased oxidative stress, induced vascular inflammation, and increased atherosclerotic plaque formation in animals [13-20] and humans [5,21-26].

Air pollution is a complex mixture of gasses, liquid droplets, and solid particles in a range of sizes from nanoparticles (Dp ≤ 100 nm) to particles with diameters greater than 10 μm. The NAAQS standards have been established to protect individuals from PM-induced adverse health effects for particles ≤ 10 um aerodynamic diameter (PM_{10}) and particles ≤ 2.5 μm ($PM_{2.5}$). Epidemiological studies have demonstrated that associations with adverse health effects become stronger when one restricts the PM particles ≤ 1 μm. There is increased evidence from animal studies that even smaller particles (Dp ≤ 0.18 μm) have greater cardiovascular toxicity than do

$PM_{2.5}$ particles with Dp > 0.18 μm, so called quasi-ultrafine particulate matter (Q-UFPM). Although these Q-UFPMs represent > 95% of particles by number, they are rarely, if ever, quantified in ambient air data used for epidemiological research. The smallest particle fraction, referred to as ultrafine PM (Dp ≤ 0.1 μm), are more pro-atherogenic than are their larger counterparts, possibly due to their greater surface area per unit mass allowing for the disproportionately higher concentration of redox-active and toxic organic chemicals carried on their surfaces [15,27-31]. Despite this, there are currently no ambient air quality regulations, or specific guidelines for ultrafine PM, however there are federal and state air quality standards for $PM_{2.5.}$

Temporal changes are one of the factors impacting the atmospheric interaction of PM with gaseous components such as O_3. PM has been reported to contain higher concentrations of more oxidized aerosols in summer months (when there are increase amounts of sunlight leading to higher levels of photochemical activity) compared to PM in winter months (when there are lower levels of sunlight leading to lower levels of photochemical) in a number of locations [32-40]. For instance, significantly greater mortality rates are associated with cardiovascular diseases during periods of higher heat and ozone [41,42]. Although the overall concentration of PM has been decreasing in recent years, PM concentration excursions associated with seasonal fluctuations and sporadic events such as wildfires (where ambient PM levels can exceed 100 $\mu g/m^3$) have potential implications for public health [43].

Regardless of the ultimate outcome, inhaled PM appears to initially promote pro-inflammatory oxidative stress responses involving the biological formation of reactive oxygen species (ROS). Components of ambient air pollution, including O_3, nitrogen oxides, mineral dusts, and environmental radiation have all been shown to enhance the generation of ROS in the

lungs [44-47]. The oxidative properties of inhaled PM and the resulting biological effects is a function of PM size, composition, and source [48,49]. Therefore, information about particle oxidative stress would be an appreciated supplement in air quality legislation.

The purpose of this research is to answer four key questions about PM-induced health effects: 1) Do exposures to PM in the summer elicit more adverse health effects compared to PM exposures in the winter; 2) Does co-exposure to O_3 and PM augment the effects of PM exposure alone; 3) Does O_3 modify the oxidative potential of ambient PM; and 4) Does the removal of semi-volatile constituents from PM alter the O_3-PM interaction.

CHAPTER 2: OBJECTIVES

2.1 Hypothesis

The goal of this thesis study was to investigate how seasonal differences in ambient PM affect changes in cardiac electrophysiology following particle inhalation. Additionally, this study analyzed how O_3 was able to modify the oxidative potential of the PM and the physiologic outcomes to PM inhalation. O_3 was expected to play a meaningful role in particle toxicity due to ability to oxidize PM-specific components thereby inducing ROS formation, such as semi-volatile organic compounds (SVOCs), polycyclic aromatic hydrocarbons (PAHs), and metallic species. Furthermore, prior studies performed by our laboratory and others have established that concentrated ambient particles (CAPs) stripped of SVOCs via thermal denudation at 120 °C (known as Denuded CAPs, or DeCAPs) exhibited decreases in tissue-specific oxidant potential and other biological effects (e.g. atherosclerosis, systemic immune response, heart rate variability (HRV), and electrocardiogram (ECG) waveform morphology).

This study provided a unique opportunity to investigate the relationship between O_3 and ambient PM regarding the manifestation of ECG waveform dysfunction using a multi-disciplinary approach (*in vivo* physiology, aerosol chemistry, and *in vitro* cell-free assays). It was hypothesized that exposures to ambient PM in the summer months (i.e., high photochemical activity) would elicit more adverse outcomes than exposure during the winter months (i.e., low photochemical activity). Additionally, O_3 was thought to exacerbate the negative effects seen following PM exposure due to the formation of more pro-oxidant PM-bound species. Furthermore, exposure to DeCAPs + O_3 are expected to produce less adverse outcomes than exposures to CAPs + O_3 due to the removal of SVOCs leading to less reactive compounds.

Implanted ECG transmitters were used to determine weekly alterations in multiple parameters associated with the cardiac conduction system in response to various PM and PM+O_3 mixtures. Data from a state-of-the-art aerosol mass monitor (AMS) allowed for the correlation between physiologic measurements and particle chemistry. The mechanism of damage for PM was thought to be due to its oxidative potential. The addition of O_3 to CAPs was expected to exacerbate antioxidant inhibition compared to PM alone. Moreover, adding O_3 to DeCAPs was thought to decrease this inhibition due to the lack of SVOCs bound to the particles.

2.2 Specific Aims and Study Design

2.2.1 Aim 1: Health Effects of Seasonal Ambient PM Exposure

The overarching hypothesis tested by this study is that there is a seasonal difference in adverse cardiovascular health effects caused by summer PM exposures as compared to winter PM exposures and that oxidative stress may play a mechanistic role. The first specific aim to test the hypothesis determined the effect of chemical modifications of PM by photochemical activation on cardiac function and conduction. Specifically, we examined whether the severity of A) ECG waveform anomalies, B) heart rate variability (HRV), and C) blood pressure detriments in apoE$^{-/-}$ mice was greater following exposures during summer (with high ambient photochemical activity) compared to the same parameters following exposures during winter (with low ambient photochemical activity). All exposures were performed on the North Campus of University of California, Irvine (UCI) and all animal exposures and procedures were approved by the UCI Institutional Animal Care and Use Committee (IACUC).

Exposure to ambient air pollution is a major public health concern. However, current mass based federal and state PM air quality standards fail to account for seasonal and regional differences in chemical composition that might provide the mode of action for PM toxicity. PM has been reported to contain higher concentrations of more oxidized aerosols in summer months (when photochemical activity is higher) compared to PM in winter months (when photochemical activity is lower) in a number of locations [32-40]. Cardiovascular disease mortality rates have been reported to increase during periods of higher heat, O_3 and photochemical activity [41,42,50]. The cardiovascular effects resulting from 8-week inhalation $PM_{2.5}$ during summer and winter seasons in a mouse model of coronary artery disease were examined. We hypothesized that since summer is a more photochemically active (PCA) season than winter, that $PM_{2.5}$ formed during periods of

high PCA would be more potent than $PM_{2.5}$ formed during low PCA periods, with respect to adverse patterns of heart rhythm, electrocardiogram (ECG) waveforms (i.e. interval changes and ventricular abnormalities) and blood pressure.

Groups of $apoE^{-/-}$ mice were exposed to concentrated ambient PM (CAPs) during periods of high or low photochemical activity while $apoE^{-/-}$ mice exposed to purified air served as a negative control. The high PCA exposures were performed July-September of 2015 while the low PCA exposure were performed August-October of 2016.

ECG waveforms were evaluated for changes in both time- and ventricular-related parameters. A tail-cuff sphygmomanometer system was used to measure effects on systolic and diastolic blood pressure after each week of exposure. The chemistry of the high and low PCA PM was determined using an Aerosol Mass Spectrometer (AMS) and measurements of UV radiation at the Earth's surface for the local area were obtained from the National Oceanic and Atmospheric administration (NOAA). The AMS provided concentrations of oxidized compounds in ambient and exposure atmospheres.

2.2.2 Aim 2: Health Effects of Exposure to PM and PM + O_3 Mixtures

The second aim of this study tested whether increased O_3 levels during high PCA periods were in part responsible for increased summer health effects. We tested whether the addition of O_3 following particle concentration (mimicking atmospheric photochemical PM activation) produces cardiovascular alterations similar to those identified following exposure to PM formed during periods of high photochemical activity.

While there are strong associations between PM exposure and cardiovascular disease, gaseous pollutants such as O_3 are also associated with adverse cardiovascular effects, independent of PM [51]. Ozone is a strong oxidant and can directly induce oxidative changes in the

lung which promote respiratory system inflammation, as does PM. In addition, O_3 can react with PM constituents and oxidize organic compounds. Hence, there may be mechanistic interactions between the effects of PM and those of O_3. Humans are often exposed to both $PM_{2.5}$ and O_3 as parts of a complex mixture of ambient air pollutants although peak exposures may vary spatially and temporally. However, little is known about potential interactions or synergisms arising from joint exposure to these two biologically active ambient pollutants.

The cardiopulmonary effects of concurrent O_3 and $PM_{2.5}$ exposures were examined to determine whether the effects of the concurrent exposures differed from those observed following exposures to $PM_{2.5}$ or O_3 alone. Both CAPs and O_3 are known inflammatory and irritant agents, we expected that the mixture would be more potent than CAPs alone with respect to adverse patterns of heart rhythm and ECG waveforms (i.e. interval changes, ventricular abnormalities). Since the VACES removes ambient O_3 from the exposure aerosol before the CAPs is delivered to the exposed mice, controlled amounts of O_3 (200 ppb) were metered into the exposure atmosphere. We also examined a secondary hypothesis that if O_3 would react with PM-bound organic compounds, and if this resulted in any interactive health effects, removing the organics could block those interactions. A thermal denuder was used in this study to produce particles that were significantly depleted of organics (DeCAPs) and the possible interactions of these particles with O_3 was also investigated.

The physical and chemical composition of inhaled PM is expected to play a substantial role in cardiac toxicity. Our laboratory and others have shown that thermally denuded PM exhibit large losses in SVOCs including PAHs while more refractory species such as metal and elemental carbon remain adsorbed to the denuded PM. Our laboratory has also found that DeCAPs had decreased concentrations of organic carbon compared to intact CAPs which

corresponded to increases in the O:C ratio of the PM. Additionally, exposure to DeCAPs was found to elicit less severe cardiovascular outcomes compared to the intact CAPs.

Groups of apoE$^{-/-}$ mice were exposed to CAPs or DeCAPs alone or in concert with O_3. The exposures occurred during two periods due to limitations of the particle concentration system. Therefore, each exposure included both a purified and an O_3 cohort which acted as a negative and positive control, respectively. As with aim 2.2.1, ECG waveforms were analyzed for changes in both time- and ventricular-related parameters with and compared with responses from the seasonal study. For this aim, the AMS provided oxygen-to-carbon (O:C) ratios, constituent-specific size distributions, and mass concentrations for generated PM atmospheres. Additionally, the AMS was used to establish correlations between specific organic species in the PM and PM + O_3 atmospheres and measurements of HRV.

2.2.3 Aim 3: Direct Effects of PM and PM + O_3 Effects on Oxidative Potential

In order to examine if PM-induced oxidative stress was, in part, a mechanism by which inhaled PM might induce toxicity at the cellular and organ level, we examined how O_3 co-exposure mediated the oxidative potential of whole or denuded CAPs by testing the direct effects of PM and PM + O_3 and measuring the response of oxidative stress enzymes using in vitro assays.

Ambient PM has been shown to exhibit oxidative properties which can promote oxidative tissue damage [34,52-57]. This oxidant capacity is thought in part to be due to adsorbed metals or quinones which can generate reactive oxygen species (ROS) through their participation in the Fenton and redox-cycling reactions. [58,59]. Inhaled oxidants react with cellular NADPH oxidase (NOX) to form superoxide, O_2. Once made, O_2, it quickly dismutates to form hydrogen peroxide (H_2O_2) either by a non-enzymatic reaction or through catalyzation with superoxide dismutase

(SOD) [60]. The H_2O_2 formed can exacerbate inflammatory processes by hypohalous (hypochlorous and hypobromous) acids [61] which can oxidize proteins in lung epithelial cells and generate additional reactive species through lipid peroxidation pathways [62]. Trace metals adsorbed to ambient particulate matter can react with H_2O_2-associated pathways, both environmentally and biologically [52,63,64]. Additionally, the organic/elemental carbon constituents as well as total surface area also play a role in PM toxicity [48].

Glutathione (γ-$_L$-glutamyl-$_L$-cysteinyl-glycine; GSH) is an antioxidant that is largely involved in mitigating the effects of cellular reactive species, including peroxides, which occurs through a series of reduction and conjugation reactions involving the sulfhydryl group (-SH) of the compound [60]. GSH exists in two redox states, reduced GSH and oxidized glutathione disulfide (GSSG). Proteins/enzymes such as glutathione peroxidase (GPx), glutathione reductase (GR), and SOD species are activated by the shift in the ratio of cellular GSH to GSSG in response to oxidative stress (ox stress). Increases in intracellular GSH have been shown to decrease pulmonary chemokine and cytokine responses by inhibiting NF-κB activation [65]. In the case of GPx, lipid hydroperoxides and cellular hydrogen peroxide are respectively reduced to alcohols and water during the oxidation of GSH to GSSG [66].

Previous studies have determined that PM is capable of directly inhibiting interacting with enzymes involved with the oxidative stress response [54,67]. The ability of multiple types of PM and PM fractions (i.e., particles with/without semi-volatile organic compounds (SVOCs) and PM+O_3 mixtures) to directly inhibit enzymes involved in biological oxidative stress outcomes was examined. We expected that CAPs would inhibit enzymatic activity to a greater degree than DeCAPs and that the addition of O_3 to PM would exacerbate the enzymatic inhibition compared to PM alone due to increased ROS elicited by the PM+O_3 mixtures.

Concentrated PM and PM + O_3 particles were collected onto Teflon membrane filters and extracted via sonication/agitation into ultrapure water. Extracts were incubated with the enzymes and their respective substrates. The enzymatic inhibition in response to PM types was measured using ultraviolet (UV) absorbance assays in the 96-well format which allowed for minimal sample quantities. The National Institute of Standards and Technology (NIST) standard reference material (SRM) 1648a was used as a positive control. The SRM 1648a is an urban particulate matter sample that contains known amounts of organic constituents like multiple PAHs and polychlorinated biphenyl (PBC) as well as numerous metallic elements.

CHAPTER 3: METHODS

3.1 Exposure

3.1.1 Versatile Aerosol Concentration Enrichment System

A Versatile Aerosol Concentration Enrichment System (VACES) [68-70] allowed for the concentration of local ambient PM, known as CAPs and has been adapted for animal exposures in real world environments and can enrich the concentration of ambient particles in the diameter range of 0.02 to 10 μm by a factor of 10 [69-71]. In this system, ambient PM is pulled in from above the laboratory at a rate of 300 liters per minute (LPM) and size-fractionated using a 2.5 μm slit impactor ($Dp \leq 2.5$ μm). The $PM_{2.5}$ is then grown to 2-3 μm droplets via a procedure that first saturates the particles in 26-30 °C water vapor and then condenses the saturated particles by passing them through a condensation tower surrounded by a -4 °C 1:1 mixture of water and ethylene glycol. The grown particles are then drawn into a system of 3 parallel virtual impactors (VI) and grown particles, which have sufficient inertia to not be deflected from a straight line are focused into the minor flow outlet located directly across from the impactor inlet operating at flow rates of 5 LPM. The bulk of the air and gaseous component molecules are diverted through a major flow outlet located to the side of the virtual impactor with a flow rate of 95 LPM per VI head. Concentrated PM in the minor flow then passes through diffusion dryers to remove excess water vapor, which returns the particles to a size distribution that closely approximates the size distribution of the sampled ambient aerosol.

3.1.2 VACES Setup to Study Seasonal Effects in Ambient PM

The schematic of the VACES used to study the seasonal effects of PM are shown in Figure 3.1. The study of season differences in ambient PM occurred in two phases. Phase 1

occurred from July-September of 2015 and is the time when animals were exposed to high PCA particles. The results of Phase 1 were contrasted with those of Phase 2, where animals were exposed to low PCA particles during August-October of 2016. Control mice for both exposure phases were exposed to air purified over potassium permanganate-impregnated alumina beads, activated carbon, and high-efficiency particle-free air (HEPA).

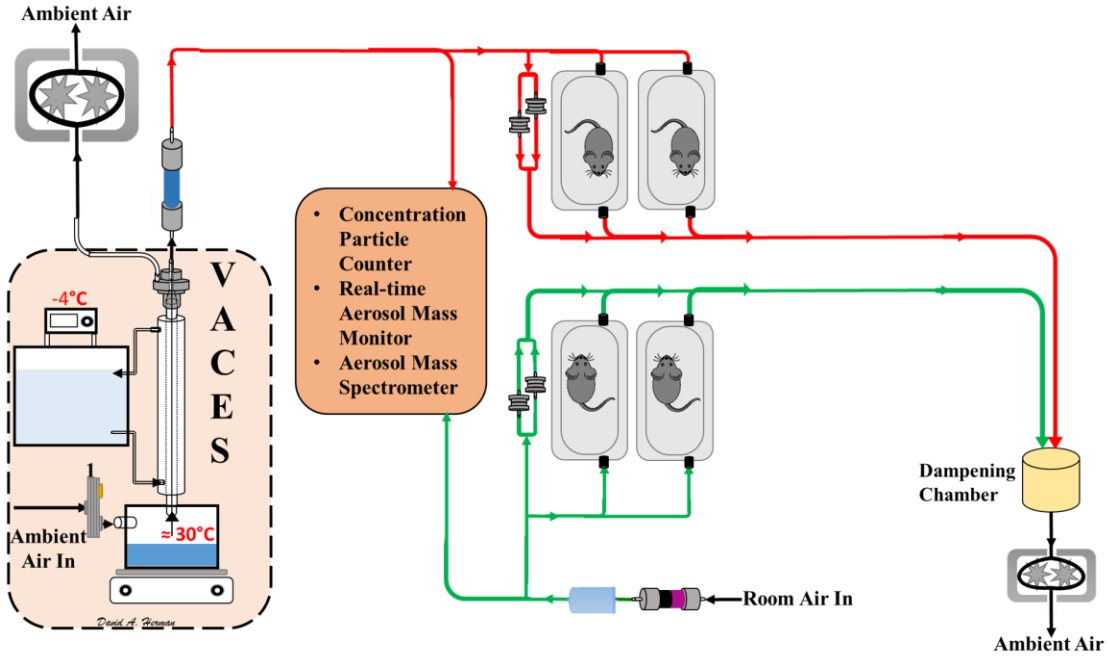

Figure 3.1. Schematic of VACES and Exposure. Red lines indicate CAPs atmosphere. Green lines indicate purified air exposure.

3.1.3 VACES Setup to Study the Effects of PM and PM + O_3

The schematic of the VACES used to study the effects of PM and PM + O_3 mixtures is shown in Figure 3.2. This portion of the study was also performed in two phases. In both Phases, O_3 was generated using a commercially available ozonizer (AquaZone, Red Sea Ozonizer) that used silent corona discharge to form O_3 from pure compressed oxygen. In Phase 1, the effects of CAPs and 200 ppb O_3, separately and in combination were contrasted, while in Phase 2 the effects of DeCAPs and O_3, separately and in combination were contrasted. DeCAPs particles during Phase 2 were produced using a thermal denuder (Dekati LTD., Finland) heated to 120 °C

to remove the SVOCs (Figure 3.B). Animals in this part of the study underwent exposure to either A) CAPs; B) CAPs + O_3 (at 200 ppb); C) DeCAPs; D) DeCAPs + O_3 (at 200 ppb); E) O_3 (at 200 ppb), or F) air purified over potassium permanganate-impregnated alumina beads, activated carbon, and high-efficiency particle-free air (HEPA).

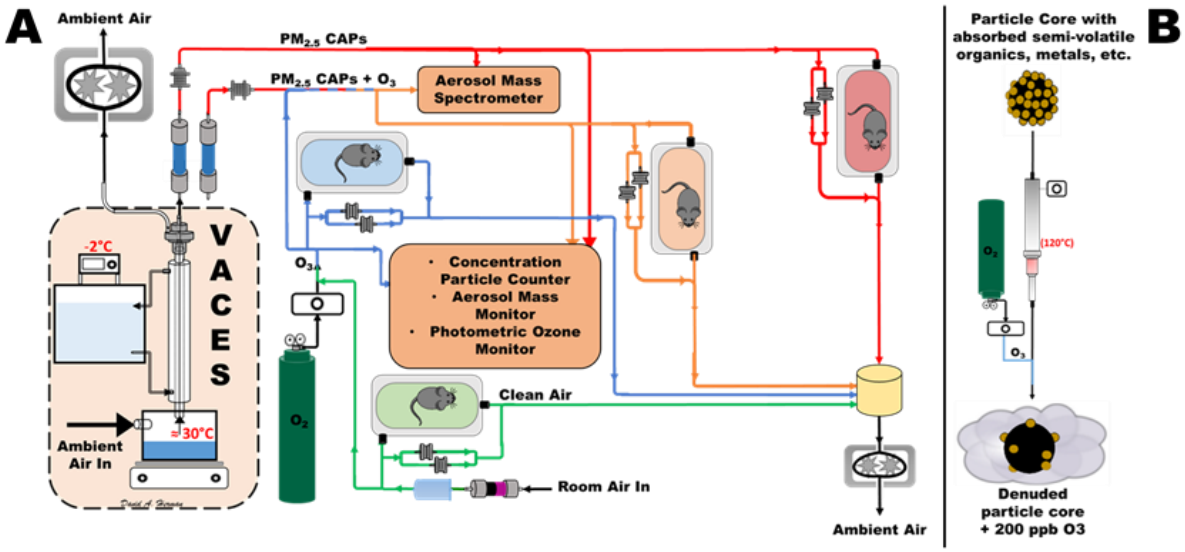

Figure 3.2. Schematic design of VACES apparatus used to examine the effects of mixtures of ozone with CAPs and DeCAPs. A) Ambient PM was concentrated using a VACES instrument and partitioned into the $PM_{2.5}$ fraction using Sioutas Cascade Impactors. Ozone was produced using pure oxygen passed through a Red Sea AquaZone Ozonizer. Real-time PM measurements were made with a Condensation Particle Counter, an Aerosol Mass monitor, and a Photometric Ozone monitor. The organic constituents of the PM were analyzed using an Aerosol Mass Spectrometer; B) The SVOCs were removed from CAPs using a thermal denuder at 120 ℃ to produce a denuded CAPs atmosphere. The stripped PM was also combined with ozone to create a denuded CAPs + O3 atmosphere.

3.1.4 VACES Setup to Collect PM and PM + O_3 in Bulk

The schematic of the VACES used to collect PM and PM + O_3 mixtures is shown in Figure 3.3. In this part of the study, the CAPs provided by the VACES were divided into two legs; one leg directly deposited CAPs onto 45 mm polytetrafluoroethylene (PTFE) filters at a rate of 7.5 LPM while DeCAPs was formed in the second leg via a thermal denuder (Dekati LTD., Finland) heated to 120 °C and collected onto a PTFE at 7.5 LPM (Figure 2, red lines). During a separate collection period, O_3 (200 ppb) was introduced into the generated CAPs at a rate of 1.0 LPM. The CAPs from the VACES was split into two legs, the first of which was unmodified and

the second was connected to the thermal denuder. O3 (0.2 parts per million; ppm) was metered into the undenuded line to produce CAPs + O3 and into the denuded line to produce DeCAPs + O_3. Particles from both lines were collected on 45 mm PTFE filters at a rate of 8.0 LPM per particle type for 7 hrs./day for 10-15 days, depending on PM type to provide sufficiently large integrated samples. Filters were stored inside their stainless steel filter holders between each exposure day. After the final collection, the loaded filers were placed in a temperature- and humidity-controlled weigh room for 24-48 hrs. until gravimetric analysis (Chapter 3.6.4)

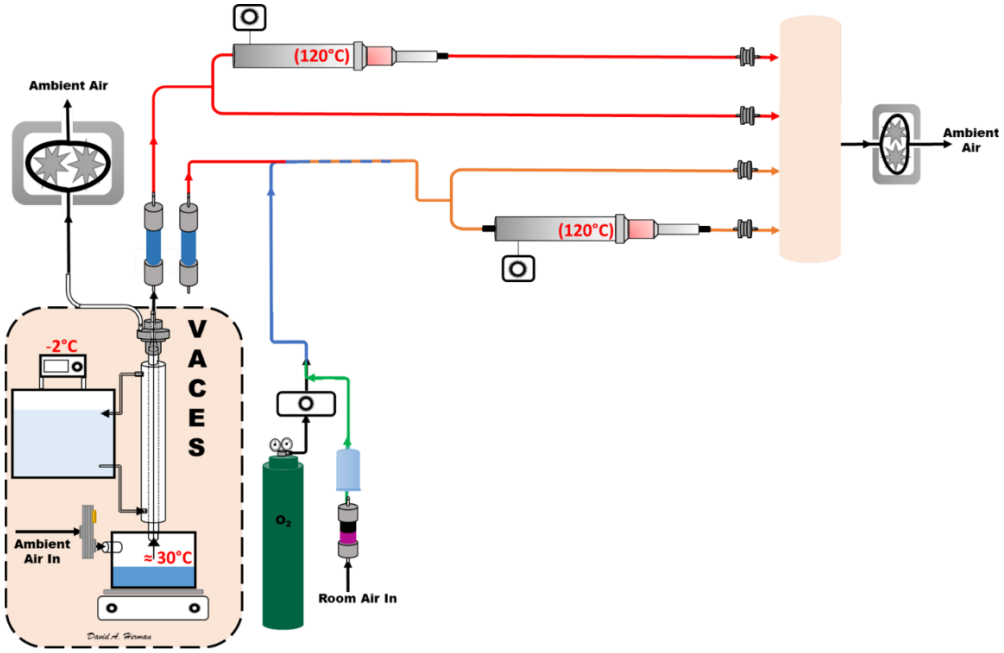

Figure 3.3. VACES and Filter Collection Schematic. Red lines represent CAPs and DeCAPs. Orange lines represent CAPs + O_3 and DeCAPs + O_3. Un-ozonated PM was collected at 7.5 LPM while ozonated PM was collected at 8.0 LPM.

3.2 Animal Husbandry and Housing

Animals were housed at the University of California, Irvine in a vivarium accredited by the Association for Assessment and Accreditation of Laboratory Animal Care (AAALAC). The vivarium maintained temperature-controlled rooms with a 12-hr light/dark cycle, and mice were housed in ventilated cages supplied with purified air. All mice received a standard chow diet (Teklad Envigo, Indianapolis, IN, USA) and water *ad lib* while in housing. Mice without telemetry implants were housed 4 per while implanted mice were housed singly to facilitate ECG monitoring.

3.3 Animals

Mice lacking the gene coding for apolipoprotein E (apoE-/-; Jackson Laboratory, Bar Harbor, ME) were used in this study because they are susceptible to developing atherosclerosis-like plaques in their coronary and aortic arteries. These mice, which have high serum levels of very low-density lipoproteins (LDL), have been used successfully in studies of the effects of PM exposure on the heart [17,72-75]. The mice were between 10-12 weeks of age at the start of all exposures. The animals were conditioned to the exposure system in purified air one week before baseline measurements were acquired.

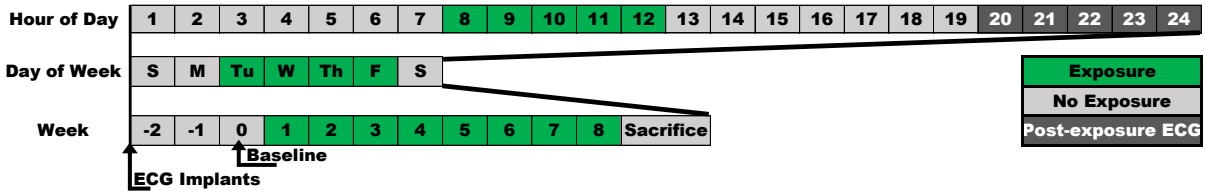

Figure 3.4. Exposure Timeline. Mice were exposed 5 hours/day, 4 days/week, for 8 weeks. Electrocardiographic (ECG) radiotelemetry devices were surgically implanted and baseline measurements obtained 3 weeks and 1 week prior to the exposure start date, respectively. ECGs were recorded continually for the duration of the experiment and analyzed during time periods immediately after exposure.

All mice (n=16 per groups) were exposed 5 hours/day (7:00 AM– 12:00 PM), 4 days/week (Tuesday – Friday) for 8 weeks during both exposure studies. Baseline ECG

measurements were obtained one week before exposure initiation and 2 two weeks following telemetry implantation (Figure3.4). Cardiac electrophysiology was monitored continuously before, during and after exposures.

Each exposure morning, all mice were transferred from their housing cages to stainless steel whole-body exposure chambers while still inside the vivarium. Perforated stainless steel grids were inserted into the cages to ensure the mice remained singly confined. Mice were allowed to move freely while constrained to their individual portion of the chambers. Once loaded, the chambers were sealed using a plexiglass cover and transferred to the exposure room. The plexiglass lid of each exposure chamber contained one inlet and one outlet port. Each chamber inlet was connected to its appropriate location on the VACES system and the CAPs was delivered to the mice using a nozzle designed and validated to provide a uniform distribution of PM within the exposure chamber [76]. The exposure atmospheres were pulled through each chamber using a vacuum pump connected to large dampening chamber. Rotameters attached inline between the pump and the chambers allowed for a steady flow of 2.0 LPM per chamber.

In all exposures, a total of 2 chambers per atmosphere were connected to their appropriate position on the VACES. The flow rate through each chamber was checked at the beginning of each exposure day to ensure that the system was providing adequate airflow for the animals. The whole-body chamber pressures, temperatures, and flow rates were monitored every 15 minutes during the exposures. Rotameters were used as a visual representation of airflow through each chamber. Chamber pressures were used to monitor pressure drop across each chamber and provided additional assurance that the cages were receiving adequate airflow. Chamber temperatures were monitored using adhesive strips and were maintained at 75 ± 5°F. Animals were observed every 15 minutes throughout the exposure period for signs of distress.

3.4 Telemetry Implantation

Radiotelemetry electrocardiographic monitors (ETA-F20, Data Sciences International, St Paul, MN, USA) allowed for continual acquisition of movement, temperature, and ECG measurements in the awake, freely moving mice. A subset of 5 mice in each exposure group was implanted with these devices. Prior to surgery, mice were anesthetized under isoflurane, secured on to a heat pad kept to a consistent 37 °, and the abdominal fur removed using Nair (Church and Dwight, Ewing NJ). The surgery began when mechanical stimulation to the mouse's foot pad did not elicit any response. The telemetry devices were implanted intraperitoneally (I.P) in a modified Lead II configuration. Surgical wounds were closed using a combination of Polyviolene braded sutures and would clips. All surgical procedures were performed using sterile technique.

Following surgery, the mice received Buprenorphine (2 days; 0.1 mg/kg body weight) for pain management and Enrofloxacin (7 days; 5.0 mg/kg body weight) to combat any possible infection. After a two-week recovery period, the mice were acclimated to the exposure system and baseline measurements of ECG parameters were obtained during which the mice were exposed to purified air. ECG signals were recorded during both exposure and non-exposure periods using PhysioTel® receivers (RMC-1, Data Sciences International, St Paul, MN, USA) connected to easyMATRIX16® amplification boxes and processed through iox2® acquisition software (EMKA Technologies S.A.S., Falls Church, VA, USA).

3.5 Exposure Atmosphere Characterization

3.5.1 Real-time particle concentration monitoring

Ambient and concentrated particle number and mass concentrations were monitored real-time during all exposures using a Condensation Particle Counter (CPC Model 3022A; TSI, Shoreview, MN, USA) a real-time optical mass monitor (DustTrak Model 8520, TSI, Shoreview, MN, USA), respectively. The monitors were located directly upstream from the exposure chambers and measurements were recorded every 15 minutes from all post-VACES atmospheres as well as from the purified air control atmosphere. The performance of VACES was determined based on the ratio of CAPs to ambient PM concentration during the entire exposure period.

3.5.2 Aerosol Mass Spectrometry

Size-resolved aerosol organic and inorganic constituent compositions were measured using a high-resolution Aerosol Mass Spectrometer (AMS, Aerodyne Research, Billerica, MA, USA) which provided size and chemical composition as well as mass concentrations in real-time for non-refractory sub-micron aerosol particles [77]. In this context, non-refractory refers to chemical species that evaporate quickly at 600 °C in a vacuum. Samples of ambient and post-VACES aerosol were sampled at a rate of 80 ml/min and the particles separated by aerodynamic diameter in a time-of-flight vacuum chamber. The particles then underwent vaporization at 600 °C followed by electron impaction ionization thereby generating small particle fragments that are detectable based on their mass:charge ratio. The AMS was not capable of identifying refractory materials such as metals or elemental carbon which are resistant to degradation at 600 °C.

The AMS was used to analyze exposure and ambient aerosol composition during the exposure studies to determine differences in PM characteristics. High resolution (V mode) data were analyzed with Igor Pro v. 6.37 (Wavemetrics, Inc.) using Squirrel (v. 1.57I) and PIKA

(1.16I) with the improved ambient method [78] to provide compositional analysis of particles. Control sampling, through a HEPA filter, was performed daily to allow adjustments to the default fragmentation table for the fragments CO_2^+ and $^{15}N^{14}N^+$. Oxygen to carbon ratio (O:C) of the particles are expected to increase as hydrocarbon compounds are progressively oxidized to aldehydes, ketones, and acids during atmospheric aging. The oxygen to carbon ratio (O:C) measurements were carried out on several exposure and non-exposure days during August through October of 2014, February of 2015, May of 2016, and August through October of 2016. Sampling was carried out at 1-2-minute time resolution and daily averages were calculated for time periods of approximately 9 am to 12 pm to overlap with the exposure timeframe.

3.5.3 O_3 Concentration

Ozone was monitored using an ultraviolet (UV) absorption analyzer (Model 400A, Teledyne API) which measures the concentration of O_3 in air by calculating the absorption of a 254 nm UV light signal in proportion to the amount of O_3 present in the sample cell. This calculation is based on the Beer-Lambert law which considers the wavelength of the UV light source and the path length of the UV sample cell. The monitor was checked daily against a calibrated transfer standard. Concentrations of O_3 were maintained at 200 ppb during all required exposures.

3.5.4 Gravimetric Analysis

Particle lines were placed in parallel with the chambers from each exposure atmosphere to collect particles on 25 mm polytetrafluoroethylene (PTFE) membrane filters for gravimetric analysis during the two animal exposures. Particles were deposited onto the filter at a rate of 1.0 LPM during each of the exposures. Pre- and post-weighed filters were placed in a temperature- and humidity-controlled weigh room for 24-48 hrs. and weighed using a microbalance (Cahn 31,

ThermoFisher, Weltham, MA, USA), with the difference in measured weight indicating the total mass of particles collected during the exposure week. Particle mass concentrations were determined for each exposure atmosphere on a weekly basis by dividing the measured weekly mass identified on the filter by the total weekly volume of air flow through the filter.

3.5.5 Elemental Carbon and Organic Carbon (EC/OC)

Particle lines were placed in parallel with the chambers from each exposure atmosphere to collect particles on 25 mm Quartz filters (Tissuquartz 2500-QAT, Pall Corp.). Filters were baked at 550 °C for 15 hrs. prior to use to purge any residual impurities from the filters. Particles were deposited onto the filter at a rate of 1.0 LPM during each of the exposures. Filters were stored inside their stainless steel filter holders at -20 °C between each exposure day. At the end of the exposure week, the Quartz filters were immediately placed in foil-line petri dishes wrapped with Parafilm M® laboratory tape (Bemis Company Inc, Oshkosh WI) and stored at -20 °C to minimize changes in the more volatile PM-bound species.

Loaded Quartz filters from the PM + O_3 exposure study (Chapter 3.3.3) were analyzed for elemental carbon (EC) and organic carbon (OC) using a Thermal Evolution/Optical Transmittance (TOT) analyzer (Lab OC-EC Aerosol Analyzer, Sunset Laboratories, Tigard, OR) [79,80] and following the predefined IMPROVE A protocol [81,82]. A 1 cm^2 punch of each filter was removed and placed into the oven of the analyzer where the collected PM is removed from the filter using thermal desorption in an inert helium environment. The vaporized OC was then oxidized under controlled heating conditions (maximum 600 °C) to form carbon dioxide and subsequently reduced to methane. A flame ionization detector (FID) is used to monitor the analysis. Some degree of pyrolysis of OC to EC is expected to occur due to the nature of this analysis and therefore is quantitated using an optical laser detector contained within the system.

Elemental carbon was also measured using the TOT analyzer. Following the OC measurements, the sample oven was heated to 850 °C and the sample chamber inundated with a helium/oxygen mixture thereby promoting the oxidation of EC to carbon dioxide. Due to the pyrolytic activity during the OC measurements, the EC measured during this stage contains both original EC from the sample and the EC produced through pyrolysis. Therefore, the final EC concentration measure for each sample was the difference between the detected EC and the pyrolysis-derived EC while the total OC concentration for each sample was calculated as the sum of the detected OC plus the pyrolytically converted OC. The mass of carbon on the entire filter was calculated by multiplying the mass of carbon detected in the sample by the ratio of the total area of the filter to the area of the punch (i.e., filter mass = sample mass x ($^{\text{Total Filter Area}}/_{\text{Punch Area}}$)). This calculated filter mass was then divided by the weekly total flow through the filter to determine the total concentration of EC and OC in each exposure atmosphere.

3.6 Non-Invasive Blood Pressure

Measures of systolic, diastolic, and mean blood pressure were collected weekly from restrained animals using a tail-cuff acquisition system (CODA, Kent Scientific, CT). This system uses a volume pressure recording (VPR) sensor to determine the systolic and diastolic blood pressure in rodents by determining tail blood volume. The VPR is clinically validated and provides a 99% correlation between telemetry and direct blood pressure measurements [83].

Mice were acclimated to the restraint tubes for 1 week prior to the start of each study. During acquisition periods, mice were placed on heated platforms which helped to maintain adequate blood volume in the tails. Blood pressure measurements were taken weekly, and data was collected on all animals one day prior to each exposure week. A total of 5 successful blood

pressure measurements during each recording session for each mouse in each cohort were acquired.

3.7 Necropsies

All mice were sacrificed 24 hrs. following their last exposure. Mice were terminally injected with 250 mg/kg of pentobarbital sodium and phenytoin sodium (Euthasol, Virbac Animal Heath, TX) to suppress neurological control of respiratory function. Once mechanical stimulation in the mouse was sufficiently suppressed, the abdominal cavity was opened and exsanguination through the vena cava acted as the ultimate cause of death.

3.8 Electrocardiogram Measurements

All ECG and HRV parameters were acquired from freely moving, conscious mice and assessed at the same time every evening beginning 6 hours following exposure period (7:00 PM–12:00 AM). The final analysis was performed on mice (n=3-5 per groups) whose telemetry signals remained consistent throughout the exposure period. All waveforms were defined using ecgAUTO® software (EMKA Technologies S.A.S., Falls Church, VA, USA) following definitions defined in Herman et al 2020 [84]. As shown in Figure 3.5, the P-wave Duration (Figure 3.5, 1) corresponds to atrial depolarization while the PR interval (Figure 3.5, 2) relates to the delay of the electrical impulse at the AV node and can be calculated as the time between of the first deflections of the P-wave and QRS wave complex. The QRS-wave complex (Figure 3.5, 3) primarily represents the start of the ventricular depolarization and the end of atrial repolarization; the time interval between consecutive QRS-waves is defined as the R-R interval. The completion of ventricular depolarization following the QRS-wave (Figure 3.5, 4) and the ventricular repolarization phase, known as the T-wave (Figure 3.5, 5), occur almost instantaneously. Due to

the absence of the murine ST segment, the T-wave was used to evaluate ventricular repolarization changes indicative of myocardial ischemia [85]. The T-wave area was defined as the area over or under the ECG tracing from the peak of the J-wave to the end of the T-wave, or where the T-wave returns to the isoelectric point. The T-wave amplitude was defined as the distance from the isoelectric line point of lowest deflection within the T-wave. The QT-interval encompasses the length of time from the onset of the Q-wave to the conclusion of the T-wave and corresponds to the ventricular repolarization phase and was measured and heart rate-corrected using Mitchell's correction [86]. Ventricular repolarization is completed by the end of the T-wave and before the subsequent atrial depolarization (Figure 3.5, 6). For this analysis, six ECG parameters were acquired: Heart Rate, RR interval, PR interval, corrected QT interval, T-wave area, and T-wave amplitude [85,87-89]. Other endpoints and waveforms were discussed for the sake of thoroughness.

HRV is the magnitude of variance explained (time-domain) in the heart's rhythm across different spectra (frequency-domain) of periodic oscillations in heart rate and was calculated using ecgAUTO® (EMKA Technologies S.A.S., Falls Church, VA, USA). ECG recordings were collected daily and analyzed in 30 second increments. Segments with less than 200 total R-waves or with a standard deviation of the averaged N-N values (SDNN) greater than 8 ms were excluded from daily exposure averages. Individual RR signal segments were averaged to obtain a single HRV value was calculated for each five-hour acquisition period. The root mean square of successive differences in the RR interval (RMSSD) was also calculated and is used here to represent the short-term deviations in heart beat and may indicate the integrity of the vagus nerve-mediated autonomic control of the heart [90]. Portions of these spectra reflect different autonomic influences on heart rate. Interpolated RR intervals underwent power spectral analysis

via Fast Fourier Transform to obtain frequency domain HRV measures. Segments with stationary stable signals and void of ectopic beats were selected following the guidelines established by the Task Force of the European Society of Cardiology [91]. The total power in both the high frequency (HF; 1.5-5.0 Hz [92]) and the low frequency (LF, 0.1-1.5 Hz) HRV band were calculated for each recording by solving for the integral of the high and low frequency bands, respectively. The HF band of the heart period power spectrum has been used to estimate cardiac vagal control [93] and decreased cardiac vagal activity in humans has been found to be associated with an increased risk of coronary atherosclerosis [94]. Heart period oscillations at lower frequencies are less well understood but may represent mixed sympathetic-parasympathetic and thermoregulatory influences [95,96].

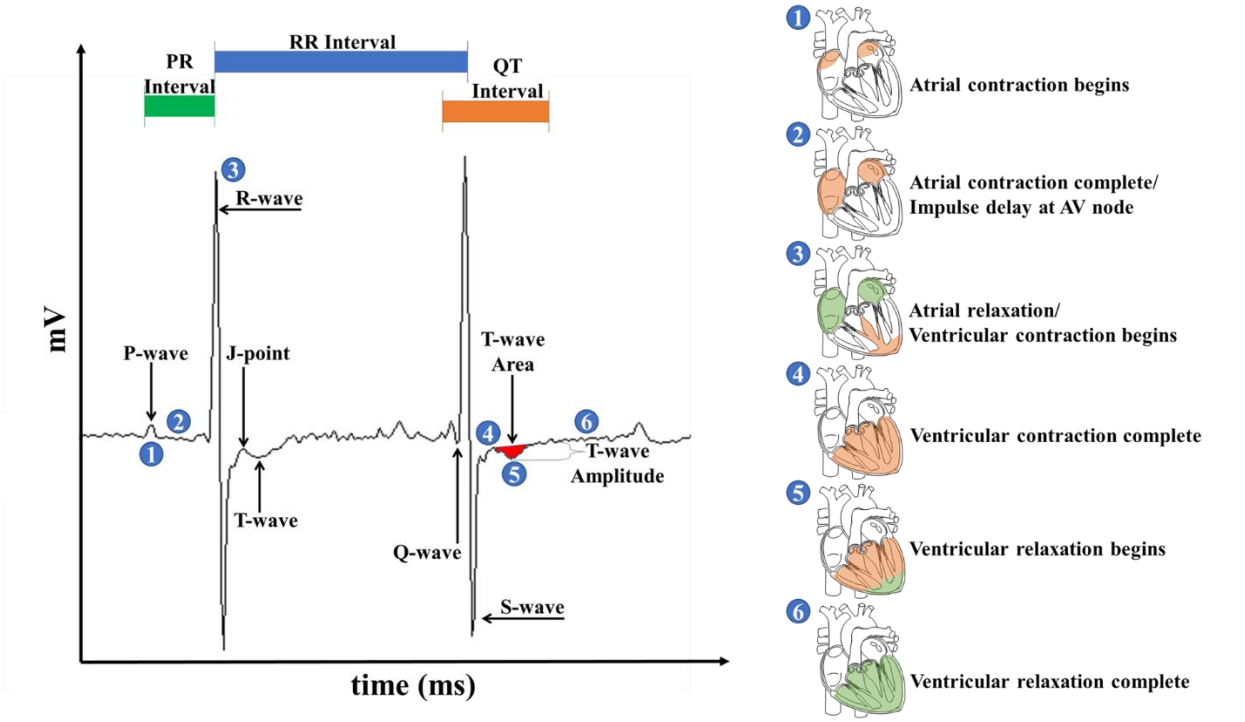

Figure 3.5. ECG Waveform Definitions. All waveform definitions were defined using ecgAUTO (see text for full definitions). Waveform libraries were assembled for each mouse using data acquired during a one-week baseline period immediately preceding the start of the exposure. Changes in ECG morphology in exposed mice were determined by comparing daily waveform measurements against baseline values. Circled numbers in the ECG trace correspond to defined contraction (orange shading) and relaxation (green shading) events in the heart highlighted on the right of the image.

3.9 Oxidative Stress-Related Assays

3.9.1 PM Extraction Procedure

Loaded filters were placed face down in clean amber glass containers. Ethanol (100 µl) was added dropwise onto the filter followed by 4 ml of water that was purified to an electrical resistance of 18.2 MΩ. The filters were twice sonicated on ice and agitated at 12000 RPM for 30 and 15 minutes, respectively. Extracted solutions were then transferred to 15 ml conical tubes and evaporated under nitrogen to a final volume of 100 µl. Extracted filters were placed back in the temperature- and humidity-controlled weigh room for 24-48 hrs. and then re-weighed to determine the final filter extraction efficiency. The evaporated samples were then diluted in order to produce PM slurries of equal concentration and stored at -20 °C until needed.

3.9.2 Oxidative Stress Assays

Two enzymes were selected for this analysis: A) glutathione Peroxidase (GPx), an enzyme that uses glutathione as the reducing substrate in the catalyzation of hydroperoxides, including hydrogen peroxide, and is a key component against oxidative stress; and B) glutathione reductase (GR), which is responsible for catalyzing the NADPH-dependent reduction of oxidized glutathione.

GPx (cat # 703102) and GR (cat # 703202) were detected using assay kits from Cayman Chemical (Ann Arbor, MI). Both assays were performed according to the provided protocols, with 20 µl of particle suspension used as a test material instead of biological samples. However, to test the inhibitory effect of PM directly, 20 µl of assay buffer was substituted for GPx control for each sample well. Absorbance at 340 nm was measured using a Synergy Mx microplate reader (BioTek Instruments, VT). The decrease in absorbance was measured every 5 minutes to assess the particle/enzyme interaction over time. Extraction media from a clean, unloaded filter

was used as background controls for both assays while urban particulate matter standard reference material (SRM) 1648a was used as a positive control. The SRM 1648a sample has been thoroughly characterized and contains known amounts of organic constituents such as multiple PAHs and polychlorinated biphenyl (PBC) as well as numerous metallic elements.

3.10 Data Analysis and Statistics

Baseline data between groups in each exposure period were compared by Student's two-tailed t-test with $P \leq 0.05$ considered significant. Differences in particle characteristics were detected using general linear model-multivariate analysis of variance (GLM-MANOVA) methods. Change from baseline measurements for ECG waveforms, HRV, and blood pressure between exposure group means were presented as weekly averages ± the standard error of the mean (SEM). Significance between exposure groups were determined at an exposure level using Bonferroni-corrected two-way analysis of variance (ANOVA) for repeated measures. Fisher's F-statistics as well as the proportion of total variance in the dependent variables, or partial η^2 was identified for each endpoint. SPSS® (IBM, Armonk, NY, USA) was used for all statistical analyses. Normalcy of the data was checked using a Shapiro-Wilk test. Significance was assessed at $P \leq 0.05$.

The oxidative stress assays measured the change in absorbance per minute at 340 nm (ΔA_{340}). This absorbance was calculated for each particle sample in duplicate and then adjusted for the non-enzymatic background ΔA_{340}. Total enzyme activity was calculated using Equation 3.1 (see below).

Equation 3.1: Antioxidant Enzyme Activity

$$GPx\ or\ GR\ Activity\ = \frac{\Delta A_{340}/min}{0.00373\ \mu M^{-1}} x \frac{0.19\ ml}{0.02\ ml}\ = nmol/min/ml$$

where 0.00373 μM^{-1} is the extinction coefficient of NADPH adjusted for well depth of the microplate for which the samples were read. Final data (based on n = 2 wells per sample type) are displayed as the enzymatic activity as a percentage of the assay control.

CHAPTER 4: RESULTS AND DISCUSSION

4.1 Health Effects of Seasonal Ambient PM Exposure

4.1.1 Results

4.1.1.1 EXPOSURE PARAMETERS AND ATMOSPHERE CHARACTERISTICS

A summary of the parameters and atmosphere characteristics to which genetically modified, hyperlipidemic (apoE-/-) mice were exposed is provided in Table 4.1. High photochemical activity (PCA) exposures to concentrated ambient particles (CAPs) were performed from July 23, 2015 through September 11, 2015 while the low PCA exposures were performed from August 23 through October 20, 2016. Ambient particle concentrations were slightly higher during the low PCA time-period compared to the high PCA period, but the average mass concentrations of the CAPs during the two exposure periods were comparable. The PM content of the filtered control air was routinely monitored for PM mass and averaged less than 0.1 $\mu g/m^3$. Ambient ozone and dewpoint levels were higher during the periods of high PCA activity; the mean ambient temperatures were comparable for both exposure periods. The mice were, however, exposed in temperature-regulated chambers and they were not affected by variations in ambient temperature.

Table 4.1. Exposure parameters and atmosphere characteristics for both high and low PCA Concentrated Ambient Particles (CAPs) $PM_{2.5}$. Data presented as exposure averages ± standard deviation.

	High PCA CAPs	High PCA Ambient Air	High PCA Filtered Air	Low PCA CAPs	Low PCA Ambient Air	Low PCA Filtered Air
Exposure Dates (Start/End)	23 July 15/ 11 Sept 15	23 July 15/ 11 Sept 15	23 July 15/ 11 Sept 15	23 Aug 16/ 20 Oct 16	23 Aug 16/ 20 Oct 16	23 Aug 16/ 20 Oct 16
Average Number Concentration (cm^{-3})	$(8.7 \pm 1.2) \times 10^4$	$(6.8 \pm 0.1) \times 10^3$	---	$(5.6 \pm 0.5) \times 10^4$	$(1.0 \pm 0.1) \times 10^4$	---
Average Mass Concentration ($\mu g\ m^{-3}$)	133 ± 20	12.5 ± 0.9	0.08±0.02	134 ± 70	12.2 ± 0.4	0.03 ± 0.04
24-hr Average Mass Equivalence	27 ± 4	27 ± 4	27 ± 4	28 ± 15	28 ± 15	28 ± 15
Average Ambient Ozone Concentration (ppb)	37.1 ± 0.8	37.1 ± 0.8	37.1 ± 0.8	24 ± 1.3	24 ± 1.3	24 ± 1.3
Average Mean Ambient Temperature (°F)	76.1 ± 4.7	76.1 ± 4.7	76.1 ± 4.7	72.1 ± 4.2	72.1 ± 4.2	72.1 ± 4.2
Average Dew Point (°F)	63.0 ± 2.5	63.0 ± 2.5	63.0 ± 2.5	57.8 ± 4.3	57.8 ± 4.3	57.8 ± 4.3

For comparison, Table 4.2 shows the relevant ambient air quality standards for O_3, $PM_{2.5}$, carbon monoxide (CO), and nitrogen dioxide (NO_2). Animals in this exposure were exposed to particles at a level below that of 24-hr national standard but above both the national and California annual standards. The South Coast AQMD (SCAQMD) also measured summer (High PCA) and winter (Low PCA) concentrations for these criteria pollutants. These measurements were calculated using data from the SCAQMD air quality station (AQS) that was both the closest in distance to our laboratory and contained the most comprehensive records (AQS # 06059007, Anaheim-Loara School). All our CAPs exposures, when calculated as time weighted 24-hr equivalented average concentrations were below the applicable state and national limits.

Table 4.2. Relevant ambient air quality standards for ozone, $PM_{2.5}$, carbon monoxide (CO), and nitrogen dioxide (NO2). Concentrations of local criteria pollutants acquired from a SCAQMD air quality station (AQS #: 060590007).

		Ambient Air Quality Standards	
		National	California
Ozone (ppb)		70	70
$PM_{2.5}$ (ug m-3)	24-hr	75	--
	Annual	12	12
CO (ppm)	1-hr	35	20
	8-hr	9	9
NO_2 (ppb)	1 hr	100	180
	Annual	53	30
		Comparative South Coast Basin Concentrations	
		Summer (High PCA)	Winter (Low PCA)
Ozone (ppb)		30	28
$PM_{2.5}$ (ug m-3)		14	12
CO (ppm)		0.35	0.62
NO_2 (ppb)		10	18

Oxygen to carbon (O:C) ratios were examined for ambient $PM_{2.5}$ over multiple seasons and years, including the exposure periods for this study. Figure 4.1 shows that particle O:C tends to be higher in spring/summer and lower in fall/winter periods. The O:C of the particles is expected to increase as hydrocarbon compounds are progressively oxidized to aldehydes, ketones, and acids during atmospheric aging. This seasonal variation in O:C was observed for both ambient PM and CAPs in the fall, showing that the average oxygen content of CAPs is similar to that of ambient particles. Figure 4.1 also shows that the seasonal trends in O:C ratios of analyzed $PM_{2.5}$ appear to track seasonal changes in UV radiation flux at the Earth's surface, which would be the driving force for atmospheric photochemical activity that influences the formation and composition of PM. While there are clearly many variables that will contribute to the composition of the organic fraction of particles, the reactive chemical species that initiate oxidation of volatile organic compounds in air are photochemically derived and thus our observed the trend in PM O:C is consistent with prior observations in Southern California [97].

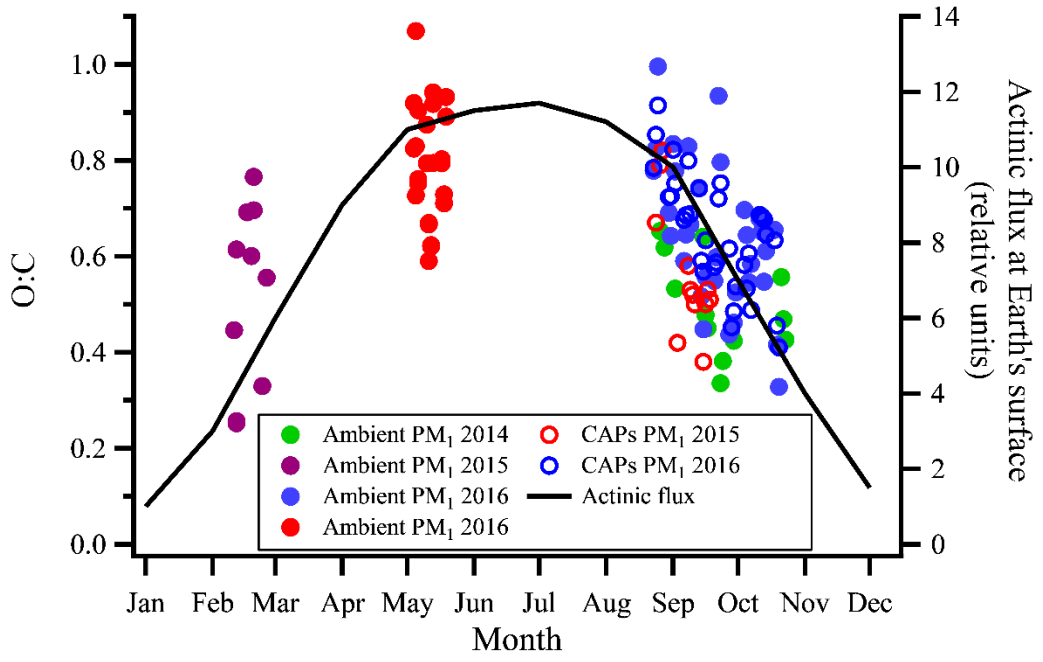

Figure 4.1. Oxygen-to-carbon ratios of PM1 sampled during different seasons compared to UV radiation at Earth's surface. Green markers indicate late fall/early winter of 2014, red markers indicate late spring/early summer of 2016. UV flux based on UV wavelength range at 30°N latitude (close to Irvine) solar zenith angles at 12:00 pm PST [97]. Exposure periods for this study occurred during periods designated by red and blue dots.

4.1.1.2 BASELINE VALUES

Baseline data for all physiologic parameters are presented in Table 4.3. Exposed and air control animals during both high and low PCA time periods exhibited comparable baseline measurements in most responses.

Table 4.3. Average baseline values for all measured endpoints ± SEM. Significant differences between cohorts during each experimental period assessed at $P \leq 0.05$ using Student's T-test and indicated by bolded italics.

	High PCA					Low PCA				
Endpoint	Air		CAPs		*P*	Air		CAPs		*P*
Heart Rate	561.71 ±	2.12	558.58 ±	3.97	0.50	576.68 ±	3.87	566.98 ±	5.14	0.14
R-R Interval	108.20 ±	0.48	109.50 ±	0.86	0.20	105.36 ±	0.76	107.09 ±	1.07	0.19
P-R Interval	34.01 ±	0.31	33.18 ±	0.47	0.16	34.10 ±	0.27	34.70 ±	0.53	0.32
QRS Interval	13.32 ±	0.12	13.73 ±	0.21	0.10	16.11 ±	0.71	14.97 ±	0.99	0.35
QTcM Interval	44.28 ±	0.63	45.46 ±	0.37	0.10	46.54 ±	0.31	45.77 ±	0.34	0.10
T-wave Area	-1.48 ±	0.11	-1.80 ±	0.16	0.07	-1.84 ±	0.22	-2.24 ±	0.10	0.10
T-wave Amplitude	-0.10 ±	0.01	-0.12 ±	0.01	0.11	-0.14 ±	0.01	-0.14 ±	0.00	0.39
SDNN	4.65 ±	0.46	5.15 ±	0.62	0.11	5.03 ±	0.09	5.05 ±	0.08	0.88
RMSSD	***3.31*** ±	***0.20***	***3.99*** ±	***0.27***	***0.04***	4.06 ±	0.10	3.79 ±	0.16	0.20
HF	0.70 ±	0.24	1.11 ±	0.39	0.21	4.80 ±	0.27	4.74 ±	0.22	0.86
LF	4.22 ±	0.38	5.32 ±	0.34	0.06	1.03 ±	0.05	0.93 ±	0.07	0.27
Systolic BP	***147.29*** ±	***5.22***	***127.31*** ±	***7.00***	***0.03***	142.01 ±	3.42	147.63 ±	7.11	0.47
Diastolic BP	116.37 ±	4.97	100.05 ±	6.95	0.07	110.29 ±	2.69	118.43 ±	7.04	0.28

4.1.1.3 HEMODYNAMICS

Mice exposed to CAPs formed during high PCA periods exhibited increased systolic and diastolic blood pressure compared to purified air controls (Figure 4.2A,C) with exposure cohort accounting for roughly forty percent of the variance in both parameters (Table 4.4). There was no observed blood pressure differences in mice exposed to CAPs formed during periods of low PCA compared to controls (Figure 4.2B, D)

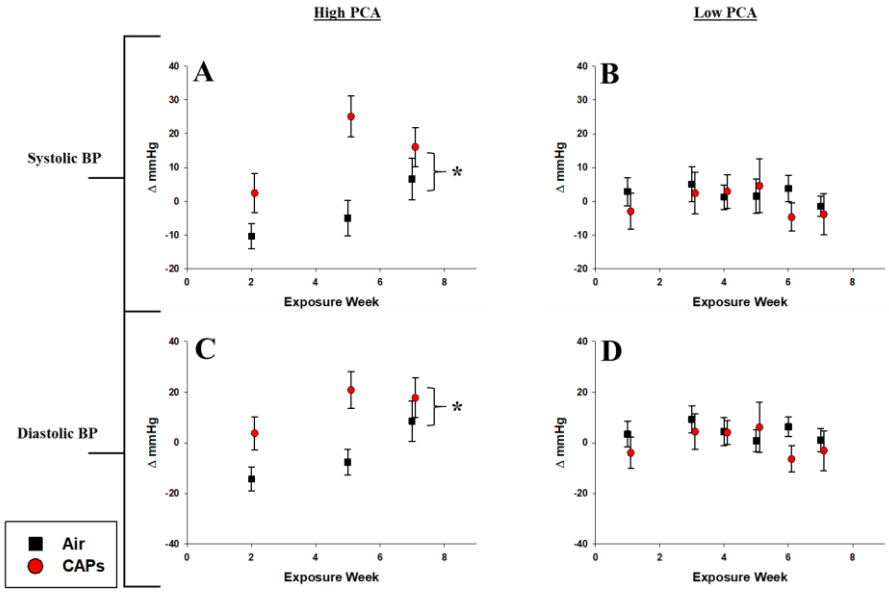

Figure 4.2. Blood pressure changes induced by particle exposure. Data represent weekly aggregates of change from baseline values for control and exposed animals during periods of high or low photochemical activity (± SEM, n = 3-5/group depending on acquisition scheduling). High PCA data set is complete and sporadic due to system availability. Low PCA CAPs data from week 2 is missing due to acquisition program errors. Significance assessed at $p \leq 0.05$; *CAPs significantly different than air over entire exposure period.

4.1.1.4 HEART RATE VARIABILITY (HRV)

8-week exposure during the high PCA time period resulted in decreased RMSSD and HF HRV parameters relative to air over the course of the exposure period (Figure 4.3A, 4.3C). This alteration in both time and frequency domain parameters may be indicative of augmented cardiac vagal control and activation of the parasympathetic nervous system. Mice exposed to low PCA CAPs experienced no change HRV parameters compared to control.

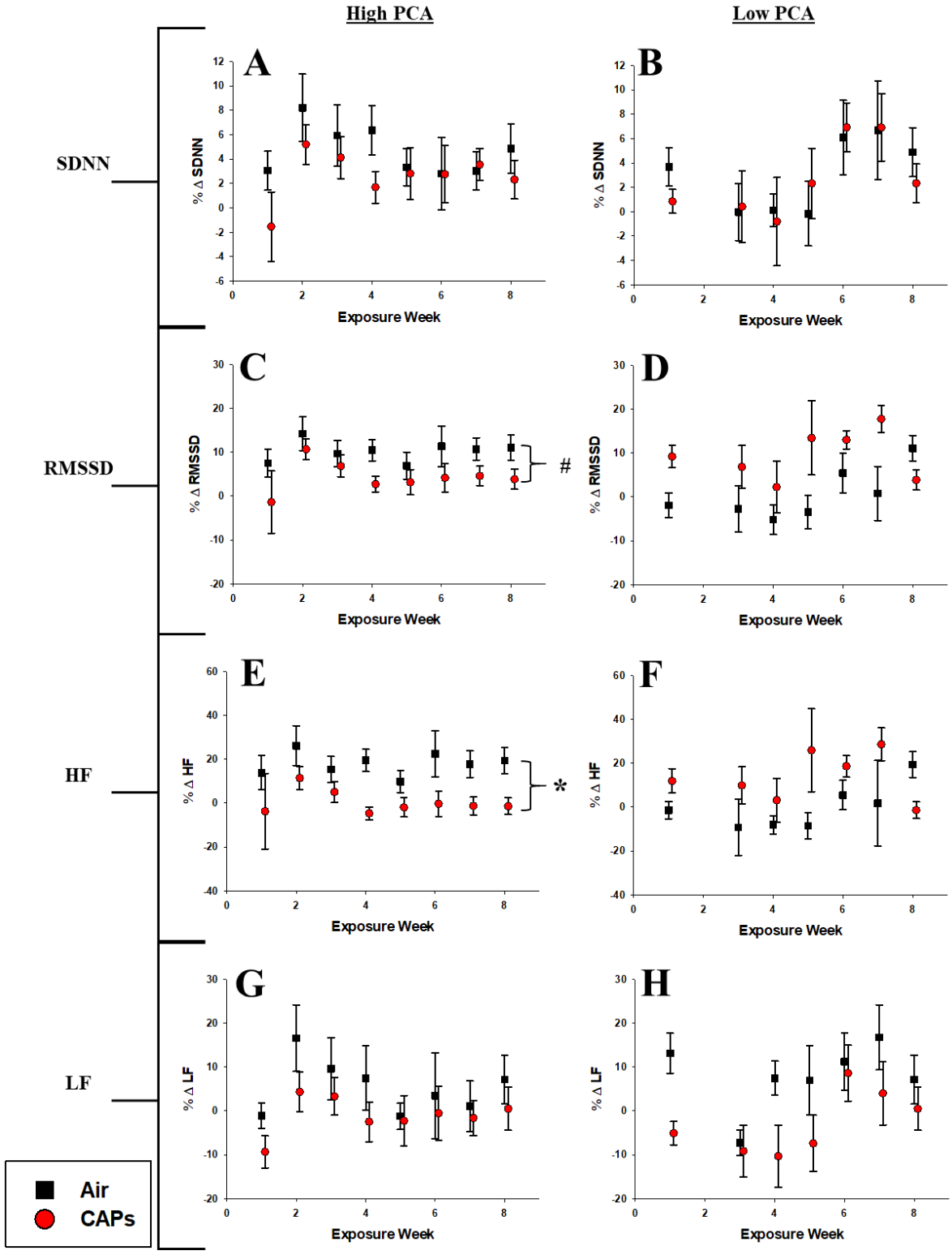

Figure 4.3. HRV averages for high and low PCA CAPs exposures. Data represent weekly aggregates of change from baseline values for control and exposed animals during periods of high or low photochemical activity (± SEM, n = 3-5/group depending on acquisition scheduling). Low PCA CAPs data from week 2 is missing due to acquisition program errors. Significance assessed at $p \leq 0.05$; *CAPs significantly different than air over entire exposure period.

4.1.1.5 ELECTROCARDIOGRAPHIC (ECG) WAVEFORM PARAMETERS

Exposure to CAPs during periods of high PCA elicited more pronounced alterations in rate-related ECG waveforms compared to exposures during periods of low photochemical activity. High PCA exposures decreased overall heart rate compared to air controls (Figure 4.4A, 4.4B) while no effect on RR interval was measured for either the high or low PCA exposures (Figure 4.4C, 4.4D). No significant differences in PR interval duration were measured during either exposure period suggesting limited atrial conduction dysfunction. However, the animals exposed during the high PCA period exhibited a consistent decrease compared to controls during most of the exposure period (Figure 4.4E). The QRS interval duration in mice exposed during the high PCA period was also significantly longer relative to air controls possibly indicating impaired cardiac depolarization (Figure 4.4G). This decreased trend, though not significant, was also present during the rate-corrected QT segment (QTcM) possibly indicating that the impairments caused by high PCA CAPs exposure may preferentially impact ventricular repolarization processes (Figure 4.4I). Interestingly, exposure to particle formed during low PCA periods resulted in phases of increased QRS intervals compared to air controls (Figure 4.4H). Additionally, the decreased QTcM duration may be attributed to the significant QRS complex prolongation (Figure 4.4G). Although not significant, these alterations may represent responses to components specific to the precise exposure period.

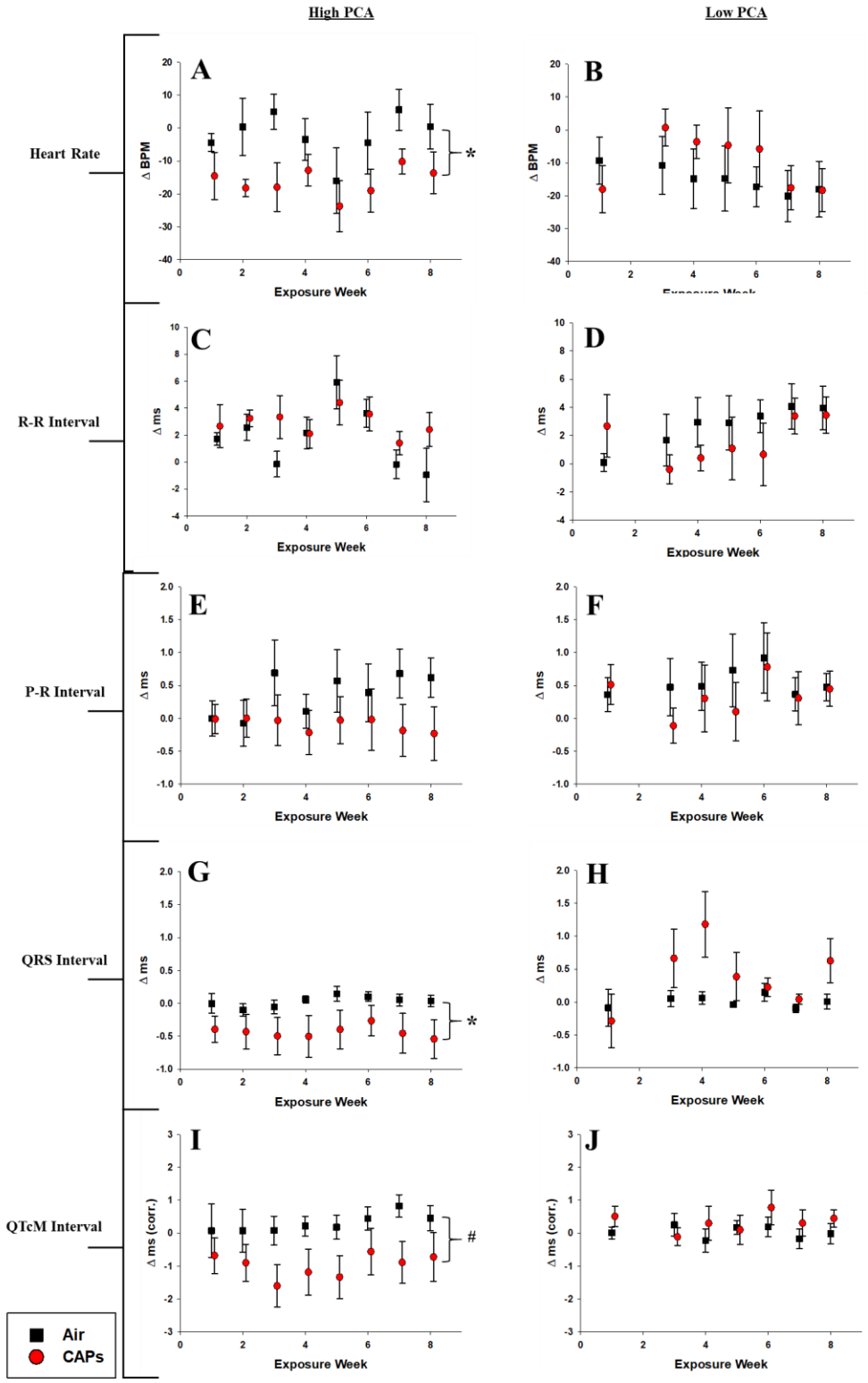

Figure 4.4. Heart rate-related ECG Waveform Changes. Data represent weekly aggregates of change from baseline values for control and exposed animals during periods of high or low photochemical activity (± SEM, n = 3-5/group depending on acquisition scheduling). Low PCA CAPs data from week 2 is missing due to acquisition program errors. Significance assessed at * $p \leq 0.05$ or $^{\#}$ $p \leq 0.1$ for CAPs compared to controls over the entire exposure period.

The effects of 8-week exposure to high and low PCA CAPs on the T-wave morphology are presented in Figure 4.5. CAPs exposed mice exhibited larger T-wave areas and amplitudes during the high PCA exposure period compared to air exposed controls over the entire exposure period (Figure 4.5A, 4.5C) and is consistent with alterations seen in the QTcM segment (Figure 4.4I). No difference between exposure and controls was seen during the low PCA exposure period.

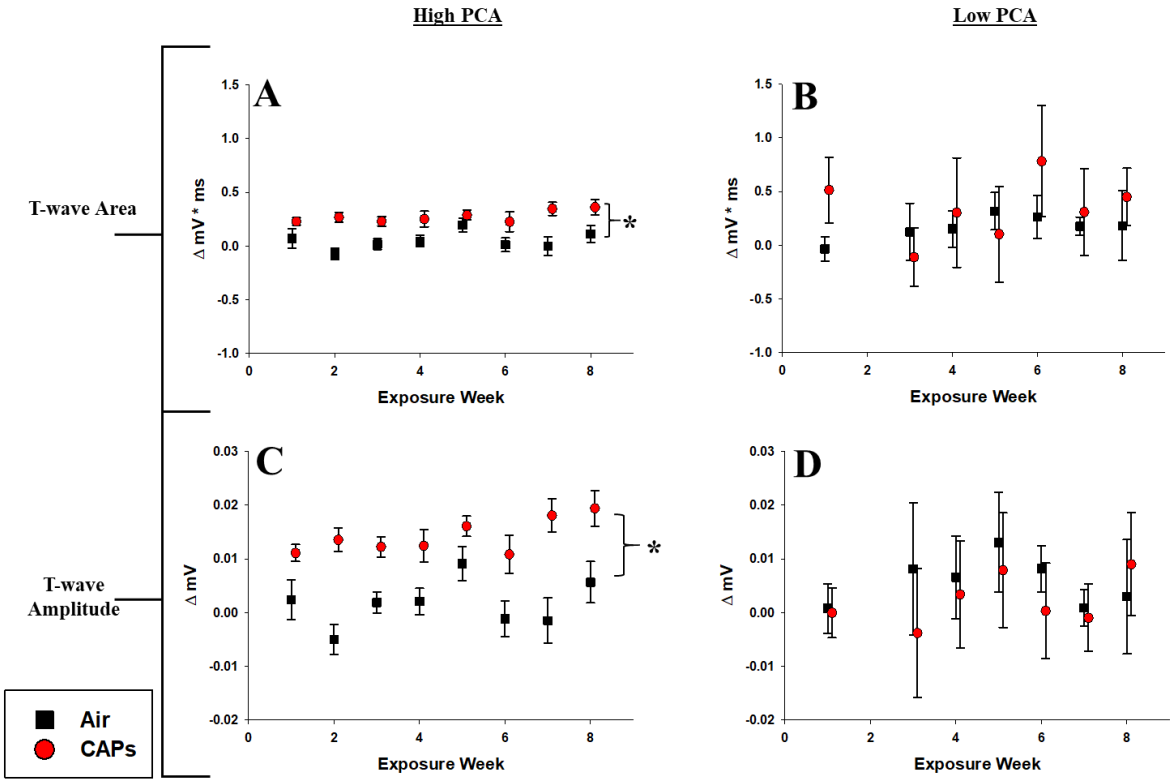

Figure 4.5. T-wave-related ECG waveform changes. Data represent weekly aggregates of change from baseline values for control and exposed animals during periods of high or low photochemical activity (± SEM, n = 3-5/group depending on acquisition scheduling). Low PCA CAPs data from week 2 is missing due to acquisition program errors. Significance assessed at $p \leq 0.05$; *CAPs significantly different than air over entire exposure period.

4.1.1.6 SUMMARY OF ANOVA-DERIVED SIGNIFICANT VALUES

The summary of statistical values for all measured parameters is presented in Table 4.4. High PCA CAPs exposures produced significant alterations in multiple cardiovascular-related measurements compared to purified air controls over the entire exposure period. Heart rate, systolic blood pressure (BP), and diastolic BP were found to account for the largest proportion of variance in the analysis at 48.5%, 40.9%, and 49.4%, respectively. Exposures to low PCA CAPs failed to elicit any significant differences in measurements compared to their respective purified air controls.

Table 4.4. Summary of ANOVA-derived significant values. Overall differences between control and CAP-exposed animals for both high and low PCA time periods. Partial Eta (η^2) are provided and represents the proportion on variance accounted for by each dependent variable. *indicates $P \leq 0.05$ while #indicates $P \leq 0.1$ by Bonferroni-corrected two-way ANOVA for repeated measures. Bolded italic font indicates significant differences.

	High PCA CAPs vs. Air				Low PCA CAPs vs. Air		
Endpoint	*F*-statistic	*P*	Partial η^2		*F*-statistic	*P*	Partial η^2
Heart Rate	***6.586***	***0.037***	***0.485***	*	0.011	0.919	0.002
R-R Interval	1.772	0.231	0.228		0.570	0.819	0.009
P-R Interval	0.696	0.432	0.090		0.018	0.897	0.003
QRS Interval	***0.899***	***0.050***	***0.114***	*	0.103	0.129	0.341
QTcM Interval	***2.470***	***0.065***	***0.261***	#	1.951	0.212	0.245
T-wave Area	***4.562***	***0.0378***	***0.174***	*	1.454	0.273	0.195
T-wave Amplitude	***2.345***	***0.025***	***0.247***	*	0.005	0.946	0.001
SDNN	0.144	0.711	0.012		0.214	0.653	0.021
RMSSD	***6.289***	***0.078***	***0.344***	#	0.353	0.566	0.034
HF	***3.763***	***0.028***	***0.255***	*	0.301	0.595	0.029
LF	1.191	0.297	0.090		1.282	0.284	0.144
Systolic BP	***11.069***	***0.004***	***0.409***	*	0.024	0.880	0.002
Diastolic BP	***11.042***	***0.004***	***0.394***	*	0.358	0.559	0.023

4.1.2 Discussion

4.1.2.1 CARDIOVASCULAR EFFECTS

Compositional and seasonal variations in PM on cardiopulmonary health effects were examined in this study. Exposures to CAPs concentrated from particles that formed or aged in ambient air during periods of high photochemical activity (July-September 2015) induced more severe adverse responses than did exposure to CAPs generated in the lower photochemical periods (August-October 2016). We analyzed ECG waveforms that relate to cardiac function and have shown that mice exposed to high PCA CAPs exhibit a decreased heart rates relative to controls which may result from decreased QRS or QT interval duration (Figure 4.4G, 4.4I) or altered autonomic nervous system input (RMSSD and HF HRV, Figures 4.3C and 4.3E). A study by Farraj and colleagues found that T-wave amplitude depressions in an acute studies exposing spontaneously hypertensive rats to residual oil fly ash [98]. Changes were seen in T-wave specific waveform structures following exposure to PM formed during periods of high or low PCA despite differences in particle concentrations between our and other studies; particles given to the animals under this exposure were 4-10 times less concentrated than those produced in the Farraj et al. study [98].

Interestingly, exposure to PM from different seasons had contrasting effects on the corrected QT interval. Animals exposed to PM during periods of high PCA experienced significantly prolonged QTcM intervals while sporadically shortened QTcM intervals were observed in animals exposed during low PCA periods (Figure 4.4I and 4.4J). Prolonged QT intervals are an established indicator for arrhythmia and sudden cardiac death and has been associated with PM air pollution in an elderly human cohort [99,100]. T-wave alterations were observed after high PCA exposures and can be indicative of myocardial ischemia [101]. Similar

studies reporting concurrent outcomes have been conducted which report altered ECG responses in rats following ambient PM inhalation. Similar to our study, the acute (3-day) study carried out by Farraj et al. in which rats were exposed to winter $PM_{2.5}$ reported a decrease in overall heart rate but also determined that exposed cardiomyocytes exhibited less sensitization to alterations in cardiac calcium homeostasis compared summer $PM_{2.5}$ exposure [102].

Furthermore, our data corroborates findings by Carll et al (2017) who showed decreased PR and QTc intervals in metabolically-challenged rats on a high fructose diet in a short-term (12 day) exposure to non-vehicular primary particles combined with photochemically derived secondary organic aerosols [103]. The consistency in results given drastically different exposure parameters (animal model, exposure time, concentration, measurement duration) may inform on the importance of the interaction between primary source particles and photochemically-derived secondary particles in environmental health effects. Additionally, opposing QRS and QTc-interval responses were observed in a ultrafine CAPs/Ozone acute co-exposure [104] which may again be due to differences in disease model, exposure duration, PM concentration, and/or monitoring periods. Regarding this study, ambient particles had undergone an atmospheric co-exposure prior to capture and concentration in our exposure system. Animals exposed to these highly photochemically active particles experienced cardiac abnormalities consistent to that previously reported human studies [105,106].

My current findings are consistent with previous findings in our research laboratory regarding high PCA exposures [13] but differ seasonally from those reported by Farraj et al. [102]. As with the Carll study, many parameters differ between this current exposure and those by Farraj et al. including animal model, duration of exposure, and the differences in source profiles in the two distinct locations (California and North Carolina); the North Carolina particle composition is

likely to be very different from that in Southern California [107]. This latter distinction may be one reason for the reversed response in the QTc interval seen by Farraj and colleagues. Other distinctions between the two studies are the animal model used and the duration of the study. Farraj and colleagues exposed rats to CAPs in three, 4-hour exposure periods. Based on our prior studies, physiological responses in rodents during the acute phase of a study may be influenced by the animal's stress responses to the novel exposure conditions in addition to the effects of exposure. The results from this 8-week study, although different from those reported by Farraj, may be represent cumulative effects of repeated exposures and possibly aging of the mice over the lengthened exposure program. The high and low PCA exposures were separated in time by roughly one calendar year and the animals were from different groups, albeit of the same strain from the same supplier. Therefore, we did not statistically contrast the measurements from one set of exposures to the other but analyzed comparisons to their respective air control groups.

4.1.2.2 HEART RATE VARIABILITY

This study found that certain markers of HRV (RMSSD and HR HRV) were decreased in mice after exposure to CAPs during the high PCA period compared to air controls with no effect seen in mice during the low PCA period (Figure 4.3C, 4.3E) indicating parasympathetic nervous system dysfunction. The degree to which these autonomic changes contribute to cardiovascular disease (CVD) is still under investigation. Reductions in both frequency domain components of HRV (LF and HF) were found in apoE-/- mice exposed to Seattle PM [108]. Similar decreases in HF HRV have been identified in apoE-/- mice exposed to concentrated PM near heavily trafficked roadways [13] reinforcing the role of primary particles in observed cardiac effects. CVD has been associated with HF HRV in humans indicating a potential predominance of the sympathetic nervous system [109]. LF HRV, on the other hand, has been associated with a plethora

of cardiovascular disorders in humans including heart failure, hypertension, and increased mortality rates after myocardial infarctions [110,111].

The HRV changes measured in Figure 4.3 indicate that inhalation of CAPs affects HRV, but the mode of action is quite different depending on the seasonal composition of the particles. Alterations in autonomic responses may be due to the presence of trace metals bound to the particulate matter. Lippmann et al (2006) reported that CAPs influenced by a 14-day incursion of nickel (Ni) during a rodent exposure study in Ney York state caused a significant decrease in SDNN stressing the importance of particle constituent on resulting health outcomes [112]. The effect of Nickel on HRV in this study is considered nominal as nickel concentrations in the South Coast air basin range from 8 -14 ng/m^3 which are about 10 times lower than concentrations present in the Lippmann study. However, the exposures from Carll and Lippmann both determined that the direction of HRV responses may be influenced by either the underlying disease state of the animal or possibly by the specific constituents of the inhaled particulate matter.

4.1.2.3 OTHER CONSIDERATIONS

This study confirmed that PM formed during periods of high PCA have different characteristics than PM formed during periods of lower PCA. The high PCA exposure occurred during the middle-late summer months of 2015 when particle O:C is shown to be at its highest at the exposure site in Irvine (Figure 4.1). The low PCA exposure occurred during the fall season when particle O:C was reduced, and ambient ozone levels were 10 ppb lower than during the high PCA period. This trend is shown to be similar in the fall for both ambient PM and CAPs. While seasonal changes in particles are dependent on the location and the sources of particles, the changes in PM O:C observed here are consistent with a number of studies that report higher

fractions of more oxidized compounds in summer months compared to PM in winter months [32-40]. Farraj et al. also examined seasonal differences in cardiac effects of PM exposure in an acute scenario and showed substantial differences in the concentration and chemistry of the ambient PM as a function of season. Their study was performed in the Northeastern region of the United States where combustion is a predominant heating method during the winter months and therefore significantly impacts the seasonal variation in ambient particulate matter. Under these conditions, Farraj and colleagues observed that exposure to PM collected during the winter months had 1.5 and 3.4 times larger concentrations of organic and elemental carbon, respectively, than did PM from summer months [102]. This is a stark contrast to our study and other ambient PM studies performed in southern California where combustion heating is minimal and variations in seasonal temperatures are less extreme than those observed in the eastern United States.

4.1.3 Limitations

This study has potential limitations. ApoE$^{-/-}$ mice were chosen for this study because they are prone to developing arterial disease similar to that seen in humans. However, these mice are also susceptible to higher levels of systemic oxidative stress and inflammation than are wild-type mice due to the apoE gene's involvement with anti-oxidative activity [113]. Additionally, existing datasets were pooled in order to determine potential seasonal effects of PM exposure. As such, the seasonal difference between the two exposure periods were not ideal. The system used to acquire the ECG and HRV data presented in this had limited recording capabilities. Therefore, a subset of each exposure cohort was recorded on any given day over the course of the exposure period. Lastly, due to the relatively small group sizes used in this exposure, the study should be repeated, and the results validated.

4.1.4 Conclusion

These findings demonstrate that exposures to particles formed during periods of high photochemical oxidation produce more adverse health effects than exposures to particles formed during periods of low photochemical activity. This finding was supported by chemical analyses which found the organic constituents present in ambient PM to be more oxidized during the high photochemical exposure period and therefore have the potential to produce increased ROS if/when inhaled. Therefore, photochemical activity may act as a surrogate for ambient levels of PM-bound organic species.

4.2 Health Effects of PM and PM+O_3 Exposure

4.2.1 Results

4.2.1.1 EXPOSURE PARAMETERS AND ATMOPHERIC CHARACTERIZATION

A summary of the exposure parameters and atmospheric characterizations are presented in Table 4.5. Exposure to CAPs + O_3 were performed for 8 weeks in July through September of 2015 while exposure to DeCAPs + O_3 were performed for 8 weeks from April through May in 2016. CAPs particle number and mass concentrations were increased by the VACES to approximately 10x ambient levels and particle mass and number concentrations for the CAPs and CAPs + O_3 exposure atmospheres were not significantly different. After removing the semi-volatile components in the denuder for the DeCAPs and DeCAPs + O_3 exposures, particle number and mass concentrations were about 50% lower those the CAPs concentrations [13] . Ozone was monitored at 200 ppb and was not statistically different between ozone exposure and the corresponding CAPs + O_3 atmosphere.

Table 4.5. Exposure parameters and atmosphere characteristics. Particle number (in particles/cm^3) and mass (in $\mu g/m^3$) concentrations compared to ambient levels are reported. Ozone concentrations are reported in ppb. Data represent average concentrations of 8-week exposures. *: $P < 0.05$. †: No detectable O_3 concentrations measured in the filtered air and CAPs/DeCAPs atmospheres at the start of the exposures.

	Filtered Air 1	Ambient 1	CAPs	CAPsO3	O3
$CAPs/O_3$ Exposure Dates (Start/End)	23 July 15/ 11 Sept 15	23 July 15/ 11 Sept 15	23 July 15/ 11 Sept 15	23 July 15/ 11 Sept 15	23 July 15/ 11 Sept 15
Average Number Concentration (#/cm^3)	---	6.8 e3 ± 1.0 e2	8.7 e4 ± 1.2 e4*	8.4 e4 ± 1.2 e4*	---
Average Mass Concentration ($\mu g/m^3$)	0.08 ± 0.02	12.5 ± 0.9	133 ± 20*	125 ± 15*	---
Average Ozone Concentration (ppb)	0†	37.1 ± 0.8	0†	200 ± 3.5	187 ± 3.8
	Filtered Air 2	Ambient 2	DeCAPs	DeCAPsO3	O3
$DeCAPs/O_3$ Exposure Dates (Start/End)	04 April 16/ 05 June 16	04 April 16/ 05 June 16	04 April 16/ 05 June 16	04 April 16/ 05 June 16	04 April 16/ 05 June 16
Average Number Concentration (#/cm^3)	---	5.7 e3 ± 2.0 e2	1.5 e4 ± 4.6 e3*	1.0 e4 ± 2.9 e3	---
Average Mass Concentration ($\mu g/m^3$)	0.29 ± 0.16	15.0 ± 4.1	33.0 ± 6.2*	31.0 ± 5.7*	---
Average Ozone Concentration (ppb)	0†	39.5 ± 0.9	0†	203 ± 3.9	197 ± 2.3

4.2.1.2 BASELINE VALUES

Baseline data for all physiologic parameters are presented in Table 4.6 for both CAPs and DeCAPs exposure periods. Significant differences were seen between the exposure groups in numerous cardiovascular parameters. Therefore, all data is presented herein are presented as change from baseline values in order to quantitate the true response of the exposure between experimental cohorts.

Table 4.6. Average baseline values for all measured endpoints ± SEM. Significant differences between cohorts during each experimental period assessed at $P \leq 0.05$ using single factor ANOVA and indicated by bolded italics.

							Whole PM						
Endpoint	Air			CAPs			CAPs + O3			O3			*P*
Heart Rate	567.21	±	3.08	558.58	±	3.97	562.67	±	6.17	571.20	±	8.01	0.41
R-R Interval	107.41	±	0.63	109.50	±	0.86	108.81	±	1.21	107.54	±	1.61	0.49
P-R Interval	***34.01***	±	***0.31***	***33.18***	±	***0.47***	***34.32***	±	***0.46***	***32.82***	±	***0.37***	***0.04***
QRS Interval	***13.32***	±	***0.12***	***13.73***	±	***0.21***	***14.40***	±	***0.26***	***15.45***	±	***0.35***	***0.00***
QTcM Interval	***44.42***	±	***0.62***	***45.73***	±	***0.43***	***48.16***	±	***0.84***	***44.52***	±	***0.42***	***0.00***
T-wave Area	**-1.74**	±	**0.16**	**-1.55**	±	**0.11**	**-1.94**	±	**0.24**	**-2.07**	±	**0.09**	**0.09**
T-wave Amplitude	***-0.11***	±	***0.01***	***-0.10***	±	***0.01***	***-0.13***	±	***0.01***	***-0.12***	±	***0.00***	***0.01***
SDNN	4.65	±	0.16	5.15	±	0.12	4.88	±	0.14	4.85	±	0.08	0.06
RMSSD	***3.31***	±	***0.10***	***3.99***	±	***0.17***	***3.70***	±	***0.20***	***3.41***	±	***0.10***	***0.01***
HF	***0.70***	±	***0.04***	***1.11***	±	***0.09***	***0.94***	±	***0.08***	***0.77***	±	***0.03***	***0.00***
LF	4.22	±	0.38	5.32	±	0.34	4.53	±	0.28	4.60	±	0.24	0.09
Systolic BP	147.29	±	5.22	127.31	±	7.00	139.33	±	4.19	135.15	±	6.12	0.12
Diastolic BP	116.37	±	4.97	100.05	±	6.95	110.04	±	3.95	106.15	±	5.77	0.22
							Denuded PM						
Endpoint	Air			DeCAPs			DeCAPs + O3			O3			*P*
Heart Rate	538.17	±	9.05	535.38	±	5.78	544.52	±	8.50	568.77	±	6.17	0.25
R-R Interval	114.01	±	1.94	113.81	±	1.25	111.39	±	1.85	106.96	±	1.46	0.24
P-R Interval	***33.66***	±	***0.32***	***34.77***	±	***0.49***	***32.36***	±	***0.26***	***32.47***	±	***0.48***	***0.00***
QRS Interval	***15.37***	±	***0.27***	***11.89***	±	***0.29***	***14.92***	±	***0.38***	***16.10***	±	***0.22***	***0.00***
QTcM Interval	***29.72***	±	***1.64***	***29.88***	±	***1.64***	***21.83***	±	***2.48***	***35.38***	±	***1.71***	***0.01***
T-wave Area	***-2.32***	±	***0.11***	***-0.83***	±	***0.20***	***-0.92***	±	***0.12***	***-1.74***	±	***0.11***	***0.01***
T-wave Amplitude	***-0.16***	±	***0.01***	***-0.06***	±	***0.01***	***-0.08***	±	***0.01***	***-0.11***	±	***0.00***	***0.00***
SDNN	***4.54***	±	***0.15***	***4.79***	±	***0.06***	***4.50***	±	***0.09***	***4.83***	±	***0.08***	***0.05***
RMSSD	***3.62***	±	***0.16***	***3.81***	±	***0.07***	***3.41***	±	***0.07***	***3.49***	±	***0.07***	***0.03***
HF	0.85	±	0.06	0.91	±	0.03	0.76	±	0.03	0.79	±	0.03	0.67
LF	***4.42***	±	***0.30***	***4.28***	±	***0.17***	***4.09***	±	***0.18***	***4.46***	±	***0.25***	***0.03***
Systolic BP	143.43	±	4.15	134.33	±	5.27	144.70	±	4.13	145.27	±	5.18	0.32
Diastolic BP	108.84	±	4.28	104.71	±	4.26	112.21	±	4.32	110.28	±	5.20	0.68

4.2.1.3 HEMODYNAMIC CHANGES

Delta baseline hemodynamic data from both exposure periods are presented in Figure 4.6. Exposure to whole PM alone or in concert with O_3 produced a significant increase in both systolic and diastolic blood pressure (Figure 4.6A, 4.6C). This increased trend became more evident towards the middle of the exposure period but subsided as the exposure period ended. Exposure to O_3 did not alter BP measurements compared to purified air exposures during either of the exposure periods. Moreover, we observed no significant effect of any exposure atmosphere on either systolic or diastolic blood pressure during the DeCAPs exposure period.

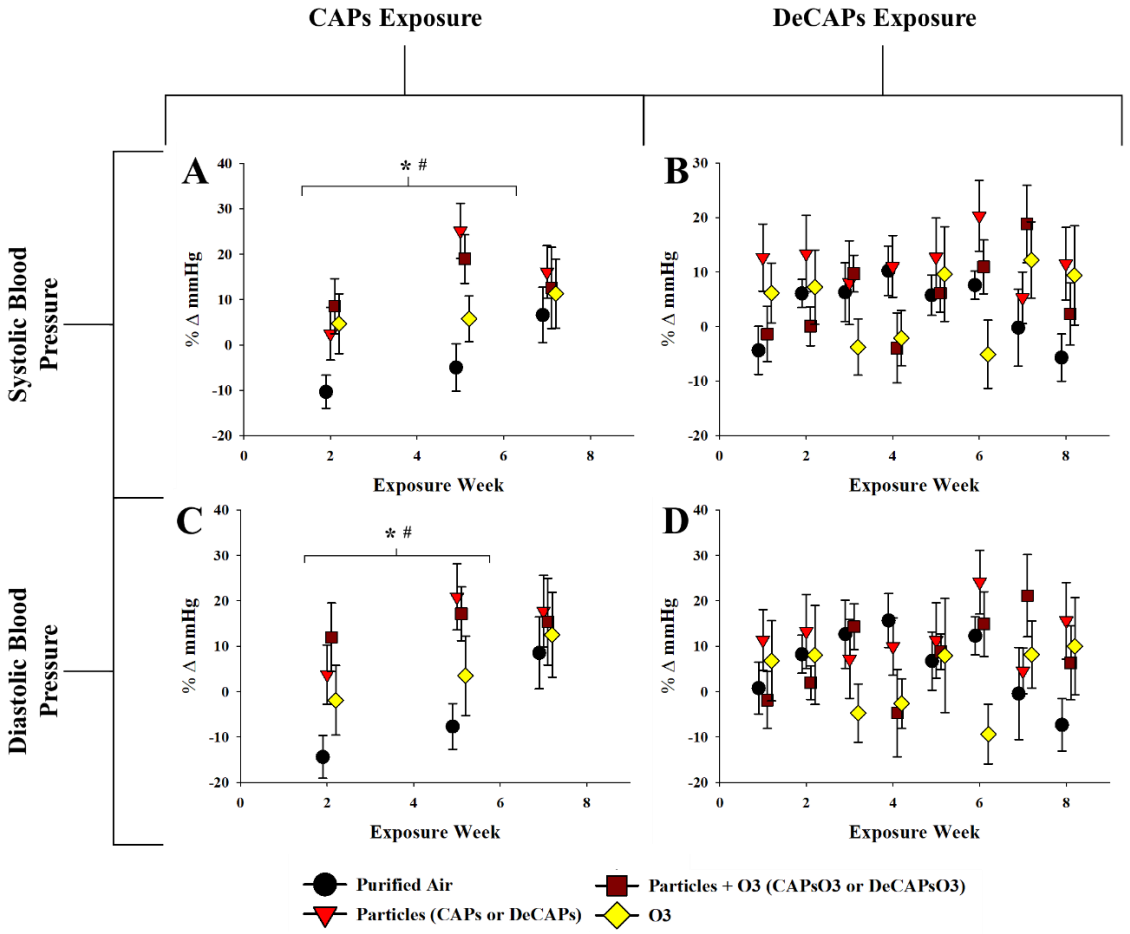

Figure 4.6. Average weekly systolic and diastolic blood pressure for both CAPs and DeCAPs exposure periods. Data represent weekly aggregates of change from baseline values for control and exposed animals during the two exposure periods (± SEM, n = 3-5/group depending on acquisition scheduling). Data from the CAPs exposure period was collected at weeks 2, 5, and 7 due to acquisition system limitations. Significance assessed at $p \leq 0.05$. *Particles vs Air; #Particles + O3 vs Air.

4.2.1.4 HEART RATE VARIABILITY

Heart rate variability responses of mice exposed to single and co-pollutant atmospheres are summarized in figure 4.7. Exposure to any pollutant atmosphere did not significantly alter the SDNN (Figure 4.7A, 4.7B). We observed a decreased RMSSD in the O_3-exposed animals during the first exposure period (Figure 4.7C). This decrease in the O_3-exposed group was evident during the first half of the DeCAPs exposure period, however this effect appears to subside as the exposure progresses (Figure 4.7D). We observed no effect of any exposure atmosphere on the low frequency HRV measure (Figure 4.7E, 4.7F). Moreover, exposure to CAPs significantly decreased high frequency HRV compared to air controls while no effect was seen in the DeCAPs exposure group (Figure 4.7G, 4.7H). Interestingly, the O_3-exposed cohort experienced a significant decrease in HF HRV during the first exposure with no effect experienced during the second exposure period (Figure 4.7G, 4.7H). However, upon closer investigation, the significance appears associated with changes during the last two weeks of exposure and appear in all HRV responses to O_3 exposure.

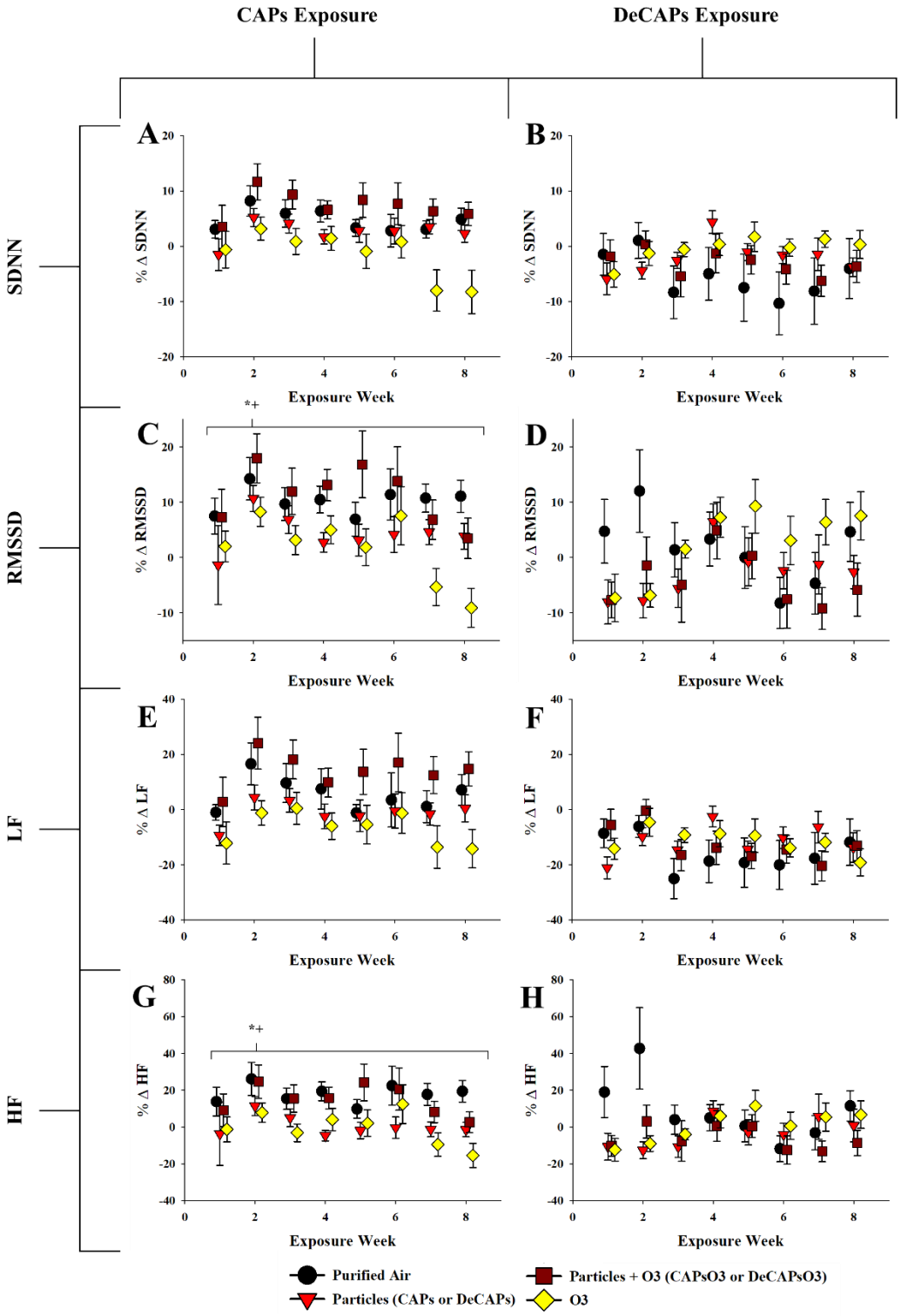

Figure 4.7. Heart Rate Variability measurements for all particle fraction exposures. Data represent weekly aggregates of change from baseline values for control and exposed animals. (± SEM, n = 3-5/group depending on acquisition scheduling). Significance assessed at $p \leq 0.05$. *Particles vs Air; $^{\#}$Particles + O3 vs Air; $^{+}$O3 vs Air based on total exposure responses.

4.2.1.5 ELECTROCARDIOGRAPHIC (ECG) WAVEFORM PARAMETERS

Heart Rate And R-R Interval: Chronic exposure to different components of ambient PM resulted in alterations in electrophysiological conduction through different cardiac regions. Exposure to O_3 with or without whole CAPs elicited a decrease in heart rate compared to controls while the heart rates of CAPs-exposed mice, although not significant, resulted in a decreased trend for the duration of the study period (figure 4.8A). Similar yet opposite patterns can be seen in the R-R interval for these animal cohorts (figure 4.8C) as this interval is inversely correlated with overall heart rate. Removal of the SVOCs from the PM ameliorated the effects seen in these measures as animals exposed to DeCAPs or DeCAPs + O_3 did not show overall heart rate or R-R interval anomalies (figure 4.8B, 4.8D). Interestingly, the effect of O_3 on heart rate during the CAPs exposure was not observed during the DeCAPs exposure despite consistencies in other ECG endpoints.

Atrial Conduction Rate: Some degree of atrial conduction anomaly was observed in mice exposed to any fraction of concentrated PM. CAPs exposure resulted in decreased PR intervals compared to controls (Figure 4.8E) while DeCAPs-exposed animals experienced a decreased trend in this measure (figure 4.8F) possibly indicating that the atrial depolarization/repolarization cycle is similarly affected by each particle fraction separately or combined. Exposure to O_3 consistently impaired PR interval duration and produced outcomes similar to that of CAPs or DeCAPs exposure alone (figure 4.8E, 4.8F). Co-exposing mice to either CAPs + O_3 or DeCAPs + O_3 failed to elicit any PR interval anomalies.

Ventricular Conduction Rate: Exposure to CAPs alone significantly decreased the QRS interval compared to purified air controls (figure 4.8G) suggesting a slowing of ventricular depolarization. This decreased rate was carried over to the corrected QT interval where CAPs exposure, albeit not to a significant degree (figure 4.8I). DeCAPs exposure did not produce any significant alterations compared to controls with respect to the QRS and QT intervals. However, there is some indication that DeCAPs exposure may increase these intervals (figure 4.8H, 4.8J) whereas CAPs exposure decreases them. No alteration in QRS interval was seen in mice exposed to O_3 in either exposure (figure 4.8G, 4.8H). However, O_3 did elicit a slight decrease in corrected QT interval during the CAPs exposure period with a significant decrease during the DeCAPs exposure period (figure 4.8I, 4.8J). Mice exposed to CAPs + O_3 did not exhibit any alterations in ventricular depolarization/repolarization. However, the DeCAPs + O_3 cohort experienced decreased QT interval durations which mimicked the effect of O_3 during this study.

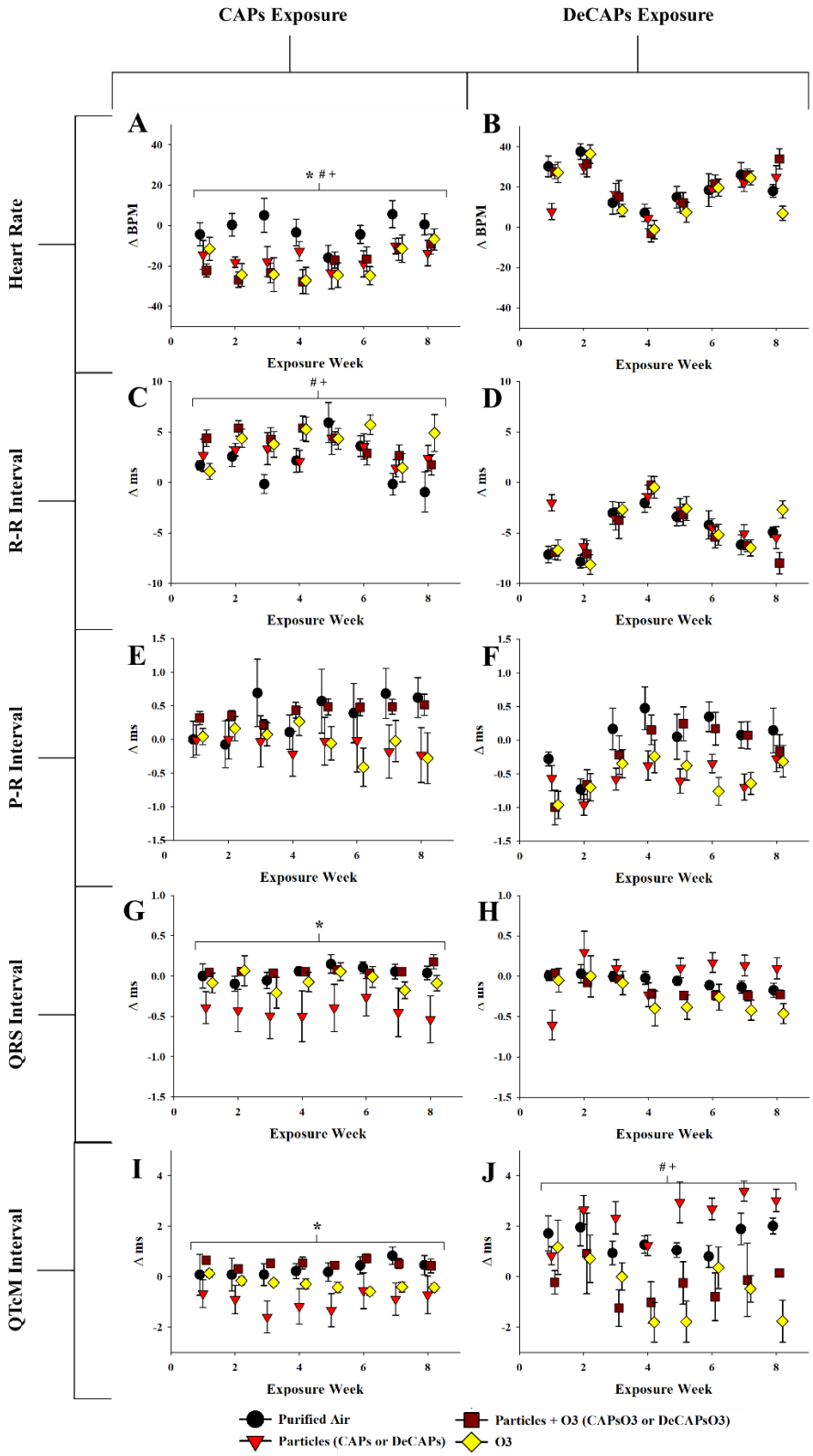

Figure 4.8. Heart rate-related ECG Waveform Changes for all particle fraction exposures. Data represent weekly aggregates of change from baseline values for control and exposed animals. (± SEM, n = 3-5/group depending on acquisition scheduling). Significance assessed at $p \leq 0.05$. *Particles vs Air; #Particles + O3 vs Air; +O3 vs Air based on total exposure responses.

Ventricular-Associated Waveforms:

The ECG waveforms associated with ventricular repolarization and cardiomyocyte relaxation were altered depending on particle fraction. 8-week exposure to whole CAPs alone resulted in significantly increased T-wave areas and amplitudes compared to control animals (figure 4.9A, 4.9C) while co-exposure to CAPs + O_3 produced a significant decrease in T-wave area with no effect seen in T-wave amplitude. Particles devoid of SVOCs ameliorate the effect of PM exposure on ventricular-associated waveforms as mice exposed to DeCAPs or DeCAPs + O_3 did not exhibit any significant changes in T-wave area or amplitude compared to controls (figure 4.9B, 4.9D). Exposure to O_3 resulted in no T-wave area impairments compared to controls animals (figure 4.9A, 4.9B). However, the T wave amplitudes in the O_3 cohort did slightly increase compared to air exposure (figure 4.9C, 4.9D).

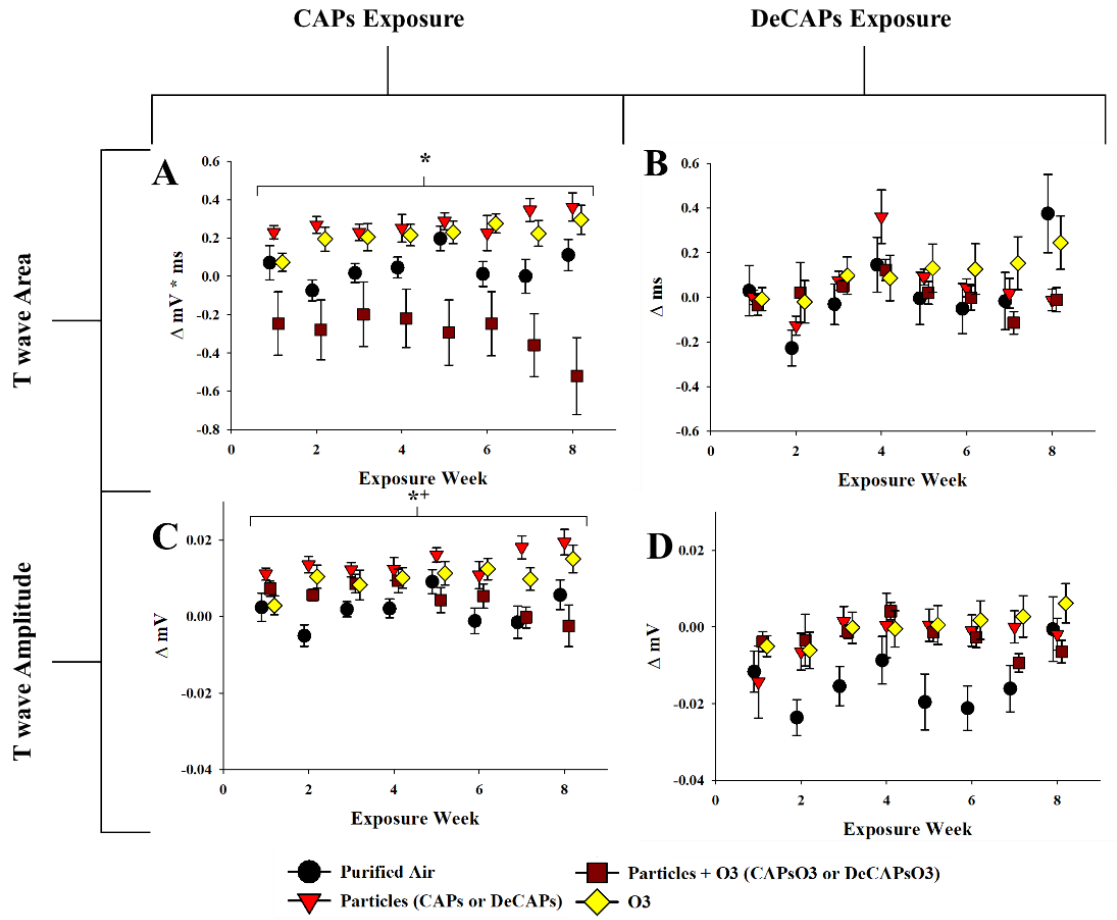

Figure 4.9. Ventricular-associated waveform data for all particle fraction exposures. Data represent weekly aggregates of change from baseline values for control and exposed animals. (± SEM, n = 3-5/group depending on acquisition scheduling). Significance assessed at $p \leq 0.05$. Significance assessed at $p \leq 0.05$. *Particles vs Air; #Particles + O3 vs Air; +O3 vs Air based on total exposure responses.

4.2.1.6 ELEMENTAL CARBON/ORGANIC CARBON

The concentration of organic carbon (OC) present in the CAPs is markedly decreased (80-90%) following thermal denudation at 120 °C. The elemental carbon (EC) content in the DeCAPs is about 30-40% lower than that measured in the CAPs, but within limits of experimental error. Adding O_3 to the PM atmospheres, specifically to the DeCAPs, results in higher OC mass compared to PM only samples which may suggest some degree of secondary organic aerosol (SOA) formation produced by the reaction of O_3 with more unstable organic constituents.

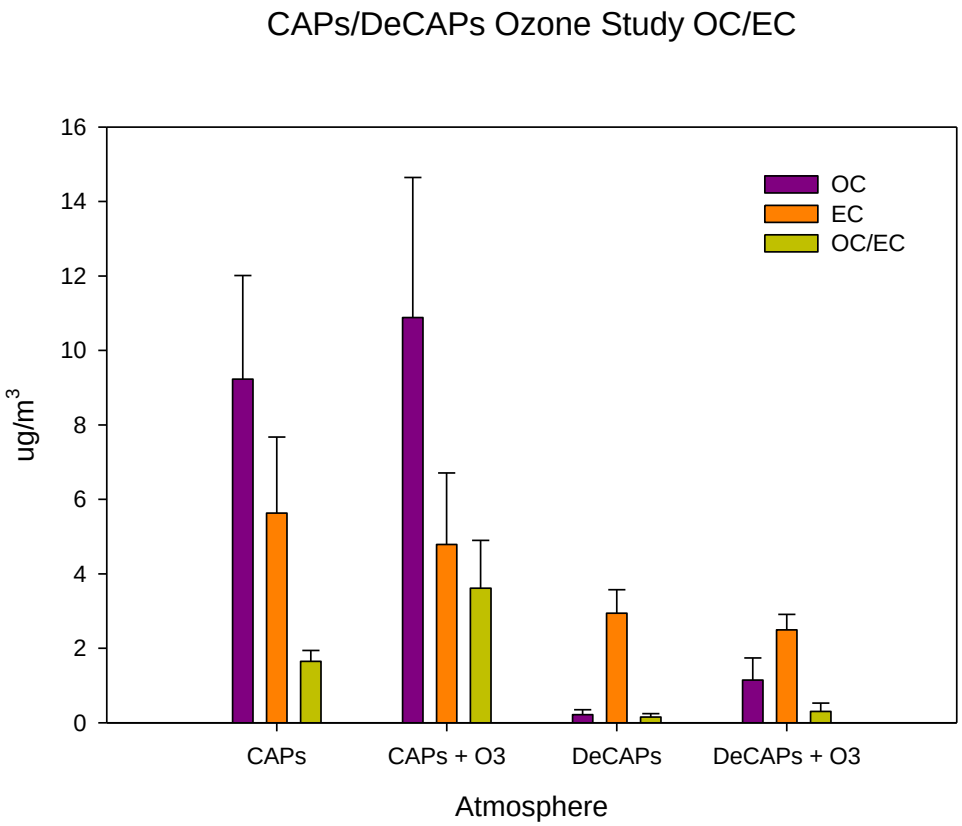

Figure 4.10. EC/OC Analysis for PM and PM + O_3 Atmospheres.

4.2.1.7 AEROSOL CONSTITUENT INFLUENCES IN HEALTH EFFECTS

Figure 4.11A shows typical PM_1 measurements of the O:C ratio for different atmospheres. CAPs samples had very similar O:C ratios to ambient PM samples, indicating that the VACES conserved O:C throughout the exposures, even with a wide daily O:C variation between 0.4 and 0.8. Examination of daily CAPs + O_3 atmospheres revealed slightly higher O:C ratios than CAPs atmospheres on most of the exposure days, as shown in Figure 4.11B. A positive change indicates an increase in O:C in the presence of O_3 and a negative change indicates a decrease in O:C. There were a few days in which CAPs + O_3 particles did not yield an increase in O:C. These were typically days in which the ambient O:C was already high or there was low mass loading. Examination of the chemically resolved size distributions for CAPs and CAPs + O_3 atmospheres showed that particles exhibited a loss in mass concentration in the presence of ozone. An example of this is shown in Figure 4.11C. The sulfate component of the particles is not expected to be affected by O_3 and is provided to show that it remains constant in the CAPs and CAPs + O_3 particles, indicating that any loss in organics is not a result of dilution. Figure 4.11D shows the change in organic mass in the particles for each exposure day. Figure 4.11E is an example size distribution showing that a large fraction of organics is removed by passage through the thermodenuder on a typical exposure day. The organic removal occurs throughout different particle sizes and inorganics are affected to some extent as well. DeCAPs O:C ratios were also generally higher than CAPs O:C ratios (Fig.4.11A), suggesting that the less oxidized organic species in the particles are preferably removed by passage through the thermodenuder. Addition of O_3 to DeCAPs did not increase O:C ratios appreciably (Figure 4.11A) as the O:C was already fairly high for DeCAPs atmospheres.

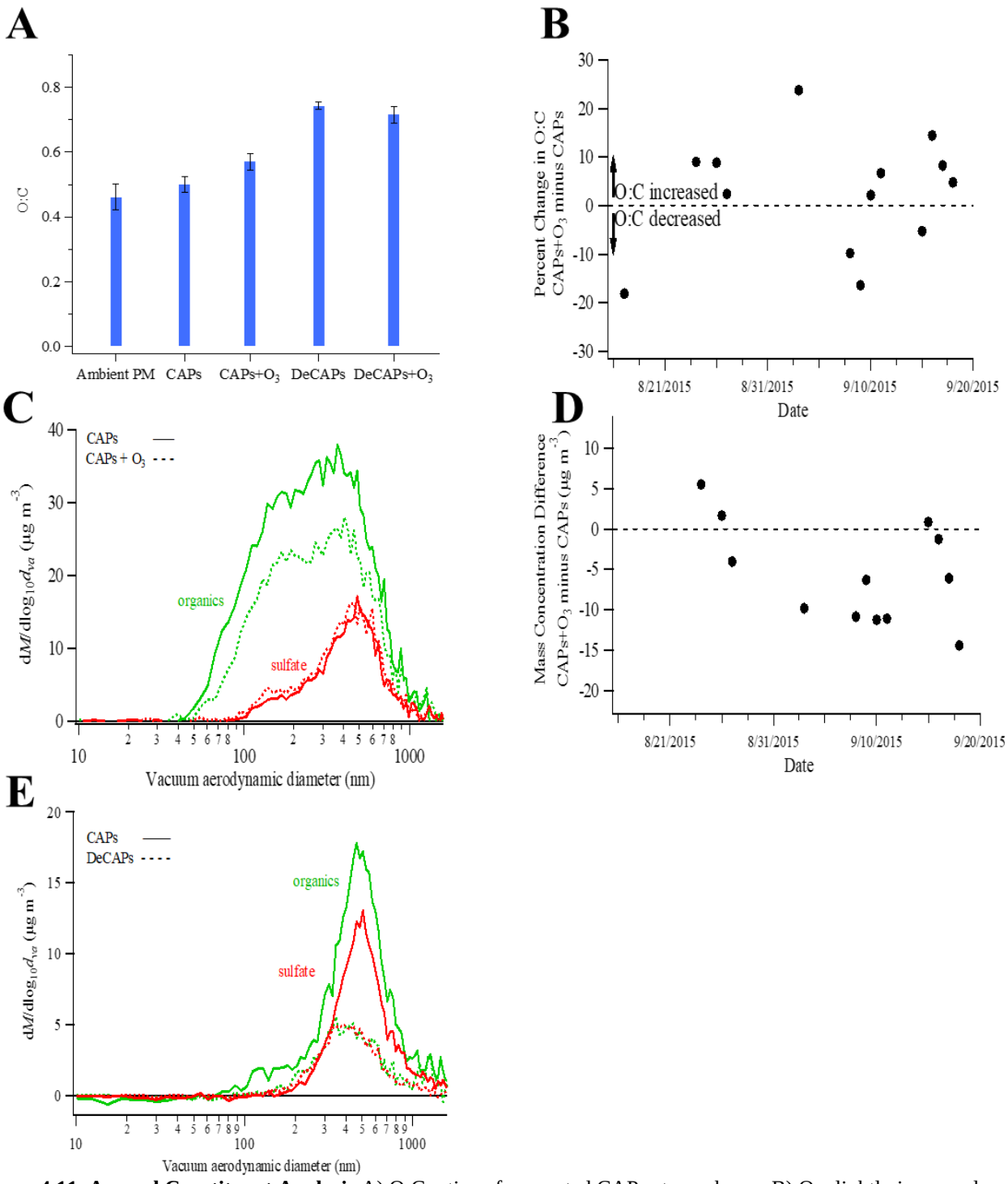

Figure 4.11. Aerosol Constituent Analysis A) O:C ratios of generated CAPs atmospheres; B) O_3 slightly increased O:C ratios in the CAPs atmosphere; C) Examination of chemically resolved size distributions for CAPs and CAPs + O_3 atmospheres. D) Difference in daily mass concentrations between CAPs and CAPs + O_3 atmospheres; E) Examination of chemically resolved size distributions for DeCAPs and DeCAPsO_3 atmospheres

4.2.1.8 CHEMICAL CORRELATIONS WITH HRV

Our laboratory has previously shown that removal of organic constituents from CAPs reduced the effect of CAPs exposure on HRV [13]. Based on results from this study, there is a significant positive correlation between HRV and O:C ratio for CAPs and for CAPs + 0.2 ppm O_3 with a larger effect seen in the co-exposure group (Figure 4.12A). That is, increases in HF HRV are prevalent on days when the O:C ratio of the CAPs is closer to one. Coupling this finding with the apparent losses of organics shown in Figure 4.11A, this might suggest that adding O_3 conserved the more toxic organic constituents bound to the PM. We also looked at the hydrogen to carbon ratio (H:C) as a "confirmation" of the data in Figure 4.12A. As expected, we measured decreases in H:C values in tandem with the O:C increase suggesting that lower H:C ratios are associated with worsened HRV (Figure 4.12B). This correlation appears to hold true, apart from one rainy day (r^2 values for fits omitting the rainy day are given in parentheses). Using the AMS we were able to identify some relationships between the presence of specific families of organic compounds and changes in HRV. Lower organic acid content represented by ions with mass fraction 44 (Figure 4.12C) and possibly higher carbonyl (mass fraction 43; Figure 4.12D) content are associated with worsened HF HRV in PM both with and without O_3.

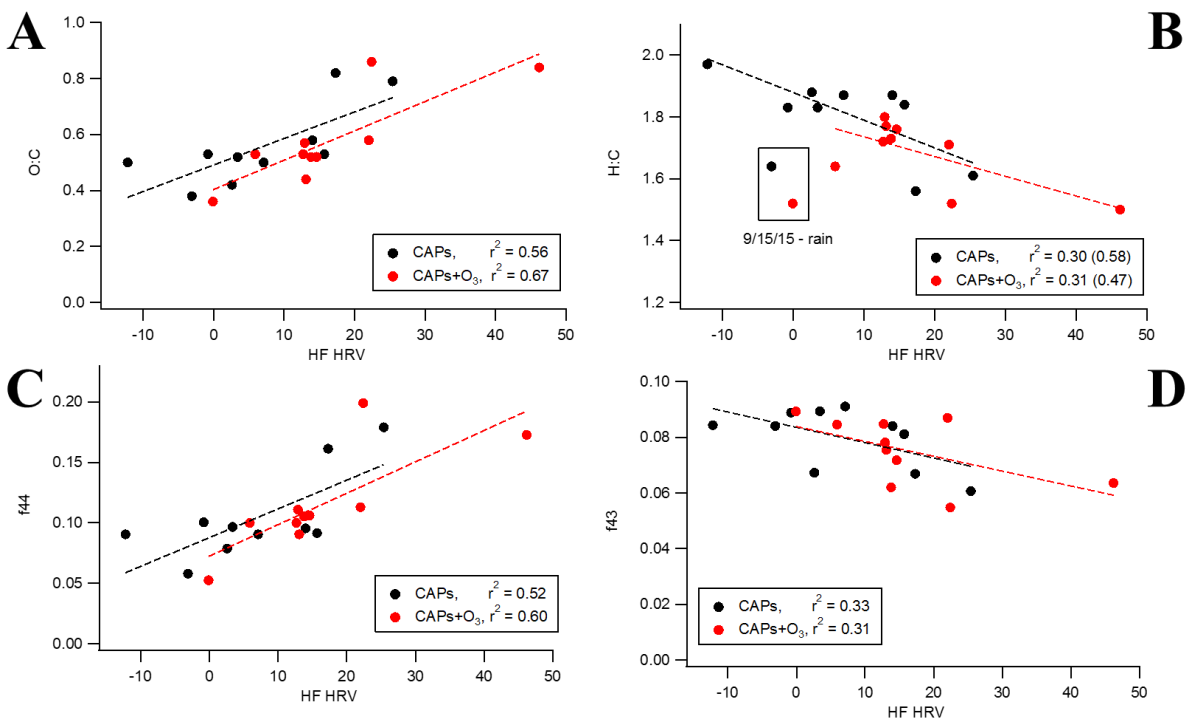

Figure 4.12. Correlations of organic species with HRV. A) Oxygen content correlates well with changes in HF HRV. B) H:C was also associated to changes in HF HRV, except for one rainy day C) Decreased concentrations of organic acids, represented by the peak at mass 44 in the mass spectrum (f44), are associated with worsened HRV. D) Increased concentrations of aldehydes may be associated with worsened HRV.

4.2.1.9 SUMMARY OF MEASURED RESPONSES

A summary of all measured parameters is presented in Table 4.7. Exposure to whole PM elicited more pronounced alterations in cardiovascular parameters compared to exposure to DeCAPs. Adding O_3 to either particle atmospheres failed to exacerbate the effects seen with exposure to PM alone. The differential response resulting from O_3 during the two exposures is unexpected and the effect seen is largely due to responses during the last weeks of exposure. Additional investigation to identify potential causes is required.

Table 4.7. Complete summary of measured responses to inhaled PM and PM mixtures

	Whole PM			Denuded PM		
Endpoint	CAPs	CAPs + O_3	O_3	DeCAPs	DeCAPs + O_3	O_3
Heart Rate	NE	↓	↓	NE	NE	NE
R-R Interval	NE	↑	↑	NE	NE	NE
P-R Interval	↓	NE	NE	NE	NE	NE
QRS Interval	↓	NE	NE	NE	NE	NE
QTcM Interval	NE	NE	NE	NE	↓	↓
T-wave Area	↑	NE	NE	NE	NE	NE
T-wave Amplitude	↑	NE	↑	NE	NE	NE
SDNN	NE	NE	NE	NE	NE	NE
RMSSD	NE	NE	↓	NE	NE	NE
HF	↓	NE	↓	NE	NE	NE
LF	NE	NE	NE	NE	NE	NE
Systolic BP	NE	NE	NE	NE	NE	NE
Diastolic BP	NE	NE	NE	NE	NE	NE

NE = No Effect, ↑ = significant increase compared to air controls, ↓ = significant decrease compared to air controls.

4.2.2 Discussion

4.2.2.1 ECG WAVEFORM ANALYSIS

This results from the current study shows that 8-week exposure to different chemical constituents of $PM_{2.5}$ causes differential effects on the rate-dependent endpoints of the cardiac conduction cycle in mice, and that specific constituents lead to varied effects with concurrent ozone exposure (see Table 4.7 for a summary of measured responses). We show here that exposure to CAPs alone was enough to elicit decreases in the PR interval and QRS complex of animals compared to air controls (Figure 4.8E-H). Exposure to $PM_{2.5}$ alone resulted in progressively worsening PR intervals while exposure to O_3 alone resulted in increased RR intervals for the duration of the exposure period. Moreover, the PM + O_3 co-exposure does not consistently produce responses different from those seen in control animals. We have previously found that denuded particles have less mass than their intact counterpart [13]. Thus, these data suggest an effect of PM may possibly depend on size.

The QT interval is a marker of ventricular repolarization and increases in this interval are a risk factor for cardiac arrhythmias, infarctions, and ischemia. Exposures to whole CAPs failed to elicit any change in the rate-corrected QT interval (Figure 4.8I). However, we did measure a decreased QT interval in mice exposed to O_3 during the DeCAPs study(Figure 4.8J). Similar decreases in QT intervals were seen in the O_3 exposure group during the CAPs exposure period possibly indicating the ability of O_3 to inhibit repolarization of the ventricular cardiomyocytes during the cardiac conduction cycle. The ability of the DeCAPs atmosphere to initiate QT abnormalities in the presence of O_3 possibly indicates an interaction between the non-volatile toxicants, such as metals[13], that remained bound to the PM following the denuding process and the gaseous oxidizer. Circulating levels of copper and nickel has been linked with relative

ventricular wall thickness and levels of these metals associated with left ventricular hypertrophy [114].

These results differ from those observed from those described by Kurhanewicz and colleagues who noted increased P-wave endpoints and rate-corrected QT intervals in rats during and immediately after concurrent acute exposures to $PM_{2.5}$ and ozone [104]. Distinctions between the current exposure and those performed by Kurhanewicz which may lead to discrepancies in ECG outcomes include, but are not limited to, animal model, PM constituents, and exposure duration. Although we exposed animals to $PM_{2.5}$, most of the particles in Irvine, CA reside in the ultrafine fraction which is a result, in part, to incomplete motor vehicle combustion. Ultrafine black carbon PM, a component of this combustion, has the ability to translocate from the lungs into the blood where it has the potential to adversely affect the cardiovascular system [115,116]. Moreover, the animals exposed in this study were exposed to 200 ppb of O_3, only a fraction of the dose delivered during the Kurhanewicz exposures. Therefore, these exposures may be missing outcomes that require higher pollutant concentrations.

Despite the discrepancies in ECG outcomes between rodent studies, both in QT interval elongation and truncation have been identified in epidemiological studies [117-119]. It has been found that both sub-chronic and long-term exposure to $PM_{2.5}$ has been associated with increases in corrected QT interval in elderly men, especially in those with a high oxidative stress allelic profile [118]. It may be the case that although both PM and O_3 produce cardiac discrepancies, the mechanisms mediating the response may be different (i.e. airway sensory irritation and particle translocation).

We have also shown that concurrent exposure of $PM_{2.5}$ and O_3 elicit alterations in ventricular-associated waveforms that are dissimilar to those seen in the rate-associated ECG

analysis. Exposure to single-pollutant whole CAPs or O_3 atmospheres resulted in increased ventricular-specific endpoints (Figure 3.9) while a co-exposure alleviates the response, and in some instances, led to a response no different than controls. Mice co-exposed to DeCAPs + O_3 also show less of an effect than the single pollutant atmospheres on ST elevation and T-wave amplitude, however, the effects decrease to those seen with air controls as time post-exposure increases. Repolarization changes, specifically changes in the T wave can be indicative of ischemia [101]. Again, this may be an instance of both toxicants producing cardiac discrepancies due to different mechanisms. The differential effects of CAPs vs. DeCAPs exposure may be a result of the varying physical and chemical characteristics of the two particle types.

4.2.2.2 HEART RATE VARIABILITY

Exposure to CAPs particles for 8 weeks generally elicited decreased HRV measurements which were exacerbated by the addition of O_3 to the atmosphere. This decreased HRV in CAPs exposed mice is consistent with those reported previously by our laboratory [13], though to a lesser extent. Other groups have reported opposing effects on apoE-/- mice following prolonged exposure to CAPs [120]. These discrepancies may be due to inherent differences in PM characteristics from the different exposure sites. PM collected from southern California is primarily produced from incomplete combustion whereas PM collected from sites in the Northeast United States are more dependent on varied atmospheric processes and combustion heating sources. Specific indices of HRV, such as SDNN and RMSSD are critical measures of cardiovascular health. SDNN has been associated with overall autonomic tone while RMSSD is generally associated with vagal pathways. Therefore, the decreases seen in the CAPs and CAPs + O_3 atmospheres may indicate the ability of these toxicants to perturb normal autonomic nervous

system controls possibly leading to episodes of bradycardia and alterations in systemic blood pressure [121].

Conversely, the effect on HRV in DeCAPs-exposed mice moderately increased compared to air controls. Altered HF and LF HRV parameters have been found in apoE$^{-/-}$ mice exposed to urban Seattle PM [108]. Additionally, these perturbations in frequency-based measures of HRV have been linked through epidemiological studies to numerous cardiovascular diseases such as heart failure, hypertension, and acute myocardial infarction [110]. These opposing responses in mice exposed to DeCAPs particles (increased HRV) versus mice exposed to whole CAPs (decreased HRV) may indicate SVOCs differential effect the body depending on their volatility and/or particle-association. Furthermore, ozone's capacity to exacerbate the effects on HRV in PM atmospheres may indicate its ability to oxidize components specific to the CAPs or DeCAPs atmospheres. Together, these types of HRV changes demonstrate that prolonged exposure to increased levels of PM and O_3 can impair cardiac function and augment normal autonomic nervous system control.

4.2.2.3 AEROSOL CONSTITUENT ANALYSIS

Measurements of the O:C ratio for the different atmospheres showed that particle composition was affected by the addition of O_3 to CAPs as well as by the thermal denudation of CAPs (Figure 4.10a). The addition of O_3 to CAPs particles led to some oxidation of particles as indicated by the slight increase in O:C on most days, as well as a decrease in organic mass concentration in the particles relative to CAPs particles. This may be attributed to reactions of O_3 with organics in the particles that often lead to molecular fragmentation [122,123]. The formation of products with lower carbon number and higher volatility is expected to lead to a loss of mass concentration due to evaporation of these products and may cause very little change in O:C.

Additionally, as the exposures continued from summer to fall, there were increased losses of organic mass concentrations in CAPs + O_3 relative to CAPs (Figure 4.10d), suggesting there may be a seasonal aspect to changes in the chemical composition of organic PM constituents [124]. As shown in Figure 4.10a, the O:C was significantly increased by passing CAPs particles through a thermodenuder. DeCAPs particles were characterized by a significant loss of SVOCs, a large remaining fraction of organic acids, and often a decrease in inorganics as well relative to CAPs. Addition of O_3 to DeCAPs did not increase O:C ratios appreciably (Figure 4.10a) as the O:C was already fairly high for DeCAPs atmospheres. In summary, the particles in the CAPs + O_3 atmospheres have very different composition than those in the CAPs atmospheres. These different particle characteristics may be one reason that the co-exposures of PM and O_3 did not result in additive adverse outcomes, namely that the particles are not the same in the CAPs and CAPs + O_3 groups.

We have previously showed that removing the semi-volatile fraction from whole PM results in a significant decrease in the organic carbon and PAH content of the particles without altering the concentration of ions or trace metals (e.g., chloride, sulphate, and ammonium) [13]. PAHs are a ubiquitous environmental contaminant and can result from incomplete combustion of fossil fuels. The addition of O_3 to CAPs (with inherent PAH compounds) is capable of inducing PAH degradation and producing less potent daughter compounds. Concerningly, Ozone-UV treatment has been shown to destroy more than 90% of PAHs with no significant toxic products produced [125]. It is therefore possible that subsequently adding O_3 to CAPs atmospheres produced during periods of high ambient photochemical activity may ultimately result in PAH destruction. Since denuded CAPs are devoid of most PAH compounds, the addition of ozone to this

atmosphere may be indicative of biologic effects driven by single toxicant interactions within the body.

4.2.3 Limitations

This study has some potential limitations. As with the seasonal study, genetically modified apoE$^{-/-}$ mice were used in this study due to their susceptibility for arterial plaque development similar to that seen in diseased humans. Unfortunately, these mice are prone to increased levels of systemic oxidative stress and inflammation compared to their wild-type counterparts due to the apoE gene's involvement with anti-oxidant activity [113]. Additionally, these exposures occurred during different time periods due to space limitations in our exposure system. The CAPs study occurred during the late summer of 2015 while the DeCAPs study occurred during the spring of 2016 culminating in roughly a 6 °C difference in ambient temperature between studies. Though not ideal, we were able to show that ambient O_3 levels were comparable between the two time periods. Turning to the exposure setup, we chose to combine the $PM_{2.5}$ and O_3 atmospheres using small diameter tubing which limited the potential mixing time of the two toxicants. Going forward, it may be beneficial to incorporate an additional mixing chamber into the experimental setup which will potentially allow for increased secondary particle formation prior to inhalation. Furthermore, exposing animals to periods of $PM_{2.5}$ and O_3 consecutively vs. concurrently may help to identify the health effects related to gaseous vs. PM irritants. The ECG acquisition system used in these studies to acquire the waveform and HRV data had limited recording capabilities. Therefore, a subset of each exposure group was recorded daily over the course of the exposure period. Given a larger subset, we anticipate a more robust analysis capable of teasing out additional exposure-based differences.

Lastly, due to the relatively small group sizes used in this exposure, the study should be repeated, and the results validated.

4.2.4 Conclusion

This study found that 8-week co-exposure to PM and O_3 are not additive or synergistic and that different components of ambient air pollution, alone and in concert, affect different portions of murine cardiac conduction. Hyperlipidemic mice exposed to whole CAPs and O_3 exhibited increases in both atrial and ventricular related conduction rates as evident by alteration in the PR and QTcM intervals. The single-pollutant atmospheres also augmented the T-wave area in the exposed animals. In most cases, co-exposing animals to whole $PM_{2.5}$ and O_3 resulted in negligible changes compared to control animals. The effects seen with whole PM exposure were diminished in animals exposed to denuded $PM_{2.5}$. Adding O_3 to DeCAPs again failed to elicit effects different from those seen in controls. The 8-week exposures of PM with O_3 at 200 ppb were enough to induce physiological modifications, justifying the importance of more realistic long-term exposure studies. Further investigation into these observed cardiovascular changes must be performed to explicate the specific mechanisms related to chronic $PM_{2.5}$ inhalation and potential interactions with downstream targets.

4.3 Oxidative Potential of PM and PM + O_3 Mixtures

4.3.1 Results

4.3.1.1 ASSAY OPTIMIZATION

Initial tests were performed on NIST SRM and CAPs samples in order to establish the effective concentration range of the PM in the enzyme inhibition assays (Figure 4.13). The highest two concentrations of SRM (2.0 and 1.0 µg/µl) had no inhibitory effect on GPx activity

compared to the assay controls possibly due to the large concentration of PM interfering with the GSH reaction by altering the PH of the reaction cell. Since this response was seen in both GR and GPx assays, the large two PM doses appear to inhibit the reduction of GSSG to GSH by interfering with NADPH processing, which is a necessary step in both assays. However, the lower SRM concentration (0.1 µg/µl) exhibited a 65% reduction in GPx activity. Low (0.5 µg/µl) and intermediate (1.25 µg/µl) levels of CAPs resulted in similar GPx inhibition (84% and 86%, respectively) while high concentrations of the CAPs (2.25 µg/µl) exhibited optimal inhibition of GPx compared to assay controls (59%). Therefore, SRM at 0.1 µg/µl was the chosen concentration for positive controls and CAPs at 2.25 µg/µl was the concentration chosen for all sample types in both enzymatic assays.

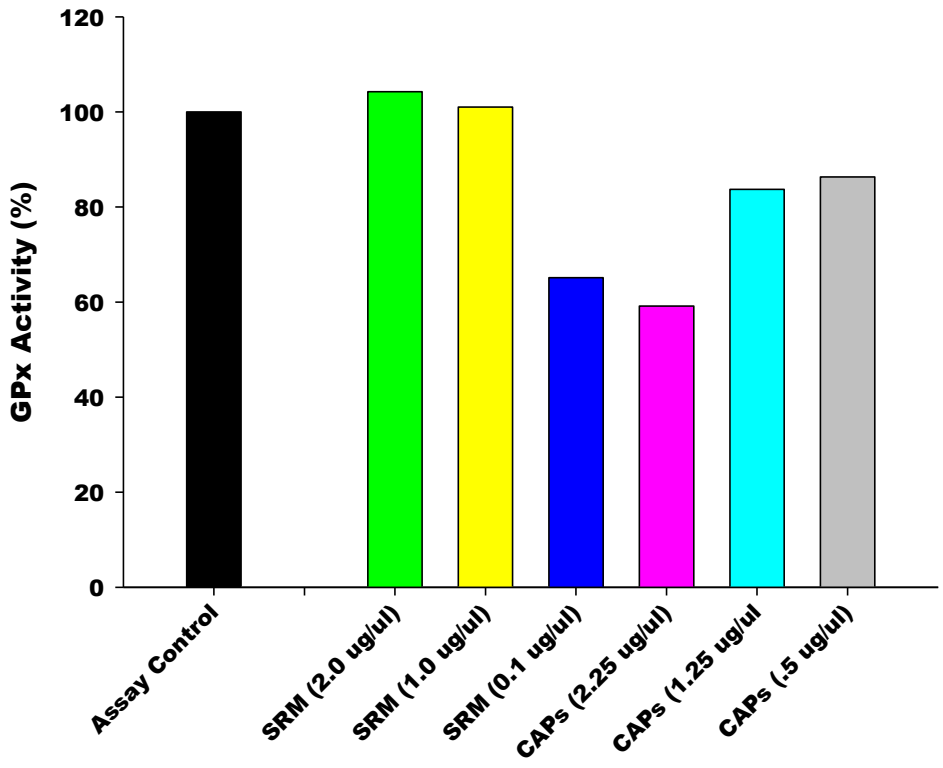

Figure 4.13. Results of range finding experiments between SRM 1648a and collected CAPs. Results (based on *n* = 2 wells per assay) presented as percentage of assay control.

4.3.1.2 ENZYMATIC RESPONSES RELATED TO OXIDATIVE STRESS

The effects of PM slurries on glutathione-specific enzymes are shown in Figure 4.14. As with the rage finding experiment (Figure 4.13), CAPs and SRM particle slurries generated similar GPx inhibition (58% and 59%, respectively; Figure 4.14A) indicating Irvine PM is less reactive than PM collected in more urban environments which potentially contain higher concentrations of metallic and organic constituents. Particles devoid of semi-volatile organic compounds (DeCAPs) were roughly 26% less inhibitory than both the CAPs and SRM materials. Particles mixed with O_3 (200 ppb) generated the largest inhibitory response in GPx activity; the CAPs + O_3 reduced the GPx activity by 47% relative to CAPs particles while a 58% reduction in GPx activity was identified in the DeCAPs + O_3 particles relative to the DeCAPs particles. Interestingly, the CAPs + O_3 and DeCAPs + O_3 particles decreased GPx activity to roughly the same percentage compared to assay controls (30% and 35%, respectively) possibly indicating an overall effect of O_3-derived particle oxidation.

Overall, glutathione reductase (GR; Figure 4.14B) appears to less sensitive to particle-induced inhibition as compared to glutathione peroxidase (GPx). Again, similar responses were seen with different concentrations of SRM and CAPs particles (79% and 81%, respectively) possibly indicating that indicating PM derived from Irvine is less reactive than PM collected in more traditional urban environments. All other responses measured in GR activity appear to be opposite of those seen in the GPx assay (Figure 4.14A). GR activity decreased approximately 35% in response to DeCAPs particles compared to the SRM and CAPs particles. CAPs + O_3 elicited a slight decrease in GR activity (12%) compared to CAPs alone while DeCAPs + O_3 decreased GR activity 33% compared to DeCAPs alone. Small but similar decreases in GR activity were measured in response to the ozonized PM compared to assay controls. Taken

together, these results indicate that equal concentrations of Irvine CAPs and traditional urban PM (NIST SRM 1648a) do not elicit a comparable oxidative stress response. However, different particle fractions/mixtures directly elicit distinct inhibitory effects on the measured antioxidant enzymes.

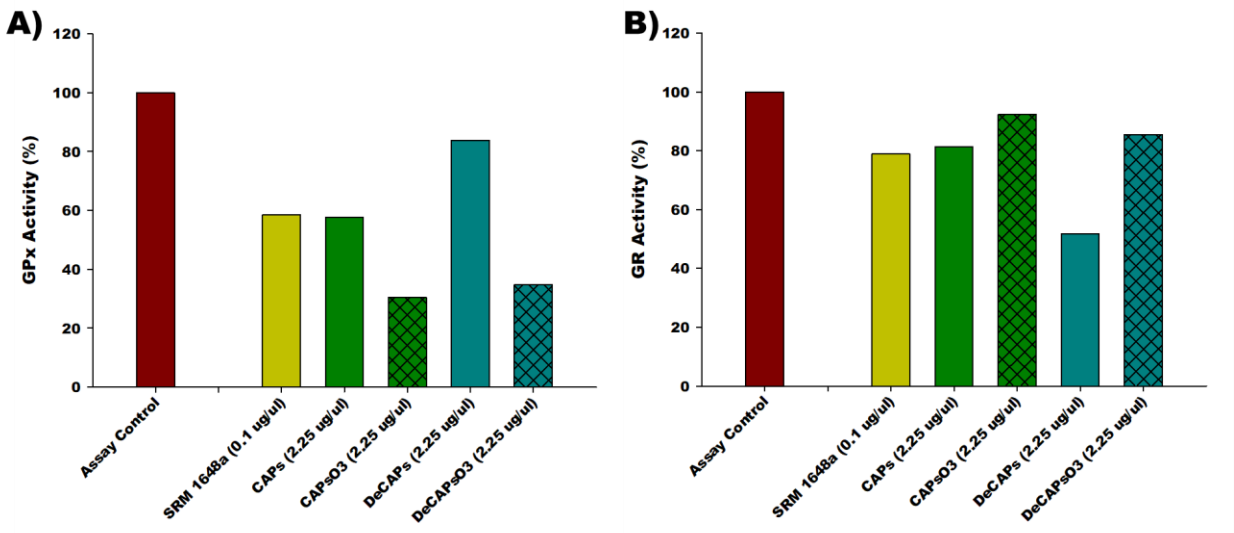

Figure 4.14. Antioxidant enzyme responses to particles with and without O_3 addition. Data represent enzyme response as a percentage of assay control. Results (based on n = 2 wells per assay) presented as percentage of assay control.

4.3.2 Discussion

The oxidative potential of inhaled PM has been traditionally based on effects in biological samples obtained by *in vivo* and *in vitro* methods. These cell-based assays are helpful, yet are hindered by numerous challenges involved with proper maintenance of biological systems and active components and multi-assay compatibility [126,127]. Using cell-free methods like enzymatic biosensors in conjunction with non-biological substrates, such as PM, offer a way to investigate the direct effects of environmental toxicants.

This study demonstrates that different particle fractions/mixtures interact directly with enzymes associated with the biological oxidative stress response. Moreover, we show that PM from Irvine, CA is less potent than traditional urban PM regarding antioxidant inhibition. A similar direct enzyme inhibition experiment performed by Hatzis et al. showed that 0.1 µg/µl of NIST SRM 1648a decreased the GPx and GR activity by 30% and 25%, respectively [54]. Ambient PM can also alter oxidative stress enzymes in biological systems. Human alveolar basal epithelial cells treated with a range of urban German PM_{10} (100 µg/ml – 1 µg/ml) altered the concentration of superoxide dismutase (SOD), catalase (CAT), and GPx relative to controls for up to 96 hours post-treatment [128], indicating the potential importance of metallic constituents found in the larger PM size fraction.

The bioavailability of specific metal ions is thought to be an essential factor leading to ROS generation. In addition to GSH-specific enzymes, the Hatzis study also determined that the SRM directly decreased the activity of copper/zinc (Cu/Zn)SOD and manganese (Mn)SOD [54], both of which participate in antioxidant defense via the dismutation of superoxide ions into molecular oxygen in the presence of specific metal substrates. The consumption rate of dithiothreitol (DTT) is also used as a measurement for PM-induced oxidative potential. Transition metals in urban $PM_{2.5}$, specifically Mn and Cu have been associated with large decreases in DTT levels [129] indicating the ability to PM to interact with SOD species thereby effecting superoxide regulation and oxidative stress responses. Data from our laboratory has shown that metals in a CAPs + O_3 atmosphere were slightly increased compared to the levels found in a comparable CAPs atmosphere [130], suggesting that O_3 can increase the bioavailability of water-soluble metals. Additionally, we have shown that thermally denuding the CAPs does not cause a large decrease in overall metal mass compared to intact particles [13].

In broader terms, PM samples alter the antioxidant enzymes GPx and GR which impact the GSH/GSSG redox cycle and overall oxidative stress. The large GPx inhibition coupled with the minimal GR inhibition seen in response to the O_3-reacted PM may indicate the ability of ozonized PM, and possibly the reactive metal components, to interact with the hydroperoxide in the system leading to an increased GSH concentration. Conversely, increased GR activity compared to the GPx activity seen in response to the DeCAPs PM may indicate a buildup of GSSG. Changes in the GPx:GR ratio in either direction have been found in response to multiple environmental stressors, including ambient PM [131-133], metals [134], and ozone [135,136]. Therefore, it is necessary to identify the oxidative potential of environmental contaminants, including PM, prior to inhalation.

4.3.4 Limitations

This study has potential limitations. Firstly, the data presented are generated from duplicate sample wells due to limited PM quantities. Therefore, appropriate statistical approaches (e.g., bootstrapping replicate absorbances with replacement) and complete assay controls (e.g., absorbance corrections for PM interactions) could not be applied. Furthermore, there may be a discrepancy between the true and presented concentration of PM used in the study due to questions surrounding the validity of the extracted PM weight. However, all weights were performed on the same scale under the same conditions, therefore equal error should be attributed to all samples. Regardless, this study demonstrated that different PM fractions/mixtures at equal concentrations elicited different oxidative stress responses. Lastly, alterations in enzymatic responses can only be attributed to general differences between PM types (e.g., with/without O_3 or SVOCs) reiterating the importance of in-depth PM analyses and metal-specific enzymes when conducting studies aimed to detect the direct effects of PM. Further investigation into the sensitivity, specificity, and reproducibility of the tests performed are needed.

4.3.4 Conclusion

This study demonstrates that different fractions or mixtures of PM are capable of directly inhibiting enzymes involved in oxidative stress. Additionally, Irvine PM appears to be less potent than urban SRM possibly due to differences in specific metal concentrations between the two particle types. Lastly, particle fractions mixed with O_3 equally diminished glutathione peroxidase activity possibly indicating increased availability of PM-bound metal constituents. Information about particle oxidative stress would be a relevant addition to current air quality legislation which currently relies on toxicity assessment using particle size as the sole determinant. Optimization of assays aimed to detect direct inhibitory effects of ambient PM at low concentrations is a current research goal.

CHAPTER 5: SUMMARY AND FUTURE DIRECTIONS

5.1 SUMMARY OF KEY FINDINGS

5.1.1 Do PM exposures during periods of high photochemical activity produce different cardiac responses compared to PM exposures during periods of low photochemical activity?

These findings indicate that particles formed during periods of high photochemical activity (PCA) (e.g. spring/summer) elicit more adverse cardiac conduction anomalies than particles formed during periods of low PCA (e.g. fall/winter) possibly due to the observed differences in PM characteristics. Both rate- and ventricular-related ECG anomalies were exacerbated during periods with high ambient O_3 levels suggesting that increased atmospheric interaction with O_3 and other atmospheric pollutants generates more biologically active PM. Furthermore, chemical differences with respect to the organic constituents in ambient particles between summer and fall aerosol were seen and were consistent with seasonal trends in atmospheric solar radiation. Therefore, photochemical activity may be a good surrogate for ambient levels of PM-bound organic species. Importantly, these results are likely to be location specific as southern California PM is formed in a region where combustion heating is minimal and variations in seasonal temperatures are less extreme than those observed in the eastern United States.

5.1.2 Do co-exposures to PM and O_3 augment the effects of exposure to PM alone AND does removing PM-bound organic compounds alter any potential interactive health effects?

These results show that exposure to intact PM is more cardiotoxic than exposure to PM with the SVOCs removed. 8-week exposure to CAPs alone was enough to elicit changes in multiple ECG waveform indices compared to purified air controls while only the QTcM interval was altered in response to DeCAPs exposure. However, animals co-exposed to either PM + O_3 atmosphere mostly failed to produce responses significantly different than those seen in purified air controls. The lack of response measured in co-exposed animals may be due to competing modes of autonomic nervous system (ANS) imbalance; O_3 is known to cause a shift of autonomic balance towards parasympathetic activity [137] while the PM exposure has been shown to alter the HF component of HRV indicating parasympathetic inhibition [92]. Measurements of the O:C ratio for the different atmospheres showed that particle composition was affected by the addition of O_3 to CAPs as well as by the thermal denudation of CAPs and may be one reason that the co-exposures of PM and O_3 did not result in additive or synergistic adverse outcomes.

Physiologic responses to PM + O_3 mixtures do not resemble those measured following exposures to PM formed during under different periods of PCA. This may be due to the interaction of PM with other environmental pollutants such as nitrogen oxides (NOx) and sulphates (SO_4^{2-}). These pollutants can produce secondary organic aerosols (species produced through oxidation of the parent NOx and SO_4^{2-} compounds) which condenses onto ambient PM creating more biologically active species [138-140]. Additionally, it is possible that subsequently adding O_3 to PM formed under periods of high photochemical activity reduced the ultimate toxicity of the PM [125].

*5.1.3. Do particles that contain semi-volatile organic compounds negatively affect oxidative stress enzymes more than thermally denuded particles **AND** does O_3 exacerbate the potential effects of PM on oxidative stress enzymes?*

Evidence indicates that inhaled PM can promote oxidative tissue damage, both locally and systemically [34,52-57,141-143]. Methods to directly measure the oxidative potential of PM have been developed such as the dithiothreitol (DTT) assay [144-146], the peroxide/ dichlorofluorescein (DFCH) reaction [147], and an electron spin resonance method designed to precisely measure the ROS-generating capacity of particle samples [148]. The results of this study demonstrate that different fractions and/or mixtures of PM are capable of directly inhibiting enzymes involved in oxidative stress. Particles that contain SVOCs elicited dissimilar inhibitory responses in glutathione peroxidase (GPx) and glutathione reductase (GR) suggesting that oxidative stress could be altered via GSH accumulation. The PM + O_3 mixtures exacerbated inhibition of GPx compared to PM alone. Moreover, the level enzymatic impairment was similar in response to the presence of PM + O_3 mixtures regardless of PM-bound SVOCs suggesting that O_3 is reacting with more stable PM-bound constituents.

The use of microplate assays such as those utilized in this study to examine oxidative stress are effective when the quantity of PM samples is limited. Furthermore, these assays can be performed on both biological and non-biological samples and therefore could provide a method for consistently measuring the oxidative potential of both PM and biological tissues following PM exposure. Although these results corroborate findings reported by other groups [54], further investigation into the sensitivity, specificity, and reproducibility of the tests performed are needed.

5.2 KEY LIMITATIONS

The key limitations for the studies presented are discussed below…

- ApoE$^{-/-}$ mice were chosen for this study because they are prone to developing arterial disease similar to that seen in humans. However, these mice are also susceptible to higher levels of systemic oxidative stress and inflammation compared to wild-type mice due to the apoE gene's involvement with anti-oxidative activity [113].
    - It would be beneficial to include a wild-type group when performing these types of studies so that strain-based oxidative stress levels could be established and accounted for when analyzing data.

- The periods/seasons during which these exposures took place occurred were not ideal.
    - Existing datasets were pooled to perform the seasonal analysis (Chapter 4.1) and thus the high PCA exposure occurred during summer/spring while the low PCA exposure occurred during fall/winter.
    - The CAPs/DeCAPs exposure occurred in two consecutive years due to exposure system limitations (Chapter 4.2). Therefore, differences between the two atmospheres may result from differences in PM prior to thermal denudation.

- The ECG and HRV reported in this study are based on relatively small group sizes (n = 3-5). These exposures should be repeated, and the results validated prior to incorporation into any regulatory guidelines.

- The results of the oxidative stress study (Chapter 4.3) are preliminary and based on duplicate sample wells due to limited PM quantities.
    - Appropriate statistical approaches (e.g., bootstrapping replicate absorbances with replacement) and complete assay controls (e.g., absorbance corrections for PM interactions) could not be applied to the analysis
    - Alterations in enzymatic responses can only be attributed to general differences between PM types (e.g., with/without O_3 or SVOCs) emphasizing the importance of in-depth PM analyses and metal-specific enzymes when performing studies on direct effects of PM.

5.3 OVERALL SIGNIFICANCE

This report describes how the inhalation of ambient PM generated during different levels of atmospheric photochemical activity differentially alters cardiovascular health. Furthermore, these studies provide insight into particle characterization and cardiac dysfunction in relation to specific PM fractions and/or PM + O_3 mixtures. Several studies have identified cardiac anomalies resulting from acute exposures to high concentrations of ambient pollutants. The work presented here utilized an 8-week *in vivo* exposure model using environmentally relevant pollutant levels which may more accurately represent PM-attributed toxicity. Additionally, these studies accurately present seven measurements derived from the ECG waveform, where most studies identify two or three.

Once inhaled, PM is thought to generate reactive oxygen species (ROS) which promote inflammatory responses leading systemic and local oxidative stress. The GSH:GSSG ratio has been used a general indicator for oxidative stress and changes of said ratio in either direction have been measured in response to multiple environmental stressors, including ambient PM [131-133], metals [134], and ozone [135,136]. Therefore, it is necessary to identify the oxidative potential of environmental contaminants, including PM, prior to inhalation. Regional and seasonal differences in $PM_{2.5}$ composition should be considered when evaluating the effects of PM exposure on cardiovascular health. Information about particle oxidative stress would be a valuable addition to current air quality analyses that rely on toxicity assessments surrounding particle size.

5.4 FUTURE DIRECTIONS

The underlying theme to this report is that different particle fractions/mixtures elicit varied responses on the cardiac conduction system which may be in response to increased generation of reactive oxygen species leading to downstream oxidative stress. The ROS hypothesis has been supported *in vitro* using cultured cardiomyocytes and lung cells [63,149-151]. There have also been *in vivo* studies linking PM exposure to augmented antioxidant enzyme function [34,47,152]. Therefore, determining the activity of general antioxidant enzymes such as GPx and GR as well as metal specific antioxidants like Cu/ZnSOD and MnSOD in the heart following chronic PM exposure would help to elucidate levels of cardiac oxidative stress. Furthermore, identifying the concentration of reduced and oxidized glutathione in the tissues of subjects exposed to PM will help explain how the glutathione-specific antioxidant enzymes are malfunctioning.

The generation of ROS in tissues has been attributed to PM-bound metals [30,134]. An inductively couple plasma mass spectrometer (ICP-MS) can be used to quantify elemental species in ambient particulate matter [13,153,154]. Going forward, determining the metal content of PM samples used during inhalation studies will help to correlate specific metals with adverse cardiac responses. Additionally, it would be useful to determine the concentration of metals in tissues of exposed animals thereby providing information about metal deposition in the lungs and about which metals may preferentially translocate to extrapulmonary organs.

Understanding how PM-associated metals cause permanent damage to the cardiac conduction system would be helpful to our knowledge of PM exposure affects the heart. This could be examined using isolated heart techniques coupled with Langendorff or working heart perfusion methods. The hearts of mice chronically exposed to concentrated ambient PM can be

assessed for alterations in electrophysiological and mechanical parameters. Metal chelators, such as ethylene diamine tetra-acetic acid (ETDA), can be used to determine the impact of metals on adverse cardiac function. An attenuation of cardiac function suggests that the PM-induced cardiac dysfunction is repairable and provides additional research avenues with therapeutic implications.

This report presented limited data on the direct inhibition of oxidative stress enzymes in response to local ambient PM. It would be worthwhile to repeat these experiments with sufficient replicates and characterize the antioxidant response in greater detail (i.e. presenting the results in terms of residual activity which takes into account multiple inter-assay controls). Additionally, it would be useful to compare the oxidative potential of different PM fraction/mixtures using different cell-free assays to identify whether there are consistent outcomes between techniques.

Lastly, the exposures presented in Chapter 4.2 of this report describe the effect of intact and thermally denuded ambient PM. However, there are still questions surrounding the possible health effects attributed to the SVOCs that were removed during the denuding process. Data aiming to provide answers to this question have been collected and are currently under analysis. Additional information about the direct oxidative potential of SVOCs would be an appropriate extension of this research. We believe that the electron spin resonance (EPR) technique currently used to detect the ROS-generating capacity of PM on filters can be modified to detect SVOCs trapped in a liquid media. If successful, this method could be used to help correlate any observed cardiovascular impairments with the direct oxidative potential of PM-derived SVOCs. Moreover, information about the oxidative potential of environmentally relevant SVOCs could provide regulatory agencies with useful information that can be considered when devising air quality legislation.

SUPPLEMENTAL: CRITICAL REVIEW OF CARDIOVASCULAR HEALTH EFFECTS RELATED TO AMBIENT PARTICULATE MATTER INHALATION

S.1 INTRODUCTION TO AMBIENT AIR POLLUTION

The correlation between adverse health effects and air pollution exposure has been known for almost a century. In 1930, several thousand residents of the Meuse Valley in Belgium were stricken with severe pulmonary symptoms when sulfur dioxide from local factory emissions combined with a bolus of dense fog; as many as 60 people reportedly died as a result of this exposure [155]. Twenty years later, hydrogen sulfide-laden factory emissions again combined with dense atmospheric fog and combustion particulates engulfed the city of London, England. This epidemic resulted in over 3000 excess deaths over 3 weeks and increasing to 12,000 pre-mature deaths by the following February, 1953 [156]. A tremendous amount of life was lost resulting from these two acute exposures reinforcing the correlative association between air pollution and health. However, mechanistic relationships between specific components of air pollution and health effects are still poorly understood. One such component, ambient particulate matter (PM), is associated with increased cardiovascular morbidity and mortality with greater risk to those residing in urban environments [27,157-161] and in individuals with immune deficiencies and preexisting cardiopulmonary conditions [162,163].

A lack of understanding behind cause/effects relationships between specific PM components and observed health effects still exists despite the wealth of epidemiological evidence linking PM inhalation to cardiovascular diseases. This is, in part, due to the heterogenous nature of ambient PM which may substantially vary in size and composition based on seasonal processes and particle sources. Therefore, the toxicological responses to similar

concentrations of chemically distinct particles could be vastly different and should be considered when drafting air quality and health effects legislation.

S.2 SIZE AND COMPOSITION OF PARTICULATE MATTER

Ambient PM is mixture of minute solid particles and liquid droplets adsorbed onto a central core. This core is composed of refractory material, usually elemental carbon while the surrounding pollutant layers are composed of redox-active metals, organic carbon compounds, secondary sulfates and nitrates, and toxic hydrocarbons. PM is traditionally subdivided according to its aerodynamic equivalent diameter (AED) into three categories depending on sources and ultimate airway deposition. The largest of these categories, PM_{10}, includes particles with a diameter less than 10 μm while particles with diameter less than 2.5 μm are designated $PM_{2.5}$. Ultrafine particulate matter ($PM_{0.1}$; < 0.1 μm) is included within the $PM_{2.5}$ mass range and is composed of vehicular emission and other products of incomplete fuel combustion; a substantial portion of $PM_{2.5}$ is found under D_p < 30 nm [164-166]. The greatest number of particles are included within the smallest PM size fraction, $PM_{0.1}$, although these particles do not account for large portions of total PM mass. However, these small particles pose additionally health risks compared to the larger PM fractions due to its ability to deeply penetrate the lung and possibly translocate into the vasculature and where it can directly and indirectly effect extra-pulmonary organs such as the heart or induce systemic effects as inflammatory mediators [142,167,168].

The potential toxicity of ambient PM is thought to be a function of its physical and chemical properties. Particle movement in the atmosphere and within the human respiratory system depends largely on air flow and particle size. Particles contained within the PM_{10} size fraction exhibit a relatively short suspension time and a large degree of filtration by the nose and upper airways [169-173]. Inhaled $PM_{2.5}$ primarily deposits in head and bronchial region of the

respiratory tract with some deposition to the deep lung where the particles can potentially interfere with alveolar gas exchange [169-173]. Current national ambient air quality standards set by the U.S. Environmental Protection Agency (EPA) consider mass concentrations of $PM_{2.5}$ and PM_{10} size fractions but do not consider composition differences. Particles in the $PM_{2.5}$ size fraction have a large degree of chemical heterogeneity which has some dependence on PM source [48]. For instance, $PM_{2.5}$ particles formed near industrial processes may have higher concentrations of metallic components while particles formed near highly trafficked roadways are mainly the result of incomplete combustion processes [48,49].

Particles produced and emitted directly from combustion sources including light- and heavy-duty vehicles, off-road vehicles, wood smoke, refinery processes, and power generation are referred to as primary source particles. In urban environments, like in southern California, these primary particles are mainly products of incomplete fuel combustion from motor vehicles, however there are contributions from marine, industrial, and natural sources [174,175]. Numerous atmospheric processes act on the aerosolized PM which alter its physical and chemical properties including nucleation, condensation, dilution, and oxidation. In the case of mobile sources, emitted particles are dispersed and diluted into the atmospheric background in two phases. The first phase, known as "tailpipe-to-road" dilutions, results from the highly turbulent air patterns generated by moving vehicles while the second phase, "atmospheric turbulence-induced" dilutions, is caused by atmospheric instabilities such as wind events. During these dilution events, exhaust particles and vapor are rapidly cooled and new, sometimes more reactive, particles are formed through nucleation of low-volatility compounds or through the condensation of new particle compounds onto pre-existing particle substrates [176].

The main components of Southern California $PM_{2.5}$ include nitrates, organic carbon and sulfates with elemental carbon, metallic species, ammonium, and other elements present in smaller quantities [174,177]. Recent studies have determined that secondary PM (particles formed through the reaction of primary PM with pollutants such as nitrogen oxides and sulphates) accounts for most of the $PM_{2.5}$ in the region, highlighting the importance of atmospheric processes in particle formation [174,178]. For instance, photochemical episodes tend to drastically alter the size distribution of ambient PM by increasing particles under 30 μm due to secondary organic aerosol (SOA) generation [179]. This phenomenon also contributes to alterations in seasonal and diurnal variations in PM concentrations.

Polycyclic aromatic hydrocarbons (PAHs), a class of semi-volatile organic compounds (SVOCs), are generated by incomplete combustion sources and are shown to be as systemic toxicants following inhalation [180]. The particle-bound PAHs are thought to be more toxic compared to their vapor-phase counterparts [180] with examples like indeno[1,2,3-cd]pyrene and benzo[a]pyrene respectively considered possible and probable carcinogens by the International Agency for Research on Cancer (IARC). Due to the predominance of anthropogenic sources, these particle-phase PAHs are present in higher concentrations in urban Southern California compared to the rural California background levels [181].

Transition metals adsorbed to PM may contribute to particle toxicity and have been implicated in several cardiopulmonary studies as a main toxicant in ambient PM air pollution [143,182-187]. The soluble fraction of PM which contains zinc salts has been shown to inhibit adenosine triphosphate (ATP)-dependent calcium (Ca^{2+}) influx [143,188]. Excess zinc concentrations in isolated cells has been shown to effect Ca^{2+}, sodium, and potassium channel regulation [189-191]. PM exposure has also been shown to increase plasma zinc levels and can interact with other

essential metals in the heart [187,192]. Transition metals that exist in two or more valence states, like copper (Cu), cadmium (Cd), and iron (Fe), can generate hydroxyl radicals through the Harbor Weiss/Fenton reaction which leads to enhanced reactive oxygen species (ROS) production and inflammation. Gurgueira et al. (2002) found Sprague-Dawley rats exposed to concentrated ambient PM experienced a significant degree of oxidative stress in the lungs and heart compared to air controls [47]. Of note, this study determined there were strong associations between the oxidative load and the CAPs content of Fe, Mn, Cu, and Zn in the lung, and with aluminum (Al), Fe, silicon (Si), and titanium (Ti) in the heart [47]. Cd, another metallic component of PM, can increase intracellular calcium concentrations through the cell-surface G protein-coupled "metal binding receptor" which in turn activates phosphatidylinositol to produce phospholipase C and 1,4,5-inositol triphosphate (IP_3) subsequently triggering Ca^{2+} release from IP_3-sensitive internal stores [193,194]. Therefore, it is possible that certain cardiac effects of PM inhalation may be due to acute elevations in circulating metal concentrations leading to adverse cardiac mitochondrial effects [192]. Taken together, these data suggest that the metallic components of PM can influence oxidative stress and inflammation, ion channel dysfunction, and interfere with normal cellular functions.

S.3 CARDIAC CONDUCTION CYCLE

S.3.1 Cardiac Ion Currents and Action Potentials

The establishment and maintenance of the membrane potential in cardiac myocytes is necessary for proper conduction of the action potential (AP). The voltage difference between the intracellular and extracellular compartments of the myocyte is referred to as the membrane potential (E_m) and it changes as cells are stimulated during the cardiac conduction cycle. One factor determining the overall E_m is the ion gradient concentration, or the concentration difference between ions located inside or outside the cells. Under normal physiologic conditions, the concentration gradient across the membrane results in ion movement from areas of high concentration to areas of low concentration until equilibrium is reached. The other requirement for membrane potential regulation is selective ion channels integrated within the cellular membrane. Erroneous activation of these channels can cause an imbalance of ion movement across the membrane leading to a charge difference between the intracellular and extracellular compartment thus establishing an electrical gradient that balances that of the chemical gradient. The Nernst equation was published by the German physical chemist Walther Nernst in 1888 [195] and calculates the established membrane potential of an ion based on the concentration gradient and valence state of said ion. The generalized form of the Nernst equation is presented below (Equation S.1) and yields the equilibrium membrane voltage of the cell when *only* a single ion contributes to the generated E_m. However, the E_m in cardiac cells are often governed by multiple ion gradients simultaneously. Under these conditions, the Goldman-Hodgkin-Katz (GHK) equation (Equation S.2) more accurately reflects the final equilibrium membrane voltage [196,197].

Equation S.2: Generalized Nernst equation…

$$V_{eq} = \frac{RT}{zF} ln \frac{[X\}_o}{[X\}_i}$$

where,

V_{eq} is the equilibrium potential of a given ion (X)
R is the universal gas constant in (Joules per Kelvin per mole)
T is the temperature (in K)
z is the valence for the ionic species (X)
F is Faraday's constant (in Coulombs per mole)
$[X]_o$ is the concentration of ion X in the extracellular fluid
$[X]_i$ is the concentration of ion X in the intracellular fluid

Equation S.3: Generalized Goldman-Hodgkin-Katz (GHK) equation…

$$V_{eq} = \frac{RT}{F} \ln \left(\frac{p_X [X\}_o}{p_X [X\}_i} + \frac{p_Y [Y\}_o}{p_Y [Y\}_i} + \frac{p_Z [Z\}_o}{p [Z\}_i} \right)$$

where,

V_{eq} is the equilibrium potential of a given ion (X)
R is the universal gas constant in (Joules per Kelvin per mole)
T is the temperature (in K)
F is Faraday's constant (in Coulombs/mole)
p_x is the membrane permeability of ion X
p_y is the membrane permeability of ion Y relative to ion x
p_z is the membrane permeability of ion Z relative to ion x
$[X]_o$ is the concentration of ion X in the extracellular fluid
[X]i is the concentration of ion X in the intracellular fluid
$[Y]_o$ is the concentration of ion Y in the extracellular fluid
$[Y]_i$ is the concentration of ion Y in the intracellular fluid
$[Z]_o$ is the concentration of ion Z in the extracellular fluid
$[Z]_i$ is the concentration of ion Z in the intracellular fluid

The image below depicts the ion currents, action potentials, and electrocardiogram (ECG) waveforms of both human and mouse during pacemaker, atrial, and ventricular cardiac conduction cycles. The contents of this image and other portions of the cardiac conduction system are discussed in detail throughout the following chapter.

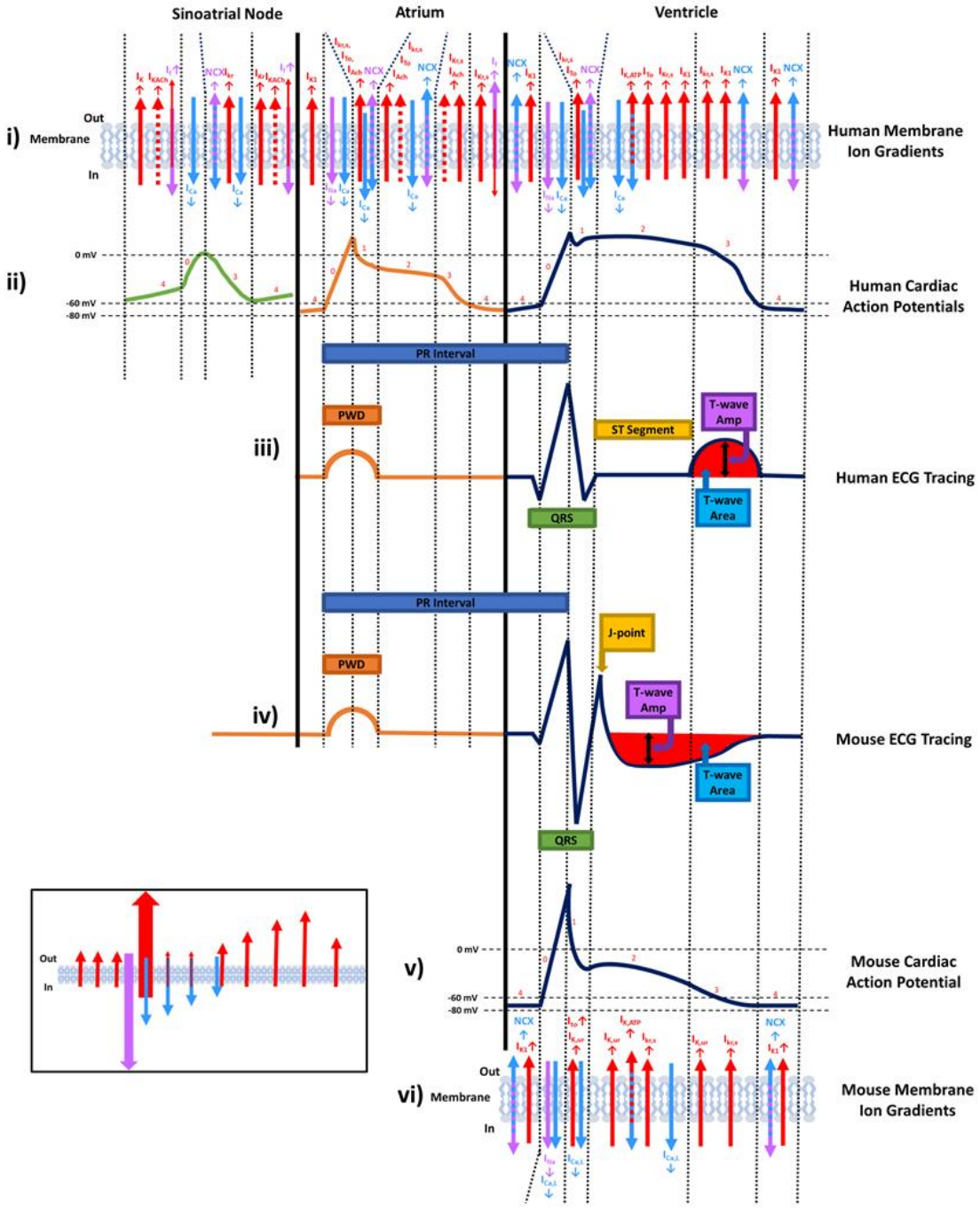

Figure S.20: The relationship between human and mouse cardiac ion channel gradients, action potentials and ECG recordings. See full figure legend on the following page.

Figure S.1: The relationship between human and mouse cardiac ion channel gradients, action potentials and ECG recordings.

Part i) depicts the ion channels and directional currents of human cardiomyocytes during activation of the sinoatrial node, the atrial compartments, and the Purkinje fibers of the ventricles while Part ii) shows the resulting action potentials in the three area of the heart during a typical cardiac conduction cycle which can be visualized using ECG techniques which produces the tracing in Part iii) of the image. Part iv) represents a typical mouse ECG waveform. The mouse ventricular action potential is depicted in Part v) with the corresponding membrane ion channels and gradients illustrated in Part vi. The inlay represents the amplitude and direction of ion channels in an idealized action potential. Solid vertical black lines separate regions of the heart. Dotted vertical black lines separate phases of the cardiac action potential and ECG waveform. For parts ii) and v), the phases of the action potential are in red font. For parts i) and vi) Ca^{2+} is in blue font, Na^{+} is in purple font, and K^{+} is in red font. NCX: Sodium Calcium Exchanger; I_{k1}: Inward Rectifier; I_{to}: Transient Outward, I_{Kr} and I_{Ks}: Delayed Rectifiers (rapid and slow); $I_{K,ATP}$: ATP-Inhibited Potassium Channels; $I_{K,ACh}$: Acetylcholine-activated Potassium Channels; $I_{Ca,L/T}$: L-type or T-type Calcium Channels; I_f: "Funny" pacemaker current; I_{Na}: Fast Sodium Channel; PWD: P wave duration; QRS: QRS interval duration; T-wave Amp: T-wave Amplitude.

S.3.1.1 THE SA NODE

The normal cardiac impulse originates in the sinoatrial node (SAN) and acts to generate a consistent heart beat necessary for adequate blood flow. Pacemaker automaticity results from spontaneous depolarization of the membrane which induces pulsing action potentials (AP). There are currently two predominant hypotheses for SAN function; the "voltage clock" theory which predominantly focuses on the activity of the "funny" current (I_f) and the "calcium clock" theory which takes into account Ca^{2+} release from the sarcoplasmic reticulum (SR) during the later stages of the pacemaker action potential [198,199].

In the "voltage clock" theory, I_f is activated during Phase 4 of the SAN action potential and, together with the outflow of potassium (K^+), provides an inward depolarizing current. The SAN does not express the inward rectifying current (I_{K1}) responsible for stabilizing the resting membrane voltage of atrial and ventricular myocardium [200]. Moreover, the rapid (I_{Kr}) and short (I_{Ks}) delayed rectifier currents that initiate the Phase 3 repolarization in the SAN diminish shortly after the start of the inward depolarizing current allows for the I_f and other inward currents to initiate another depolarization phase (Phase 0) [201,202]. In addition to the K^+ channels, the SAN also possess both L- and T-type calcium (Ca^{2+}; I_{CaL} and I_{CaT}, respectively) channels. The I_{CaL} current is primarily responsible for the upstroke of the SAN action potential while the I_{CaT} current is involved in the final depolarization stages (Phase 0) [200,203,204]. Lastly, the upstroke of the SAN action potential during this depolarization phase is slower than in working atrial and ventricular myocardium predominantly due to the lack of fast inward sodium (Na^+) currents and the dependence of the slow I_{CaL} channels [200,203,205].

Intracellular Ca^{2+} distribution is also thought to contribute to pacemaker automaticity in the SAN. It has been shown that the SR spontaneously releases Ca^{2+} during the later stages of the SAN action potential [206,207] which directly induces additional Ca^{2+} release from the cytosol by

the Na^+-Ca^{2+} exchanger (NCX) in a process known as calcium-induced calcium release. The opening of the NCX generates a net inward current by exchanging 3 Na^+ ions for 2 Ca^{2+} ions and ultimately contributes to the late depolarization stage of the SAN[208].

S.3.1.2 THE ATRIUM

Electrical depolarization of the atria is the first phase of the cardiac cycle and initiated by the influx of Na^+ ions from neighboring SAN cells. The increased Na^+ concentration in the atrial cells leads to a rapid AP upstroke (Phase 0) and results in the P wave of the electrocardiogram (ECG). Following the AP upstroke, a small influx of Ca^{2+} via I_{CaL} flows into the cell causing a large Ca^{2+}-induced Ca^{2+} release form the SR via Ryanodine receptors (RyRs) [202]. This increased cellular Ca^{2+} concentration initiates atrial muscular contraction due to the interaction of Ca^{2+} with myofilaments. Increases in Ca^{2+} begin during late ventricular diastole of the previous cardiac cycle when the pressure within the atrial compartments increases over that of the ventricular compartments thereby allowing the atrioventricular valves to open [202].

Relaxation of the atrial cells occur when Ca^{2+} concentrations decrease in the cell by exiting through the membrane-bound NCX and the Ca^{2+}-ATPase or being re-absorbed into the SR through the SR Ca^{2+}-ATPase (SERCA). This Ca^{2+} decrease is coupled with large fluxes in K^+ currents that are predominantly involved with atrial membrane repolarization [202]. The transient outward K^+ current (I_{to}) produces the initial, rapid repolarization (Phase 1) immediately following the AP upstroke while the AP plateau (Phase 2) and subsequent repolarization (Phase 3) is maintained by the ultra-rapid delayed-rectifier currents (I_{Kur}), together with the I_{Ks} and I_{Kr} and the Na^+-K^+ ATPase (I_{NKA}) currents [209]. Once the atrial myocardium has fully repolarized, the resting membrane potential (RMP, Phase 4 of the AP) is upheld by the inward rectifier current

(I_{K1}) and the G-protein gated K^+ channel ($I_{K,ACh}$) which mainly operate at negative membrane potentials [202,209].

S.3.1.3 ATRIOVENTRICULAR NODE

The atrioventricular node (AVN) is located in the triangle of Koch at the base of the atrial septum [210] and is involved in several crucial processes. Primarily, the AVN provides a pause in conduction between the atrial and ventricular compartments of the heart providing adequate time for the atria to complete the current conduction cycle prior to the initiation of ventricular systole. Due to its relatively long refractory period, the AVN acts as a buffer between the atria and the ventricles from atrial arrhythmias by blocking high frequency atrial APs. In extreme cases, the AVN can act as a back-up pacemaker if there are complications with normal SAN function due similarities between the SAN and AVN action potential; both exhibit a large I_f current and decreased expression of the I_{K1} and I_{Na} currents [200,211-215]. It has been found that AVN removal in excised rabbit hearts results in an almost doubling of cardiac cycle length [216] underscoring the importance of normal AVN function.

Differences exist in ion expression between the AVN and the SAN. The AVN produces a pronounced increase in the transient outward K^+ (I_{To}) currents relative to the working atrial myocardium while slightly downregulating the I_{Kur} and I_{Kr} currents which is opposite of that found in the SAN which exhibits a marked decrease in the I_{to}, I_{Kur}, and I_{Kr} [200,212]. Additionally, differences in Ca^{2+} handling between the two nodal regions exists with the SAN displaying a large down-regulation of the SERCA and RyRs receptors compared to the atrial myocardium while the AVN only shows a modest decrease in these receptors [212].

S.3.1.4 HIS-PURKINJE SYSTEM

Following the delay at the AVN, the electrical impulse moves to the bundle of His. The His bundle is isolated from the AVN within connective tissue and located in the bottom of the left atrium. Under normal conditions, conduction through the AVN is the only pathway connecting the electrical activity of the atria to the ventricles. Therefore, His bundle dysfunctions can lead to multiple degrees of heart block ranging from conduction delays between the upper and lower chambers of the heart (first-degree blockages) to a complete disassociation between these two cardiac regions (third degree blockages) [217]. Right and Left bundle branches form at the distal end of the bundle of His and extend through the cardiac septum towards the apex of the heart. The cells of the bundle branches are insulated by connective tissue sheaths allowing for fast, uninterrupted AP conduction to the apex of the ventricles without activating ventricular myocardium along the way [218]. The bundles innervate the ventricular myocardium at specific sites through networks of Purkinje cells where subsequent excitation occurs.

A key characteristic of the His-Purkinje system is fast conductance relative to other ventricular myocardia. This is due in part to an abundance of the large and intermediate gap junctions (Cx40 and Cx43, respectively) [215,219,220]. Additionally, the AP of Purkinje fibers have a quicker upstroke velocity and longer duration compared to the working ventricular AP which contribute to the fast conduction rate [221,222]. The Purkinje fibers also exhibit pacemaker capabilities and can pace the ventricles in cases of AV block. However, this pacemaker function is suppressed under normal sinus rhythm due to extrinsic excitation at frequencies above their intrinsic rate [202]. In humans, the Purkinje system exists primarily in the subendocardial space and accounts for roughly 1-2% of the total ventricular mass [223,224].

S.3.1.5 VENTRICLES

Blood moves from the atria to the ventricles while the ventricular myocardium is at rest and the pressure within the ventricular compartments is below the pressure inside the atrial compartments. Once the AP propagates down through the His-Purkinje system, it flows into the ventricular myocardium where depolarization can be visualized via ECG as the QRS complex. Ventricular depolarization is coupled with myocardial cytosolic Ca^{2+} increases which initiate ventricular muscle contraction (systole) and cause the pressure within the ventricular compartment to rise and the atrioventricular valves to close. When ventricular pressure exceeds that of the atrial pressure, the aortic and pulmonary valves open and blood is ejected to the systemic and pulmonary systems [225]. Repolarization of the ventricular myocardium, viewed as the T-wave on the ECG, is necessary for Ca^{2+} removal and myocyte relaxation (diastole). Once the pressure within the ventricular compartment has dropped below that of the atrial compartment, blood begins to passively fill the ventricles and the cycle repeats.

The AP of the ventricles is similar to that seen in the atria. The rapid upstroke seen in ventricular depolarization is generated by the fast activation of Na^+ channels and results in a large inward Na^+ current (I_{Na}). However, the velocity of the upstroke and duration of the resulting plateau phase (Phase 2) compared to the atrial AP are larger and longer, respectively [226,227]. A small repolarization (Phase 1) immediately following ventricular depolarization (Phase 0) results from the simultaneous inactivation of the I_{Na} current and activation of the transient outward K^+ currents (I_{to}) [228,229]. At this same time, L-type calcium channels begin to open resulting in a slow influx of Ca^{2+} ($I_{Ca,L}$) into the cells which leads to further increases in cellular Ca^{2+} levels via Ca^{2+}-induced Ca^{2+} release from RyRs in SR [202,230]. This increase in Ca^{2+} binds to the myofilaments of the ventricular myocytes and generates the ventricular contraction. Ventricular systole begins when the increased Ca^{2+} levels in the myocytes are purged from cell

through the sodium calcium exchanger (NCX) and Ca^{2+}-ATPase or re-sequestered into the SR through the SERCA channels [231].

The last channels to activate during ventricular repolarization are the delayed K^+ rectifier currents ($I_{Kr,s}$). The balance between the $I_{Kr,s}$ currents and the $I_{Ca,L}$ current enable the plateau phase (Phase 2) of the ventricular AP to remain depolarized for an extended duration which is essential for proper excitation-contraction coupling and normal AP waveform propagation. Repolarization of the ventricles (Phase 3) occurs when the $I_{Ca,L}$ channels inactivate. The outward $I_{Kr,s}$ currents begin to dominate during this phase and is coupled with the activation of inward rectifying I_K currents. Once repolarization is complete, the AP returns to resting membrane potential (Phase 4), a period primarily maintained by the I_K current [232,233].

S.3.2 Differences Between Mouse and Man

Animal models are primarily used to investigate cardiac cellular electrophysiology. Therefore, it is wise to consider species-specific differences when comparing results to human outcomes. The first detailed descripting of the murine ECG was described in 1968 by Goldbarg et al. [87] with more recent groups utilizing mouse models to study cardiac conduction and repolarization relevant to gene mutations seen in human subjects [234-236].The most noticeable difference between human and animal is overall heart rate. Smaller animals, such as mice and rats, have faster heart rates compared to humans (~600 or 400 bpm, respectively) which correlate with numerous differences in ventricular AP regulation [89,237,238]. This section will go in depth into the atrial and ventricular AP differences between human and mouse and how they manifest on the surface ECG.

The AP of the SAN in mice exhibit similar upstroke velocities, amplitudes, and diastolic potentials compared to those in humans indicating only small differences in the L-type Ca^{2+}

current responsible for the SAN AP [239]. However, mice possess substantially shorter SAN AP durations compared to humans possibly due to differences in delayed rectifier K^+ currents ($I_{to,}$ $I_{Kr,s}$) and the pacemaker current (I_f) [240,241]. Atrial AP are also similar between these two species and result in comparable P-wave morphology, albeit with different AP durations. Furthermore, the PR interval in both species is often used as a measure of atrial repolarization [237,242,243]. Similarities between the human and mouse cardiac electrophysiology end at the AVN where only minor difference in connexon expression and gap junction formation are present but manifest through differences in AVN conduction delays [212,244].

The ventricular AP conduction cycle in the mouse is vastly different than that seen in humans. The ultra-rapid transient outward K^+ current (I_{Kur}) is responsible for the initial repolarization phase of the AP (Phase 1) in mice [245]. The I_{kur} current is absent in humans; the initial repolarization is guided by fast transient outward K^+ currents ($I_{to,f}$). In mice, ventricular repolarization is primarily facilitated by numerous rate-varying transient outward K^+ currents (i.e., $I_{to,f}$ and $I_{to,s}$) [241,246], Mice also express a smaller L-type Ca^{2+} current (I_{CaL}) compared to humans which manifests in a gradual repolarization instead of a true plateau phase (Phase 2) [247,248]. The rapid and slow delayed K^+ rectifier currents ($I_{Kr,s}$) have large impacts on Phase 2 and Phase 3 of the human ventricular AP whereas these currents have negligible effects in the murine myocytes during these AP phases [241,247].

These species-dependent ion current differences result in noticeable alterations to the ECG waveform. The shape of the ECG waveform in mice is different than that of other mammalian species. Boukens and colleagues argue ventricular depolarization is most accurately portrayed by assessing the duration of the QRS complex between the onset of the Q wave and the point where the S wave intersects with the isoelectric line [89,238]. Additionally, the mouse ECG

includes the presence of a J wave while lacking an isoelectric ST segment [85,238], both of which are not present in the human ECG. The J wave and ST segment in mice are used as a proxy to identify partial or complete ventricular repolarization. The end of the J wave has been shown to correspond with about 90% of total ventricular repolarization [249]. Other groups have shown that complete ventricular repolarization occurs at the point when the negatively-deflected T wave returns to isoelectric levels [85,238]. These differences between the human and mouse ECG can lead to improper detection of underlying cardiac issues and should be accounted for when attempting to compare effects between species.

S.4 EPIDEMIOLOGY

Exposure to elevated concentrations of ambient PM is implicated as a risk factor for increased cardiovascular disease [5,11,12,121,250,251]. Short-term exposure to PM air pollution is associated with increased risk of myocardial infarctions and incidence of ischemic strokes [6,250,252-255]. It is possible that sudden atrial constriction and/or endothelial disruption resulting from PM inhalation could initiate these types of coronary abnormalities by disrupting plaque stability or by decreasing the degree of myocardial perfusion in patients with pre-existing atherosclerosis. Additionally, decreases in parasympathetic tone triggered by PM exposure can potentially induce arrhythmias resulting in episodes of bradycardia and ultimately sudden death [121]. Zanobetti and colleagues determined that there is an increased risk of hospitalizations in elderly individuals for myocardial infarctions per 10 $\mu g/m^3$ increases of ambient PM_{10} mass [6]. It is therefore possible that fine and ultrafine fraction of PM, which is included within the PM_{10} mass fraction, is responsible for a portion of the cardiovascular effects due to the large surface area/unit mass which allows for a higher adsorption of reactive organic molecules and increased ability for interaction with cellular targets [46].

S.5 TARGET-ORGAN TOXICITY

Ambient PM is composed of a heterogeneous mixture of compounds which vary in mass, concentration, shape, surface area, reactivity, solubility, and origin which all impact toxicological outcomes. The following chapter outlines a proposed mechanistic framework for $PM_{2.5}$ and O_3 toxicity relevant to cardiac abnormalities (Figure S.2) and includes several possible interactions between inhaled particulate matter and downstream biological endpoints**.** Mechanisms leading to free radical generation, increased inflammation, and oxidative damage will be the topics on which the following sections will focus.

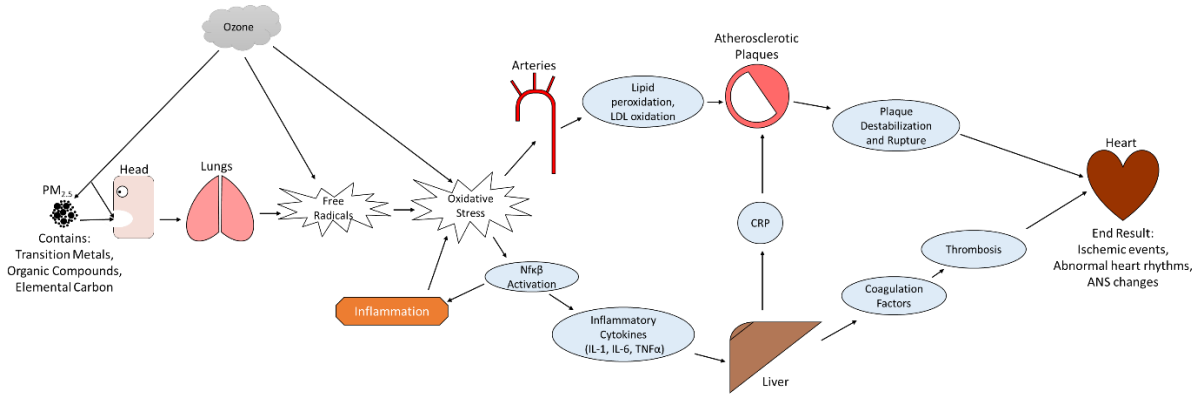

Figure S.2: Hypothesized Mechanistic Framework for PM and O_3 Toxicity Following Inhalation.

S.5.1 Pulmonary System

S.5.1.1 PULMONARY INFLAMMATION

Pulmonary inflammation is one of the more widely established health effects resulting from PM inhalation. Early research looking into the effects of PM in the lungs was performed using PM-treated cell culture experiments. These studies show that macrophages, the resident defense cells of the lungs, release several interleukins (IL) including IL-8, IL-6, and IL-1β in addition to granulocyte macrophage colony-stimulating factor (GM-CSF) and macrophage inflammatory protein (MIP)-2 [256-259]. The generation and release of these factors into the respiratory environment initiate the recruitment of circulating inflammatory cells including

monocytes, lymphocytes, phagocytes, and neutrophils in response to *in vivo* PM exposure. It has been shown in animal models that PM stimulates the production of inflammatory cytokines thereby initiating the infiltration of immune cells such as neutrophils [260], and macrophages [261].

Additionally, alveolar macrophages exposed to PM *in* vitro exhibited decreased levels of anti-inflammatory cytokines (IL-4, IL-13, and IL-10) [262-264]. Macrophages appear to release different products when interacting with different sized PM; both macrophages and epithelial cells have been shown to produce a substantial proportion of the respiratory immune response when exposed to coarse PM ($PM_{2.5-10}$) compared to smaller particle fractions which may be due to the inclusion of more reactive components such as transition metals. [256,265-269]. Immune cells are also able to modify the responses of airway epithelial cells. Macrophages have been shown to exacerbate the epithelial cell response to PM in both co-culture [270-272] and conditioned media [257,273] through the release of tumor necrosis factor (TNF)-α [273] thereby increasing the expression of transcription factors like nuclear factor (NF)-κB and the mitogen activated protein kinase (MAPK) pathway which both are involved with inflammatory cytokine production. [151,274].

Studying the effects of PM on lung cells is essential for understanding the mechanisms underlying its toxicity. Numerous experiments using *in vivo* exposure paradigms aim to corroborate results identified under *in vitro* conditions. Increased numbers of neutrophils and macrophage have been identified in the bronchial alveolar lavage fluid (BALF) of rodents instilled through the trachea with PM [152,275-277]. Cytokines and other signaling molecules (i.e., IL-6, monocyte chemoattractant protein (MCP)-1), MIP-2, and TNF-α were also found to be increased in PM-instilled mice [152,275,277-281]. Similar markers for pulmonary inflammation have been identified in sputum or BALF from human subjects following a controlled inhalation exposure to PM or purified air. Inflammatory cells in exposed individuals were found to be

increased compared to control subjects [282,283] with the effect specific to the bronchiole region of the lungs [284]. Inflammatory cytokines like IL-8 and eotaxin were also increased in lung fluids of these subjects [282,283,285] indicating that PM can initiate pulmonary inflammatory responses in both children and susceptible populations [11,286,287].

S.5.1.2 PULMONARY OXIDATIVE STRESS

ROS generation and free radical peroxidation also play a significant role in PM-associated respiratory decrements as many PM-induced inflammatory mediators are susceptible to oxidation reactions [288]. The metals, organic components, and free radicals adsorbed to the PM can elicit free radical production which oxidizes lung cells [57,289-291]. It has been found that cytochrome P450 can metabolize PAHs to produce a variety of redox cycling quinones which in turn damage lung tissue through ROS production [292,293]. The transitions metals bound to PM produce ROS via hydroxyl radical (• OH) catalyzed by Fenton-like reactions [293,294]. Once inhaled, these reactive components can increase the concentration of free radicals in the lung which deplete antioxidant reserves and induce oxidative stress through the activation of the nuclear factor (erythroid-derived 2)-like (Nrf)2 pathway [151]. Excess ROS production in the lungs in response to PM exposure has been identified using both *in vitro* and *in vivo* methods [55,295]. A study in healthy mice found that low doses of $PM_{2.5}$ (15 μg; intranasal instillation) increased catalase levels and reduced the GSH:GSSG ratio (a measure of oxidative damage) in the lungs [296]. Additionally, it has been shown that the ROS generated by water-soluble particles can generate hydroxyl radicals that can damage DNA and lead to downstream mutagenesis and ameliorate DNA repair mechanisms [297-299].

S.5.1.3 PULMONARY EFFECTS OF PM AND OZONE CO-EXPOSURE

Ambient air pollution exposures have also been investigated in the context of PM and gaseous co-exposures. O_3 is thought to be one of the dominant gas pollutants contributing to cardiopulmonary toxicity. Healthy individuals exposed to 300 $\mu g/m^3$ of diesel exhaust PM followed by 0.2 ppm of O_3 experienced significant increases in pulmonary neutrophil and macrophage concentrations compared to sham controls [300]. Multiple rodents studies have identified adverse pulmonary responses with PM + O_3 co-exposures [133,301-303] Spontaneously hypertensive rats acutely exposed to ultrafine PM ($Dp \leq 0.1$ μm; 250$\mu g/m^3$) in combination with O_3 (1.0 ppm) experienced more severe bronchi and central acinar injuries compared to single atmosphere exposures [304] possibly due to the reaction of organic constituents (e.g. PAHs) with O_3 in the co-exposure atmosphere [305]. In another study, mice co-exposed to PM + O_3 (0-50μg $PM_{2.5}$ intranasally instilled, 0.8 ppb O_3) exhibited a marked increase in pulmonary neutrophil levels without generating a standard Type 2 inflammatory and epithelial response compared to O_3 exposure alone [306]. These studies indicate that O_3 and PM co-exposures can produce pulmonary outcomes separate from exposures to individual pollutants.

S.5.2 Vasculature

S.5.2.1 PARTICLE TRANSLOCATION FROM LUNGS TO VASCULATURE

The translocation of PM from the lungs into the systemic circulation depends on the physical and chemical makeup of the PM at the air-blood interface. Experiments using tracheally-instilled ^{99m}Tc-labelled albumin particles ($D_p \leq 80$ nm) in hamster models discovered a substantial transfer of PM into the systemic circulation and numerous extra-pulmonary organs including kidneys, liver, heart, and spleen 1-hour post exposure [167]. Additionally, ^{192}Ir-labeled ultrafine PM was found to persist in rat circulatory systems up to 1 week post exposure [307].

Furuyama and colleagues instilled mice with both gold and fluorescently labeled PM (Dp = 20 nm , 200 nm) and found appreciable amounts of particles in the same extra-pulmonary organs as identified above [308]. Human experiments attempting to identify PM translocation have identified disparate results; some studies report negligible lung clearance of ^{99m}Tc-labelled particles within 3 days of exposure [309-311] while others report immediate clearance [168]. The differences in PM clearance studies underscores possible methodological issues including detection methods, tracer retention/leaching, and PM generation/dose administration.

S.5.2.2 SYSTEMIC INFLAMMATION

Once in circulation, PM has been shown to produce systemic inflammation which negatively impacts cardiovascular health. Clinical studies have identified a positive correlation between plasma C-reactive protein (CRP) and acute PM exposure in both healthy patients [312] and those who are elderly and/or sick [163,287,313]. Links between real-world ambient PM concentrations have been investigated with data acquired from personal PM samplers. These studies found that PM exposure was positively correlated with increases in plasma CRP levels [314] as well as augmented inflammatory cell counts with increased levels of white blood cells and fibrinogen [315,316]. These markers have also been found to be increased in populations exposed chronically to PM [317,318]. Importantly, children living in polluted areas were found to have increased levels of numerous inflammatory markers including, but not limited to, TNF-α, IL-1β, endothelin-1, and CRP compared to children living in less polluted regions [319].

The effects of PM exposure on systemic inflammation in human subjects has been confirmed in multiple animal studies. Rodents exposed to PM through various exposure routes exhibited increased levels of serum inflammatory cell counts with increased inflammatory protein levels [276,320]. Other animal studies indicate that PM exposure can increase circulating

neutrophil concentrations by decreasing the transit time of polymorphonuclear leukocytes (PMN) from the bone marrow [321-323]. This decreased PMN transit time resulting from direct PM instillation was substantiated in studies that tracheally instilled media from PM-conditioned cells [272,324], indicating the importance of PM-induced lung responses in downstream systemic inflammation.

S.5.2.3 SYSTEMIC OXIDATIVE STRESS

Vascular oxidative stress is primarily produced through the activation of enzymes such as uncoupled endothelial nitric oxide synthase, xanthine oxidase, or NADH/NADPH [325]. Vascular ROS production can also result from the numerous toxic constituents adsorbed to the PM (see section S.5.2.3). Exposure to PM has been correlated with systemic oxidative stress which can be identified through altered expression of certain circulatory biomarkers or factors produced by downstream organs. Associations between levels of PM and 8-hydroxy-2'-deoxyguanosine (8-OHdG), a DNA oxidant, in healthy subjects [326] during short term PM exposure were found to be significantly associated with increased plasma homocysteine levels in both smokers [327] and elderly individuals [328]. Additionally, the effects of PM on plasma GSH and Cu/ZnSOD were attenuated by supplementation with the antioxidant omega-3 fatty acids when administered in an elderly cohort [329].

Studies using *in vitro* models have been helpful in solidifying the role of PM in ROS formation and oxidative stress. Diesel exhaust particles (DEP) have been shown to induce superoxide in cell-free systems [58]. Mice exposed to PM were found to promote NADPH oxidase-mediated ROS formation through an in infiltrating monocytes and vascular tissue [320] with other studies identifying increases in both NADPH oxidase and superoxide in murine aortas [330].

Moreover, an analysis of liver tissue in hyperlipidemic mice identified increased expression of multiple antioxidant genes including catalase, Nrf-2, and SOD2 [15].

S.5.2.4 BLOOD PRESSURE

Exposure to PM has also been shown to elicit alteration in systemic blood pressure (BP) in both acute and chronic studies. Coogan et al. identified a positive relationship between PM exposure and increased BP and risk for developing hypertension [331]. Other epidemiological approaches have also established links between PM exposure and BP at a population level which have been able to tease out relationships between specific PM components (i.e., carbon type) and certain at-risk populations [332-340]. Despite a small number of studies showing a slight negative association between PM exposure and BP [83,341-343], the majority of studies have identified that PM exposure is associated with increases in both systolic and diastolic BP. It is therefore necessary to evaluate these changes when properly assessing PM-induced cardiovascular function.

The effects of PM exposure on BP have been assessed on an individual level using personal PM samplers. As with the population-based approaches, PM has been shown to positively correlate with increased measures of BP [344-346]. Notably, it was found that individuals acutely exposed to DEP (two hour duration on two separate occasions) also exhibited similar BP anomalies [347] emphasizing the substantial short-term effects of PM exposure. Some researchers have utilized interventional approaches to help solidify the effects of inhaled PM on BP. One study identified that BP was increased in individuals exposed to PM compared to individuals wearing PM-filtering face masks during the same period [348]. Another study established that BP increases associated with unventilated cooking areas were ameliorated following additional ventilation and PM removal from the cooking area [349]. PM has also been found to cause BP

changes in animal models. The BP in mice repeatedly exposed to DEP was found to be increased over control animals with curcumin administration able to adequately mitigate these changes [276]. Decreases in BP were also noted following chronic exposure to photochemically activated concentrated ambient PM [124]. These data adequately suggest that PM exposure is capable of altering BP in both human and animal models, and the mechanisms behind these changes should be accounted for when assessing ultimate cardiotoxicity.

S.5.2.5 VASCULAR DYSFUNCTION AND ATHEROSCLEROSIS

Particulate matter has been linked to increased atherosclerosis and vascular dysfunction in a plethora of studies. Exposure to increased levels of $PM_{2.5}$ has been shown to correlate with significant increases in carotid intima-media thickness suggesting increased risk for atherosclerotic development with a greater association in vulnerable populations [350-352]. Other studies have identified increased coronary [100] and thoracic [101] artery calcification in healthy individuals with increased PM exposure levels. Additionally, increased PM exposure was found to correlate with decreases in nitroglycerine-related vascular activity (necessary for arterial dilation) and increases in brachial artery flow-mediated diameter (a measure of arterial dilation) [344,353].

Animal studies have provided a wealth of insight into the vascular changes associated with PM inhalation. Atherosclerotic lesion development was shown to be exacerbated in numerous PM-exposed animal models including rabbits, low-density lipoprotein receptor (LDLR)-deficient mice, and apolipoprotein E knockout ($apoE^{-/-}$) mice compared to air exposed controls [15,120,354]. Increased atherosclerosis was measured in mice sub-chronically exposed to environmentally relevant levels of Beijing ambient PM (17 μg/m3 $PM_{2.5}$ and 99 μg/m3 PM_{10}) [16].

Moreover, long term exposure to concentrated ambient particle (CAPs) resulted in increased vascular inflammation and atherosclerotic plaque lesions in apoE$^{-/-}$ mice fed high-fat diets compared to control animals [355]. The effects of CAPs on atherosclerotic progression may be a function of particle size as it was found that mice sub-chronically exposed to ultrafine CAPs exhibited greater lesion area in the thoracic artery compared to both air controls and mice exposed to a larger concentration of concentrated $PM_{2.5}$ [356] suggesting that increased surface area with additional adsorbed chemical constituents may be partly responsible for atherogenesis.

Oxidative stress and ROS generation is also a significant promoter of atherosclerosis. Insights from experiments with DEP established that there was a dose-dependent increase in lipid peroxidation and fibrotic deposits found in the aortic plaque lesions of apoE$^{-/-}$ mice [18]. Furthermore, the effects of DEP exposure were attenuated when animals were given particle-filtered DEP at comparable concentration to the unfiltered DEP, indicating that atherosclerotic plaque composition is, in part, driven by the particle phase of ambient air pollution. Our laboratory has previously shown that mice exposed to $PM_{2.5}$ thermally-stripped of most semi-volatile compounds (SVOCs) decreased overall plaque formation compared to mice exposed to whole PM [13]. However, the thermal denudation of PM results in a decrease in overall particle and mass concentration which hinders the ability to clearly delineate between dose and compositional effects of SVOC removal.

S.5.2.6 VASCULAR EFFECTS OF PM AND OZONE CO-EXPOSURE

Particulate matter and O_3 co-exposures have helped to better understand the vascular effects of real-world air pollution events. A randomized crossover study found that healthy adults acutely exposed to CAPs + O_3 via inhalation (~ 150 μg/m^3 CAPs; 120 ppb O_3) exhibited significant brachial artery vasoconstriction compared to filtered air exposures [357] possibly due to increased sympathetic nervous system stimulation via afferent pulmonary vagal nerves or perhaps acute increases in plasma endothelin (ET) concentrations [301]. Additionally, the inhaled PM may induce inflammation and cytokine production due to free radical generation which can also contribute to vascular ET expression through oxidative stress pathways [358]. PM + O_3 co-exposure in animals have led to less conclusive results. Rats chronically exposed to a DEP or O_3 singly (~ 2.0 mg/m^3 DEP; 500 ppb O_3) were found to exhibit significant mRNA upregulation of proteins associated with oxidative stress, microvascular thrombosis, protease/antiprotease concentrations, and vasoconstriction in the aorta with no effect seen in the DEP + O_3 co-pollutant atmosphere [359]. This lack of co-pollutant response was also observed in mice acutely exposed to CAPs in combination with O_3 (~ 150 μg/m^3 CAPs; 120 ppb O_3) where animals exposed to single pollutant atmosphere exhibited a larger change in HDL antioxidant/anti-inflammatory capacity compared to filtered air controls. The lack of response to PM + O_3 atmospheres may be due to the ability of O_3 to diminish the health effects of PM exposure, such as the case with diastolic blood pressure in humans [360] or on heart rate variability in rats [104,361,362].

S.5.3 Heart

S.5.3.1 HEART RAVE VARIABILITY AND AUTONOMIC DYSFUNCTION

Exposure to PM has be shown to elicit multiple effects on heart rate variability (HRV), an index that looks at the interval deviation between consecutive heartbeats. Increased PM exposure

was associated with a decrease in the standard deviation of normal-to-normal beat intervals (SDNN) in a cohort of elderly patients expressing specific mutations in a gene involved in the methionine cycle [363]. Other human studies have identified contrasting HRV associations with increased PM exposure, as patients with a history of myocardial infarction (MI) experience decreased SDNN but patients with a history of chronic obstructive pulmonary disorder (COPD) experienced an increase [364] highlighting the importance of underlying health in HRV outcomes. Studies in animals have also determined that PM exposure can produce disparate results on HRV parameters. Rats that inhaled either concentrated ambient PM or DEP exhibited decreases in both SDNN and the root mean square of successive differences (RMSSD) of the normal-to-normal beat intervals [365,366]. Chen et al. found that SDNN and RMSSD in apoE$^{-/-}$ mice were both increased and decreased in response to PM exposure depending the period of acquisition [120]. Furthermore, apoE$^{-/-}$ mice exhibited decreases in both time- and frequency-dependent parameters of HRV following intranasal instillation [367] or chronic whole body inhalation or $PM_{2.5}$ [13,124] suggesting an impairment of the parasympathetic limb of the autonomic nervous system (see detailed discussion below).

The autonomic nervous system (ANS) is critical for proper function and maintenance of HRV. Air pollution may induce dysregulation of the sympathetic and parasympathetic branches of the ANS through the excitation of excitatory/inhibitory afferent nerves. Oxidative stress produced by inhaled PM has been shown to produce acute autonomic disruptions via stimulation of the transient receptor potential (TRP) vanilloid 1 (TRPV1) or TRP ankyrin 1 (TRPA1) on pulmonary irritant-sensitive afferent vagal nerve fibers (aka C-fibers) [368,369], and, when activated alter efferent autonomic nerve activity to the cardiovascular system [370,371]. Additionally, acute

PM exposure was shown to induce parasympathetic cardiac dysautomation through the methylation of interferon (INF) γ via changes in inflammation and sympathetic control [372].

Chronic ANS dysfunction resulting from prolonged PM exposure can result from alterations in normal cardiac baroreflex function [370]. As mentioned previously in this chapter, PM exposure can exacerbate atherosclerotic plaque formation through increased inflammatory processes and oxidative stress. In humans, measurements of decreased cardiac baroreflex sensitivity has been found to correspond with coronary atherosclerotic impairments [373]. Neuroplasticity is also though to affect chronic ANS function as acute exposure to $PM_{2.5}$ reduced central cardiac vagal excitability and baroreflex responsiveness in a mouse model [374]. Endothelial dysfunction in arterial walls can augment baroreflex sensitivity by changing how stretch receptors respond to vascular pressure changes.

S.5.3.2 CARDIOMYOCYTE DYSFUNCTION

Multiple pathways have been proposed to help explain the effect of PM exposure on cardiac function. A study using human cardiomyocytes (AC16 cells) determined that $PM_{2.5}$ exposure induced an upregulation in proteins associated with the mitochondria-mediated apoptosis pathway (Caspase-3, Caspase-9, and BAX) ultimately inducing cell apoptosis [375]. Wang et al. measured increased cardiomyocyte apoptosis resulting from $PM_{2.5}$ exposure in a rat model where it was determined that PM elicited larger alterations in myocardial enzyme profiles, increased CRP levels and decreased SOD activity compared to control animals [376]. The Wang study also identified increased cellular apoptosis stemming from increased phosphorylation of myocardial c-Jun NH2-terminal kinase (JNK) and p53 which act to upregulate levels of B-cell lymphoma 2(BCL2)-Associated X Protein (BAX) and caspase-3 while downregulating levels of Bcl-2 [376]. Upregulation of JNKs and p38 MAPK levels leading to altered BAX/Bcl-2 ratios and

increased caspase-3 levels were also identified in cultured rat cells (H9C2 cells) exposed to PM *in vitro* [149] suggesting a significance of the JNK/MAPK pathway in PM-induced cardiovascular toxicity.

Apoptosis is only one hypothesized mechanism for PM-induced cardiomyocyte toxicity. Data from an exploratory panel study found a positive association between traffic-related pollutants and Nrf2-mediated genes (SOD2, heme oxygenase (HMOX1), and NAD(P)H dehydrogenase quinone 1 (NQO1)) at the transcription level [377] implying an increased oxidative potential of freshly derived vehicle emissions. An *in* vitro study using human cardiomyocytes (HL-1 cells) determined that cells exposed directly (incubated in culture) to PM increased ROS generation without overall metabolic alterations while cells indirectly exposed to PM (conditioned media from PM-exposed macrophages) induced a marked reduction in cardiac metabolism [150]. The differential response between the direct and indirect PM exposures may be due to Nrf2's ability to translocate into cell nuclei where it participates in cellular antioxidant responses and reaffirms the importance of lung-derived mediators in downstream cardiac function. The effects of direct and indirect PM exposure were further investigated using harvested rat cardiomyocytes where it was determined that cells exposed directly and indirectly to DEP exhibited ROS-dependent contractile and calcium handling dysfunction [378]. PM exposure was also found to increase cellular apoptosis rates and intracellular ROS production in a dose-dependent manner in an *in vitro* rodent cardiomyocyte model [149].

S.5.3.3 ECG WAVEFORM ANOMALIES AND UNDERLYING IMPAIRMENTS

PM exposure is an established risk factor for functional cardiac impairments. Increases in PR interval duration were found to be correlated with increased PM exposure in a human study [379] which could indicate a perturbation of parasympathetic activation, sympathetic withdrawal, or

cardiomyocyte Ca^{2+} channel blockages. The mechanistic explanations behind P-wave alterations have been investigated using several rodent models. Dianat and colleagues acutely exposed rats to PM (2.5 mg/kg or 5.0 mg/kg body weight via intratracheal instillation) with high metal content exhibited increased PR durations with decreased levels of antioxidant enzymes (GPx, SOD, and CAT) [380] suggesting that PM exposure initiates ROS formation and oxidative stress. The Dianat study also established that supplementation with vanillic acid, an antioxidant, was able to attenuate the negative effects of PM exposure [380]. The protective effects of vanillic acid and the importance of its receptor, TRPV1 (previously discussed in section S.5.3.1), was further investigated in a study by Ghelfi et al. [381]. Rats chronically exposed to PM exhibited increased P-wave durations, QRS durations, and QT intervals with concomitant increases in oxidative stress measurements (cardiac *in situ* chemiluminescence and lipid peroxidation) compared to control animals with s(CPZ) administration, a TRPV1 antagonist, capable of reversing the effects [381]. These studies indicate the usefulness of ECG waveform changes to detect possible ANS impairments.

Myocardial ischemia and alterations to ventricular repolarization can be identified by assessing changes in the T-wave of the surface ECG. In humans, PM exposure has been associated with decreases in T-wave amplitude and T-wave area in patients with ischemic heart disease [254] with another study associating a 10 $\mu g/m^3$ increase in ambient PM to a 4-5% increased odds of developing decreased T-wave amplitudes [382]. Rodents studies examining the effects of inhaled PM on ventricular function have produced inconsistent results. Farraj et al. noted increases in both T-wave area and T-wave amplitude in rats acutely exposed to residual oil fly ash (ROFA)-like $PM_{2.5}$ (450 $\mu g/m^3$ via nose-only inhalation) [98] while failing to elicit a significant pulmonary inflammatory response. However, these same T-wave measurements

increased in rats when exposed to higher doses of the ROFA-like $PM_{2.5}$ (3.5mg/m^3 via nose-only inhalation) while also producing a significant pulmonary immune response [98]. This pattern of response seen in the T-wave measurements, together with the lack of inflammatory response in the low-dose exposure group, may be caused by direct oxidative damage to cardiomyocytes resulting from the translocation of metals to the heart [141].

Increased systemic oxidative stress may also impact ECG waveform morphology. Our laboratory has previously shown that $apoE^{-/-}$ mice exposed to quasi-ultrafine PM ($D_p \leq 0.18$ μm) experienced increases in PR interval duration, QRS interval duration, and T-wave amplitude (as a percent change from baseline) compared to control animals which were accompanied by increases in atherosclerotic plaque size, arterial lipid accumulation, and serum malondialdehyde (MDA) levels [13]. The toxic effects of PM inhalation in this previous study were ameliorated in mice similarly exposed to thermally denuded PM [13] possibly indicating the PM-associated SVOCs as the primary toxic agent in PM-driven cardiovascular injury. Alterations in T-wave area with an upregulation in Endothelin (ET)-1 were also identified by Campen et al. in $apoE^{-/-}$ mice exposed to PM from freshly generated gasoline emission but not from gasoline emissions sans particles [383]. Similar to the study discussed above by Farraj et al., the T-wave alterations identified in the Campen study occurred without increased pulmonary inflammatory markers suggesting that oxidative damage to cardiomyocytes may result from the direct translocation of metals to the heart.

S.5.3.4 CARDIAC EFFECTS OF PM AND OZONE CO-EXPOSURE

The cardiac effects of PM + O_3 co-exposures have also been investigated. In one study, rats were exposed to O_3 (800 ppb) following an intratracheal instillation of $PM_{2.5}$ at a dose of either 0.2, 0.8, or 3.2 mg/rat [133]. Animals exposed to the medium or high dose exhibited periods

of ST-segment anomalies and QRS interval prolongation/J-wave inversions, respectively [133]. This study also established a dose-dependent response between the administered concentrations of PM+ O_3 and the levels of 1) inflammatory markers such as CRP and IL-6, and 2) heart oxidants and antioxidants such as SOD and MDA, the latter of which was increased nearly 3-fold in the highest PM + O_3 dose compared to controls [133]. In another study, Kurhanewicz et al. found that mice exposed to ultrafine CAPs (140 μg/m^3 via inhalation) in concert with O_3 (300 ppb) experienced longer QRS intervals and rate-corrected QT intervals compared to filtered air or PM-exposed mice [104]. These co-exposed animals also had a greater number of non-conductive P-waves compared to controls and compared to both PM and O_3 atmospheres. Non-conductive P-waves accompanied by widened QRS complexes are suggestive of atrioventricular conduction block with possible downstream ventricular conduction impairments [384]. The Kurhanewicz study also found that glutathione S-transferase was significantly reduced in the ultrafine PM+ O_3 exposure but not in the single PM exposure which may indicate increased systemic oxidative stress [104].

REFERENCES

1. Pope CA, Ezzati M, Cannon JB, Allen RT, Jerrett M, Burnett RT. Mortality risk and PM2.5 air pollution in the USA: an analysis of a national prospective cohort. Air Qual Atmos Hlth 2018;11:245-52.
2. Pope CA, Cohen AJ, Burnett RT. Cardiovascular Disease and Fine Particulate Matter: Lessons and Limitations of an Integrated Exposure-Response Approach. Circ Res 2018;122:1645-7.
3. Burnett R, Chen H, Szyszkowicz M, et al. Global estimates of mortality associated with long-term exposure to outdoor fine particulate matter. Proc Natl Acad Sci U S A 2018;115:9592-7.
4. Landrigan PJ, Fuller R, Acosta NJR, et al. The Lancet Commission on pollution and health. The Lancet 2017.
5. Pope CA, Burnett RT, Thurston GD, et al. Cardiovascular mortality and long-term exposure to particulate air pollution: epidemiological evidence of general pathophysiological pathways of disease. Circulation 2004;109.
6. Zanobetti A, Schwartz J. The effect of particulate air pollution on emergency admissions for myocardial infarction: a multicity case-crossover analysis. Environ Health Perspect 2005;113:978-82.
7. Tonne C, Yanosky J, Gryparis A, et al. Traffic particles and occurrence of acute myocardial infarction: a case-control analysis. Occup Environ Med 2009;66:797-804.
8. Jerrett M, Burnett RT, Ma R, et al. Spatial analysis of air pollution and mortality in Los Angeles. Epidemiology 2005;16:727-36.
9. Krewski D, Jerrett M, Burnett RT, et al. Extended follow-up and spatial analysis of the American Cancer Society study linking particulate air pollution and mortality. Res Rep Health Eff Inst 2009:5-114; discussion 5-36.
10. Koton S, Molshatzki N, Yuval, et al. Cumulative exposure to particulate matter air pollution and long-term post-myocardial infarction outcomes. Prev Med 2013;57:339-44.
11. Dockery DW, Pope CA, Xu X, et al. An association between air pollution and mortality in six U.S. cities. N Engl J Med 1993;329.
12. Pope CA, 3rd, Dockery DW. Health effects of fine particulate air pollution: lines that connect. J Air Waste Manag Assoc 2006;56:709-42.
13. Keebaugh AJ, Sioutas C, Pakbin P, Schauer JJ, Mendez LB, Kleinman MT. Is atherosclerotic disease associated with organic components of ambient fine particles? Sci Total Environ 2015;533:69-75.
14. Sun Q, Wang A, Jin X, et al. LOng-term air pollution exposure and acceleration of atherosclerosis and vascular inflammation in an animal model. JAMA 2005;294:3003-10.
15. Araujo JA, Barajas B, Kleinman M, et al. Ambient Particulate Pollutants in the Ultrafine Range Promote Early Atherosclerosis and Systemic Oxidative Stress. Circulation Research 2008;102:589.
16. Chen T, Jia G, Wei Y, Li J. Beijing ambient particle exposure accelerates atherosclerosis in ApoE knockout mice. Toxicol Lett 2013;223:146-53.
17. Floyd HS, Chen LC, Vallanat B, Dreher K. Fine ambient air particulate matter exposure induces molecular alterations associated with vascular disease progression within plaques of atherosclerotic susceptible mice. Inhalation Toxicology 2009;21:394-403.
18. Campen MJ, Lund AK, Knuckles TL, et al. Inhaled diesel emissions alter atherosclerotic plaque composition in ApoE(-/-) mice. Toxicol Appl Pharmacol 2010;242:310-7.
19. Xu Z, Xu X, Zhong M, et al. Ambient particulate air pollution induces oxidative stress and alterations of mitochondria and gene expression in brown and white adipose tissues. Part Fibre Toxicol 2011;8:20.
20. Mirowsky JE, Jin L, Thurston G, et al. In vitro and in vivo toxicity of urban and rural particulate matter from California. Atmos Environ (1994) 2015;103:256-62.
21. Hajat A, Allison M, Diez-Roux AV, et al. Long-term Exposure to Air Pollution and Markers of Inflammation, Coagulation, and Endothelial Activation: A Repeat-measures Analysis in the Multi-Ethnic Study of Atherosclerosis (MESA). Epidemiology 2015;26.
22. Kunzli N, Jerrett M, Mack WJ, et al. Ambient air pollution and atherosclerosis in Los Angeles. Environ Health Perspect 2005;113:201-6.
23. Kunzli N, Jerrett M, Garcia-Esteban R, et al. Ambient air pollution and the progression of atherosclerosis in adults. PLoS One 2010;5:e9096.
24. Hoffmann B, Moebus S, Mohlenkamp S, et al. Residential exposure to traffic is associated with coronary atherosclerosis. Circulation 2007;116:489-96.
25. Hoffmann B, Moebus S, Kroger K, et al. Residential exposure to urban air pollution, ankle-brachial index, and peripheral arterial disease. Epidemiology 2009;20:280-8.

26. Allen RW, Criqui MH, Diez Roux AV, et al. Fine particulate matter air pollution, proximity to traffic, and aortic atherosclerosis. Epidemiology 2009;20:254-64.
27. Araujo JA, Nel AE. Particulate matter and atherosclerosis: role of particle size, composition and oxidative stress. Particle and Fibre Toxicology 2009;6.
28. Oberdorster G. Pulmonary effects of inhaled ultrafine particles. Int Arch Occup Environ Health 2001;74:1-8.
29. Borm PJA, Robbins D, Haubold S, et al. The potential risks of nanomaterials: a review carried out for ECETOC. Particle and Fibre Toxicology 2006;3:11.
30. Ntziachristos L, Froines JR, Cho AK, Sioutas C. Relationship between redox activity and chemical speciation of size-fractionated particulate matter. Particle and Fibre Toxicology 2007;4:5.
31. Brown DM, Wilson MR, MacNee W, Stone V, Donaldson K. Size-Dependent Proinflammatory Effects of Ultrafine Polystyrene Particles: A Role for Surface Area and Oxidative Stress in the Enhanced Activity of Ultrafines. Toxicology and Applied Pharmacology 2001;175:191-9.
32. Xu L, Suresh S, Guo H, Weber RJ, Ng NL. Aerosol characterization over the southeastern United States using high-resolution aerosol mass spectrometry: spatial and seasonal variation of aerosol composition and sources with a focus on organic nitrates. Atmos Chem Phys 2015;15:7307-36.
33. Arhami M, Shahne MZ, Hosseini V, Roufigar Haghighat N, Lai AM, Schauer JJ. Seasonal trends in the composition and sources of PM2.5 and carbonaceous aerosol in Tehran, Iran. Environ Pollut 2018;239:69-81.
34. Pardo M, Xu F, Qiu X, Zhu T, Rudich Y. Seasonal variations in fine particle composition from Beijing prompt oxidative stress response in mouse lung and liver. Sci Total Environ 2018;626:147-55.
35. Freney EJ, Sellegri K, Canonaco F, et al. Seasonal variations in aerosol particle composition at the puy-de-Dôme research station in France. Atmos Chem Phys 2011;11:13047-59.
36. Kuhn T, Biswas S, Sioutas C. Diurnal and seasonal characteristics of particle volatility and chemical composition in the vicinity of a light-duty vehicle freeway. Atmospheric Environment 2005;39:7154-66.
37. Russell M, Allen DT, Collins DR, Fraser MP. Daily, Seasonal, and Spatial Trends in PM2.5 Mass and Composition in Southeast Texas Special Issue of Aerosol Science and Technology on Findings from the Fine Particulate Matter Supersites Program. Aerosol Science and Technology 2004;38:14-26.
38. Martin M, Chang RYW, Sierau B, et al. Cloud condensation nuclei closure study on summer arctic aerosol. Atmos Chem Phys 2011;11:11335-50.
39. Avery Anita M, Waring MS, DeCarlo PF. Seasonal variation in aerosol composition and concentration upon transport from the outdoor to indoor environment. Environmental Science: Processes & Impacts 2019;21:528-47.
40. Rogge WF, Mazurek MA, Hildemann LM, Cass GR, Simoneit BRT. Quantification of urban organic aerosols at a molecular level: Identification, abundance and seasonal variation. Atmospheric Environment Part A General Topics 1993;27:1309-30.
41. Knowlton K, Hogrefe C, Lynn B, Rosenzweig C, Rosenthal J, Kinney PL. Impacts of Heat and Ozone on Mortality Risk in the New York City Metropolitan Region Under a Changing Climate. In: Thomson MC, Garcia-Herrera R, Beniston M, eds. Seasonal Forecasts, Climatic Change and Human Health: Health and Climate. Dordrecht: Springer Netherlands; 2008:143-60.
42. Ren C, Williams GM, Morawska L, Mengersen K, Tong S. Ozone modifies associations between temperature and cardiovascular mortality: analysis of the NMMAPS data. Occupational and Environmental Medicine 2008;65:255.
43. Michaels RA, Kleinman MT. Incidence and Apparent Health Significance of Brief Airborne Particle Excursions. Aerosol Science and Technology 2000;32:93-105.
44. Biswas SK, Rahman I. Environmental toxicity, redox signaling and lung inflammation: the role of glutathione. Mol Aspects Med 2009;30:60-76.
45. Janssen YM, Van Houten B, Borm PJ, Mossman BT. Cell and tissue responses to oxidative damage. Lab Invest 1993;69:261-74.
46. Li N, Sioutas C, Cho A, et al. Ultrafine particulate pollutants induce oxidative stress and mitochondrial damage. Environ Health Perspect 2003;111:455-60.
47. Gurgueira SA, Lawrence J, Coull B, Murthy GG, Gonzalez-Flecha B. Rapid increases in the steady-state concentration of reactive oxygen species in the lungs and heart after particulate air pollution inhalation. Environ Health Perspect 2002;110.
48. Kelly FJ, Fussell JC. Size, source and chemical composition as determinants of toxicity attributable to ambient particulate matter. Atmospheric Environment 2012;60:504-26.

49. Velali E, Papachristou E, Pantazaki A, et al. Redox activity and in vitro bioactivity of the water-soluble fraction of urban particulate matter in relation to particle size and chemical composition. Environmental Pollution 2016;208:774-86.
50. Romero Lankao P. Are we missing the point?: Particularities of urbanization, sustainability and carbon emissions in Latin American cities. Environment and Urbanization 2007;19:159-75.
51. Mirowsky JE, Carraway MS, Dhingra R, et al. Ozone exposure is associated with acute changes in inflammation, fibrinolysis, and endothelial cell function in coronary artery disease patients. Environ Health 2017;16:126.
52. Pardo M, Porat Z, Rudich A, Schauer JJ, Rudich Y. Repeated exposures to roadside particulate matter extracts suppresses pulmonary defense mechanisms, resulting in lipid and protein oxidative damage. Environmental Pollution 2016;210:227-37.
53. Carll AP, Haykal-Coates N, Winsett DW, et al. Cardiomyopathy confers susceptibility to particulate matter-induced oxidative stress, vagal dominance, arrhythmia and pulmonary inflammation in heart failure-prone rats. Inhal Toxicol 2015;27:100-12.
54. Hatzis C, Godleski JJ, Gonzalez-Flecha B, Wolfson JM, Koutrakis P. Ambient particulate matter exhibits direct inhibitory effects on oxidative stress enzymes. Environ Sci Technol 2006;40:2805-11.
55. Beck-Speier I, Dayal N, Karg E, et al. Oxidative stress and lipid mediators induced in alveolar macrophages by ultrafine particles. Free Radic Biol Med 2005;38:1080-92.
56. Tao F, Gonzalez-Flecha B, Kobzik L. Reactive oxygen species in pulmonary inflammation by ambient particulates. Free Radical Biology and Medicine 2003;35:327-40.
57. Kelly FJ. Oxidative stress: its role in air pollution and adverse health effects. Occup Environ Med 2003;60:612-6.
58. Kumagai Y, Arimoto T, Shinyashiki M, et al. Generation of reactive oxygen species during interaction of diesel exhaust particle components with NADPH-cytochrome P450 reductase and involvement of the bioactivation in the DNA damage. Free Radic Biol Med 1997;22:479-87.
59. Stohs SJ, Bagchi D, Hassoun E, Bagchi M. Oxidative mechanisms in the toxicity of chromium and cadmium ions. J Environ Pathol Toxicol Oncol 2001;20:77-88.
60. Forman HJ, Zhang H, Rinna A. Glutathione: overview of its protective roles, measurement, and biosynthesis. Molecular aspects of medicine 2009;30:1-12.
61. Bakkenist AR, de Boer JE, Plat H, Wever R. The halide complexes of myeloperoxidase and the mechanism of the halogenation reactions. Biochim Biophys Acta 1980;613:337-48.
62. Pullar JM, Vissers MC, Winterbourn CC. Living with a killer: the effects of hypochlorous acid on mammalian cells. IUBMB Life 2000;50:259-66.
63. Wang J, Huang J, Wang L, et al. Urban particulate matter triggers lung inflammation via the ROS-MAPK-NF-κB signaling pathway. Journal of thoracic disease 2017;9:4398.
64. Wei J, Yu H, Wang Y, Verma V. Complexation of iron and copper in ambient particulate matter and its effect on the oxidative potential measured in a surrogate lung fluid. Environmental science & technology 2018;53:1661-71.
65. Antonicelli F, Parmentier M, Drost EM, et al. Nacystelyn inhibits oxidant-mediated interleukin-8 expression and NF-kappaB nuclear binding in alveolar epithelial cells. Free Radic Biol Med 2002;32:492-502.
66. Muthukumar K, Rajakumar S, Sarkar MN, Nachiappan V. Glutathione peroxidase3 of Saccharomyces cerevisiae protects phospholipids during cadmium-induced oxidative stress. Antonie van Leeuwenhoek 2011;99:761-71.
67. Staimer N, Nguyen TB, Nizkorodov SA, Delfino RJ. Glutathione peroxidase inhibitory assay for electrophilic pollutants in diesel exhaust and tobacco smoke. Analytical and Bioanalytical Chemistry 2012;403:431-41.
68. Kim S, Jaques PA, Chang M, Froines JR, Sioutas C. Versatile aerosol concentration enrichment system (VACES) for simultaneous in vivo and in vitro evaluation of toxic effects of ultrafine, fine and coarse ambient particles Part I: Development and laboratory characterization. Journal of Aerosol Science 2001;32:1281-97.
69. Kleinman MT, Hamade A, Meacher D, et al. Inhalation of Concentrated Ambient Particulate Matter near a Heavily Trafficked Road Stimulates Antigen-Induced Airway Responses in Mice. Journal of the Air & Waste Management Association 2005;55:1277-88.
70. Li N, Harkema JR, Lewandowski RP, et al. Ambient ultrafine particles provide a strong adjuvant effect in the secondary immune response: implication for traffic-related asthma flares. American Journal of Physiology-Lung Cellular and Molecular Physiology 2010;299:L374-L83.

71. Kim S, Jaques PA, Chang M, et al. Versatile aerosol concentration enrichment system (VACES) for simultaneous in vivo and in vitro evaluation of toxic effects of ultrafine, fine and coarse ambient particles Part II: Field evaluation. Journal of Aerosol Science 2001;32:1299-314.
72. Sun QH, Wang AX, Jin XM, et al. Long-term air pollution exposure and acceleration of atherosclerosis and vascular inflammation in an animal model. Jama-J Am Med Assoc 2005;294:3003-10.
73. Chen T, Jia G, Wei YJ, Li JC. Beijing ambient particle exposure accelerates atherosclerosis in ApoE knockout mice. Toxicology Letters 2013;223:146-53.
74. Keebaugh AJ, Sioutas C, Pakbin P, Schauer JJ, Mendez LB, Kleinman MT. Is atherosclerotic disease associated with organic components of ambient fine particles? Science of the Total Environment 2015;533:69-75.
75. Ramanathan G, Yin F, Speck M, et al. Effects of urban fine particulate matter and ozone on HDL functionality. Particle and Fibre Toxicology 2016;13.
76. Oldham MJ, Phalen RF, Robinson RJ, Kleinman MT. Performance of a portable whole-body mouse exposure system. Inhal Toxicol 2004;16:657-62.
77. DeCarlo PF, Kimmel JR, Trimborn A, et al. Field-Deployable, High-Resolution, Time-of-Flight Aerosol Mass Spectrometer. Analytical Chemistry 2006;78:8281-9.
78. Canagaratna MR, Jimenez JL, Kroll JH, et al. Elemental ratio measurements of organic compounds using aerosol mass spectrometry: characterization, improved calibration, and implications. Atmospheric Chemistry and Physics 2015;15:253-72.
79. Birch ME, Cary RA. Elemental carbon-based method for monitoring occupational exposures to particulate diesel exhaust. Aerosol Sci Tech 1996;25:221-41.
80. Birch ME, Cary RA. Elemental carbon-based method for occupational monitoring of particulate diesel exhaust: methodology and exposure issues. Analyst 1996;121:1183-90.
81. Chow JC, Watson JG, Chen LW, et al. The IMPROVE_A temperature protocol for thermal/optical carbon analysis: maintaining consistency with a long-term database. J Air Waste Manag Assoc 2007;57:1014-23.
82. Winquist A, Schauer JJ, Turner JR, Klein M, Sarnat SE. Impact of ambient fine particulate matter carbon measurement methods on observed associations with acute cardiorespiratory morbidity. Journal of Exposure Science & Environmental Epidemiology 2015;25:215-21.
83. Feng M, Whitesall S, Zhang Y, Beibel M, D'Alecy L, DiPetrillo K. Validation of volume-pressure recording tail-cuff blood pressure measurements. Am J Hypertens 2008;21:1288-91.
84. Herman DA, Wingen LM, Johnson RM, et al. Seasonal Effects of Ambient PM2.5 on the Cardiovascular System of Hyperlipidemic Mice. Journal of the Air & Waste Management Association 2020;70:307-23.
85. Speerschneider T, Thomsen MB. Physiology and analysis of the electrocardiographic T wave in mice. Acta Physiol (Oxf) 2013;209:262-71.
86. Mitchell GF, Jeron A, Koren G. Measurement of heart rate and Q-T interval in the conscious mouse. Am J Physiol 1998;274:H747-51.
87. Goldbarg AN, Hellerstein HK, Bruell JH, Daroczy AF. Electrocardiogram of the normal mouse, Mus musculus: general considerations and genetic aspects. Cardiovasc Res 1968;2:93-9.
88. Farraj AK, Hazari MS, Haykal-Coates N, et al. ST depression, arrhythmia, vagal dominance, and reduced cardiac micro-RNA in particulate-exposed rats. Am J Respir Cell Mol Biol 2011;44:185-96.
89. Boukens BJ, Rivaud MR, Rentschler S, Coronel R. Misinterpretation of the mouse ECG: 'musing the waves of Mus musculus'. The Journal of Physiology 2014;592:4613-26.
90. DeGiorgio CM, Miller P, Meymandi S, et al. RMSSD, a measure of vagus-mediated heart rate variability, is associated with risk factors for SUDEP: the SUDEP-7 Inventory. Epilepsy & behavior : E&B 2010;19:78-81.
91. Heart rate variability: standards of measurement, physiological interpretation and clinical use. Task Force of the European Society of Cardiology and the North American Society of Pacing and Electrophysiology. Circulation 1996;93:1043-65.
92. Rowan WH, Campen MJ, Wichers LB, Watkinson WP. Heart rate variability in rodents: uses and caveats in toxicological studies. Cardiovasc Toxicol 2007;7:28-51.
93. Liao DP, Cai JW, Barnes RW, et al. Association of cardiac autonomic function and the development of hypertension - The ARC study. Am J Hypertens 1996;9:1147-56.
94. Hayano J, Yamada A, Mukai S, et al. Severity of Coronary Atherosclerosis Correlates with the Respiratory Component of Heart-Rate-Variability. American Heart Journal 1991;121:1070-9.
95. Fleisher LA, Frank SM, Sessler DI, Cheng CT, Matsukawa T, Vannier CA. Thermoregulation and heart rate variability. Clinical Science 1996;90:97-103.

96. Lossius K, Eriksen M, Walloe L. Thermoregulatory Fluctuations in Heart-Rate and Blood-Pressure in Humans - Effect of Cooling and Parasympathetic Blockade. Journal of the Autonomic Nervous System 1994;47:245-54.
97. Finlayson-Pitts BJ, Pitts JN. CHAPTER 3 - Spectroscopy and Photochemistry: Fundamentals. In: Finlayson-Pitts BJ, Pitts JN, eds. Chemistry of the Upper and Lower Atmosphere. San Diego: Academic Press; 2000:71.
98. Farraj AK, Hazari MS, Haykal-Coates N, Lamb C, Winsett DW, Ge Y. ST depression, arrhythmia, vagal dominance, and reduced cardiac micro-RNA in particulate-exposed rats. Am J Respir Cell Mol Biol 2011;44.
99. Scott JL, Walls RM. QT interval prolongation. J Emerg Med 1985;3:221-5.
100. Straus SM, Kors JA, De Bruin ML, et al. Prolonged QTc interval and risk of sudden cardiac death in a population of older adults. J Am Coll Cardiol 2006;47:362-7.
101. Mirvis DM. Physiologic bases for anterior ST segment depression in patients with acute inferior wall myocardial infarction. Am Heart J 1988;116:1308-22.
102. Farraj AK, Walsh L, Haykal-Coates N, et al. Cardiac effects of seasonal ambient particulate matter and ozone co-exposure in rats. Particle and Fibre Toxicology 2015;12:12.
103. Carll AP, Crespo SM, Filho MS, et al. Inhaled ambient-level traffic-derived particulates decrease cardiac vagal influence and baroreflexes and increase arrhythmia in a rat model of metabolic syndrome. Part Fibre Toxicol 2017;14:16.
104. Kurhanewicz N, McIntosh-Kastrinsky R, Tong H, Walsh L, Farraj AK, Hazari MS. Ozone co-exposure modifies cardiac responses to fine and ultrafine ambient particulate matter in mice: concordance of electrocardiogram and mechanical responses. Particle and Fibre Toxicology 2014;11:54.
105. Baja ES, Schwartz JD, Wellenius GA, et al. Traffic-Related Air Pollution and QT Interval: Modification by Diabetes, Obesity, and Oxidative Stress Gene Polymorphisms in the Normative Aging Study. Environmental Health Perspectives 2010;118:840-6.
106. Tong H, Rappold Ana G, Diaz-Sanchez D, et al. Omega-3 Fatty Acid Supplementation Appears to Attenuate Particulate Air Pollution–Induced Cardiac Effects and Lipid Changes in Healthy Middle-Aged Adults. Environmental Health Perspectives 2012;120:952-7.
107. Davis JA, Meng Q, Sacks JD, Dutton SJ, Wilson WE, Pinto JP. Regional variations in particulate matter composition and the ability of monitoring data to represent population exposures. Science of The Total Environment 2011;409:5129-35.
108. Corey LM, Baker C, Luchtel DL. Heart-rate variability in the Apo lipoprotein E knockout transgenic mouse following exposure to Seattle particulate matter. J Toxicol Environ Health Part A 2006;69.
109. Simula S, Vanninen E, Lehto S, et al. Heart rate variability associates with asymptomatic coronary atherosclerosis. Clinical Autonomic Research 2014;24:31-7.
110. Zanobetti A, Gold DR, Stone PH, Suh HH, Schwartz J, Coull BA. Reduction in heart rate variability with traffic and air pollution in patients with coronary artery disease. Environ Health Perspect 2010;118.
111. Colhoun HM, Francis DP, Rubens MB, Underwood SR, Fuller JH. The association of heart-rate variability with cardiovascular risk factors and coronary artery calcification: a study in type 1 diabetic patients and the general population. Diabetes Care 2001;24:1108-14.
112. Lippmann M, Ito K, Hwang JS, Maciejczyk P, Chen LC. Cardiovascular effects of nickel in ambient air. Environ Health Perspect 2006;114:1662-9.
113. Getz GS, Reardon CA. ApoE knockout and knockin mice: the history of their contribution to the understanding of atherogenesis. J Lipid Res 2016;57:758-66.
114. Lind PM, Olsén L, Lind L. Elevated circulating levels of copper and nickel are found in elderly subjects with left ventricular hypertrophy. Ecotoxicology and Environmental Safety 2012;86:66-72.
115. Takenaka S, Karg E, Roth C, et al. Pulmonary and systemic distribution of inhaled ultrafine silver particles in rats. Environ Health Perspect 2001;109.
116. Furuyama A, Kanno S, Kobayashi T, Hirano S. Extrapulmonary translocation of intratracheally instilled fine and ultrafine particles via direct and alveolar macrophage-associated routes. Arch Toxicol 2009;83:429-37.
117. Liao D, Cai J, Barnes RW, et al. Association of cardiac autonomic function and the development of hypertension: the ARIC study. Am J Hypertens 1996;9:1147-56.
118. Mordukhovich I, Kloog I, Coull B, Koutrakis P, Vokonas P, Schwartz J. Association between Particulate Air Pollution and QT Interval Duration in an Elderly Cohort. Epidemiology (Cambridge, Mass) 2016;27:284-90.
119. Van Hee VC, Szpiro AA, Prineas R, et al. Association of long-term air pollution with ventricular conduction and repolarization abnormalities. Epidemiology 2011;22:773-80.

120. Chen LC, Hwang J-S. Effects of Subchronic Exposures to Concentrated Ambient Particles (CAPs) in Mice: IV. Characterization of Acute and Chronic Effects of Ambient Air Fine Particulate Matter Exposures on Heart-Rate Variability. Inhalation Toxicology 2005;17:209-16.
121. Brook RD, Rajagopalan S, Pope CA, 3rd, et al. Particulate matter air pollution and cardiovascular disease: An update to the scientific statement from the American Heart Association. Circulation 2010;121:2331-78.
122. Kroll JH, Seinfeld JH. Chemistry of secondary organic aerosol: Formation and evolution of low-volatility organics in the atmosphere. Atmospheric Environment 2008;42:3593-624.
123. Kroll JH, Smith JD, Che DL, Kessler SH, Worsnop DR, Wilson KR. Measurement of fragmentation and functionalization pathways in the heterogeneous oxidation of oxidized organic aerosol. Physical Chemistry Chemical Physics 2009;11:8005-14.
124. Herman DA, Wingen LM, Johnson RM, et al. Seasonal Effects of Ambient PM2.5 on the Cardiovascular System of Hyperlipidemic Mice. Journal of the Air & Waste Management Association 2020:null-null.
125. Vollmuth S, Niessner R. Degradation of PCDD, PCDF, PAH, PCB and chlorinated phenols during the destruction-treatment of landfill seepage water in laboratory model reactor (UV, Ozone, and UV/Ozone). Chemosphere 1995;30:2317-31.
126. Bousse L. Whole cell biosensors. Sensors and Actuators B: Chemical 1996;34:270-5.
127. Rudolph AS, Reasor J. Cell and tissue based technologies for environmental detection and medical diagnostics. Biosensors and Bioelectronics 2001;16:429-31.
128. Michael S, Montag M, Dott W. Pro-inflammatory effects and oxidative stress in lung macrophages and epithelial cells induced by ambient particulate matter. Environmental Pollution 2013;183:19-29.
129. Charrier JG, Anastasio C. On dithiothreitol (DTT) as a measure of oxidative potential for ambient particles: evidence for the importance of soluble transition metals. Atmospheric chemistry and physics 2012;12:11317-50.
130. Kleinman MT, Herman DH, Johnson R, Wingen LM, Keebaugh AJ. Cardiovascular Effects of Multi-Pollutant Exposure: Mechanisms and Interactions. California Air Resources Board2017.
131. Beeh KM, Beier J, Koppenhoefer N, Buhl R. Increased glutathione disulfide and nitrosothiols in sputum supernatant of patients with stable COPD. Chest 2004;126:1116-22.
132. Kodavanti UP, Schladweiler MC, Ledbetter AD, et al. The spontaneously hypertensive rat as a model of human cardiovascular disease: evidence of exacerbated cardiopulmonary injury and oxidative stress from inhaled emission particulate matter. Toxicol Appl Pharmacol 2000;164:250-63.
133. Wang G, Zhao J, Jiang R, Song W. Rat lung response to ozone and fine particulate matter (PM2.5) exposures. Environmental Toxicology 2015;30:343-56.
134. Magnani ND, Marchini T, Garcés M, et al. Role of transition metals present in air particulate matter on lung oxygen metabolism. The International Journal of Biochemistry & Cell Biology 2016;81:419-26.
135. Boehme DS, Hotchkiss JA, Henderson RF. Glutathione and GSH-dependent enzymes in bronchoalveolar lavage fluid cells in response to ozone. Experimental and Molecular Pathology 1992;56:37-48.
136. Todokoro M, Mochizuki H, Tokuyama K, et al. Effect of Ozone Exposure on Intracellular Glutathione Redox State in Cultured Human Airway Epithelial Cells. Inflammation 2004;28:105-14.
137. Kuz'mina V, Khokhlov Iu K, Savin AA. The effect of ozone therapy on the activity of the autonomic nervous system. Zh Nevrol Psikhiatr Im S S Korsakova 2012;112:18-23.
138. Yang Y, Ruan Z, Wang X, et al. Short-term and long-term exposures to fine particulate matter constituents and health: a systematic review and meta-analysis. Environmental pollution 2019;247:874-82.
139. Boningari T, Smirniotis PG. Impact of nitrogen oxides on the environment and human health: Mn-based materials for the NOx abatement. Current Opinion in Chemical Engineering 2016;13:133-41.
140. Morakinyo OM, Mokgobu MI, Mukhola MS, Hunter RP. Health outcomes of exposure to biological and chemical components of inhalable and respirable particulate matter. International journal of environmental research and public health 2016;13:592.
141. Wallenborn JG, McGee JK, Schladweiler MC, Ledbetter AD, Kodavanti UP. Systemic translocation of particulate matter-associated metals following a single intratracheal instillation in rats. Toxicol Sci 2007;98:231-9.
142. Geiser M, Rothen-Rutishauser B, Kapp N, et al. Ultrafine particles cross cellular membranes by nonphagocytic mechanisms in lungs and in cultured cells. Environ Health Perspect 2005;113:1555-60.
143. Bagate K, Meiring JJ, Gerlofs-Nijland ME, et al. Ambient particulate matter affects cardiac recovery in a Langendorff ischemia model. Inhal Toxicol 2006;18.

144. Biswas S, Verma V, Schauer JJ, Cassee FR, Cho AK, Sioutas C. Oxidative potential of semi-volatile and non volatile particulate matter (PM) from heavy-duty vehicles retrofitted with emission control technologies. Environ Sci Technol 2009;43:3905-12.
145. Cho AK, Sioutas C, Miguel AH, et al. Redox activity of airborne particulate matter at different sites in the Los Angeles Basin. Environ Res 2005;99.
146. Cho SH, Tong H, McGee JK, Baldauf RW, Krantz QT, Gilmour MI. Comparative toxicity of size-fractionated airborne particulate matter collected at different distances from an urban highway. Environ Health Perspect 2009;117.
147. Crobeddu B, Aragao-Santiago L, Bui L-C, Boland S, Squiban AB. Oxidative potential of particulate matter 2.5 as predictive indicator of cellular stress. Environmental Pollution 2017;230:125-33.
148. Briedé JJ, de Kok TMCM, Hogervorst JGF, Moonen EJC, op den Camp CLB, Kleinjans JCS. Development and application of an electron spin resonance spectrometry method for the determination of oxygen free radical formation by particulate matter. Environmental science & technology 2005;39:8420-6.
149. Cao J, Qin G, Shi R, et al. Overproduction of reactive oxygen species and activation of MAPKs are involved in apoptosis induced by PM2.5 in rat cardiac H9c2 cells. Journal of Applied Toxicology 2016;36:609-17.
150. Orona NS, Astort F, Maglione GA, Yakisich JS, Tasat DR. Direct and Indirect Effect of Air Particles Exposure Induce Nrf2-Dependent Cardiomyocyte Cellular Response In Vitro. Cardiovascular Toxicology 2019;19:575-87.
151. Baulig A, Garlatti M, Bonvallot V, et al. Involvement of reactive oxygen species in the metabolic pathways triggered by diesel exhaust particles in human airway epithelial cells. Am J Physiol Lung Cell Mol Physiol 2003;285:L671-9.
152. Wegesser TC, Franzi LM, Mitloehner FM, Eiguren-Fernandez A, Last JA. Lung antioxidant and cytokine responses to coarse and fine particulate matter from the great California wildfires of 2008. Inhal Toxicol 2010;22:561-70.
153. Arı A, Arı PE, Gaga EO. Chemical characterization of size-segregated particulate matter (PM) by inductively coupled plasma–Tandem mass spectrometry (ICP-MS/MS). Talanta 2020;208:120350.
154. Mishra SK, Chattopadhyay B, Kadjo AF, Dasgupta PK. Continuous measurement of elemental composition of ambient aerosol by induction-coupled plasma mass spectrometry. Talanta 2018;177:197-202.
155. Nemery B, Hoet PH, Nemmar A. The Meuse Valley fog of 1930: an air pollution disaster. Lancet 2001;357:704-8.
156. Bell ML, Davis DL. Reassessment of the lethal London fog of 1952: novel indicators of acute and chronic consequences of acute exposure to air pollution. Environmental health perspectives 2001;109 Suppl 3:389-94.
157. Schwartz J, Morris R. Air pollution and hospital admissions for cardiovascular disease in Detroit, Michigan. Am J Epidemiol 1995;142:23-35.
158. Schwartz J. Air pollution and hospital admissions for heart disease in eight U.S. counties. Epidemiology 1999;10:17-22.
159. Wong TW, Lau TS, Yu TS, et al. Air Pollution and Hospital Admissions for Respiratory and Cardiovascular Diseases in Hong Kong. Occupational and Environmental Medicine 1999;56:679-83.
160. Simkhovich BZ, Kleinman MT, Kloner RA. Air pollution and cardiovascular injury epidemiology, toxicology, and mechanisms. J Am Coll Cardiol 2008;52:719-26.
161. Chen R, Chu C, Tan J, et al. Ambient air pollution and hospital admission in Shanghai, China. Journal of Hazardous Materials 2010;181:234-40.
162. Delfino RJ, Sioutas C, Malik S. Potential Role of Ultrafine Particles in Associations between Airborne Particle Mass and Cardiovascular Health. Environmental Health Perspectives 2005;113:934-46.
163. Delfino RJ, Staimer N, Tjoa T, et al. Air pollution exposures and circulating biomarkers of effect in a susceptible population: clues to potential causal component mixtures and mechanisms. Environ Health Perspect 2009;117:1232-8.
164. Zhu Y, Hinds WC, Kim S, Shen S, Sioutas C. Study of ultrafine particles near a major highway with heavy-duty diesel traffic. Atmospheric environment 2002;36:4323-35.
165. Ntziachristos L, Ning Z, Geller MD, Sioutas C. Particle Concentration and Characteristics near a Major Freeway with Heavy-Duty Diesel Traffic. Environmental Science & Technology 2007;41:2223-30.
166. Kittelson DB. Engines and nanoparticles: a review. J Aerosol Med 1998;29.
167. Nemmar A, Vanbilloen H, Hoylaerts MF, Hoet PH, Verbruggen A, Nemery B. Passage of intratracheally instilled ultrafine particles from the lung into the systemic circulation in hamster. Am J Respir Crit Care Med 2001;164:1665-8.

168. Nemmar A, Hoet PH, Vanquickenborne B, et al. Passage of inhaled particles into the blood circulation in humans. Circulation 2002;105:411-4.
169. Phalen RF, Raabe OG. Aerosol particle size as a factor in pulmonary toxicity. 1974.
170. Brown JH, Cook KM, Ney FG, Hatch T. Influence of particle size upon the retention of particulate matter in the human lung. American Journal of Public Health and the Nations Health 1950;40:450-80.
171. Hatch TF, Gross P. Pulmonary deposition and retention of inhaled aerosols: Elsevier; 2013.
172. Phalen R, Kenoyer J, Davis J. Deposition and clearance of inhaled particles: Comparison of mammalian species. 1977: National Technical Information Service Springfield, VA. p. 159-70.
173. Stuart BO. Deposition and clearance of inhaled particles. Environmental health perspectives 1976;16:41-53.
174. Hasheminassab S, Daher N, Saffari A, Wang D, Ostro BD, Sioutas C. Spatial and temporal variability of sources of ambient fine particulate matter (PM2.5) in California. Atmospheric Chemistry and Physics 2014;14:12085-97.
175. Arhami M, Sillanpaa M, Hu SH, Olson MR, Schauer JJ, Sioutas C. Size-Segregated Inorganic and Organic Components of PM in the Communities of the Los Angeles Harbor. Aerosol Science and Technology 2009;43:145-60.
176. Olsson PQ, Benner RL. Atmospheric Chemistry and Physics: From Air Pollution to Climate Change By John H. Seinfeld (California Institute of Technology) and Spyros N. Pandis (Carnegie Mellon University). Wiley-VCH: New York. 1997. $89.95. xxvii + 1326 pp. ISBN 0-471-17815-2. Journal of the American Chemical Society 1999;121:1423-.
177. Kim B, Teffera S, Zeldin M. Characterization of PM2.5 and PM10 in the South Coast Air Basin of southern California: Part 1 - Spatial variations. Journal of the Air & Waste Management Association 2000;50:2034-44.
178. Hasheminassab S, Daher N, Ostro BD, Sioutas C. Long-term source apportionment of ambient fine particulate matter (PM2.5) in the Los Angeles Basin: A focus on emissions reduction from vehicular sources. Environmental Pollution 2014;193:54-64.
179. Moore KF, Ning Z, Ntziachristos L, Schauer JJ, Sioutas C. Daily variation in the properties of urban ultrafine aerosol—Part I: Physical characterization and volatility. Atmospheric Environment 2007;41:8633-46.
180. ATSDR (Agency for Toxic Substances and Disease Registry): Toxicological Profile for Polycyclic Aromatic Hydrocarbons (PAHs). Atlanta, GA: U.S. Department of Health and Human Services, Public Health Service; 1995.
181. Eiguren-Fernandez A, Miguel AH, Froines JR, Thurairatnam S, Avol EL. Seasonal and spatial variation of polycyclic aromatic hydrocarbons in vapor-phase and PM 2.5 in Southern California urban and rural communities. Aerosol Science and Technology 2004;38:447-55.
182. Bagate K, Meiring JJ, Cassee FR, Borm PJ. The effect of particulate matter on resistance and conductance vessels in the rat. Inhal Toxicol 2004;16:431-6.
183. Bagate K, Meiring JJ, Gerlofs-Nijland ME, Vincent R, Cassee FR, Borm PJ. Vascular effects of ambient particulate matter instillation in spontaneous hypertensive rats. Toxicol Appl Pharmacol 2004;197:29-39.
184. Kodavanti UP, Schladweiler MC, Ledbetter AD, et al. Pulmonary and systemic effects of zinc-containing emission particles in three rat strains: multiple exposure scenarios. Toxicol Sci 2002;70:73-85.
185. Kodavanti UP, Schladweiler MC, Ledbetter AD, et al. Temporal association between pulmonary and systemic effects of particulate matter in healthy and cardiovascular compromised rats. J Toxicol Environ Health A 2002;65:1545-69.
186. Kodavanti UP, Moyer CF, Ledbetter AD, et al. Inhaled environmental combustion particles cause myocardial injury in the Wistar Kyoto rat. Toxicol Sci 2003;71:237-45.
187. Kodavanti UP, Schladweiler MC, Gilmour PS, et al. The role of particulate matter-associated zinc in cardiac injury in rats. Environ Health Perspect 2008;116:13-20.
188. Mubagwa K, Flameng W. Adenosine, adenosine receptors and myocardial protection: an updated overview. Cardiovasc Res 2001;52:25-39.
189. Aedo F, Delgado R, Wolff D, Vergara C. Copper and zinc as modulators of neuronal excitability in a physiologically significant concentration range. Neurochemistry International 2007;50:591-600.
190. Graff DW, Cascio WE, Brackhan JA, Devlin RB. Metal particulate matter components affect gene expression and beat frequency of neonatal rat ventricular myocytes. Environmental Health Perspectives 2004;112:792-8.
191. Maret W. Crosstalk of the group IIa and IIb metals calcium and zinc in cellular signaling. Proc Natl Acad Sci U S A 2001;98:12325-7.
192. Gilmour PS, Schladweiler MC, Nyska A, et al. Systemic Imbalance of Essential Metals and Cardiac Gene Expression in Rats Following Acute Pulmonary Zinc Exposure. Journal of Toxicology and Environmental Health, Part A 2006;69:2011-32.

193. Faurskov B, Bjerregaard HF. Evidence for cadmium mobilization of intracellular calcium through a divalent cation receptor in renal distal epithelial A6 cells. Pflugers Arch 2002;445:40-50.
194. Misra UK, Gawdi G, Akabani G, Pizzo SV. Cadmium-induced DNA synthesis and cell proliferation in macrophages: the role of intracellular calcium and signal transduction mechanisms. Cell Signal 2002;14:327-40.
195. Nernst W. Zur Kinetik der in Lösung befindlichen Körper. Z physik Chem 1888;2:613-37.
196. Goldman DE. Potential, impedance, and rectification in membranes. J Gen Physiol 1943;27:37-60.
197. Hodgkin AL, Katz B. The effect of sodium ions on the electrical activity of the giant axon of the squid. The Journal of Physiology 1949;108:37-77.
198. Maltsev VA, Lakatta EG. The funny current in the context of the coupled-clock pacemaker cell system. Heart rhythm 2012;9:302-7.
199. Lakatta EG, Maltsev VA, Vinogradova TM. A coupled SYSTEM of intracellular Ca2+ clocks and surface membrane voltage clocks controls the timekeeping mechanism of the heart's pacemaker. Circulation research 2010;106:659-73.
200. Chandler NJ, Greener ID, Tellez JO, et al. Molecular architecture of the human sinus node: insights into the function of the cardiac pacemaker. Circulation 2009;119:1562-75.
201. Trautwein W, Kassebaum DG. On the mechanism of spontaneous impulse generation in the pacemaker of the heart. J Gen Physiol 1961;45:317-30.
202. Bartos DC, Grandi E, Ripplinger CM. Ion Channels in the Heart. Comprehensive Physiology 2015;5:1423-64.
203. Kodama I, Nikmaram MR, Boyett MR, Suzuki R, Honjo H, Owen JM. Regional differences in the role of the Ca2+ and Na+ currents in pacemaker activity in the sinoatrial node. Am J Physiol 1997;272:H2793-806.
204. Hagiwara N, Irisawa H, Kameyama M. Contribution of two types of calcium currents to the pacemaker potentials of rabbit sino-atrial node cells. The Journal of physiology 1988;395:233-53.
205. Tellez JO, Dobrzynski H, Greener ID, et al. Differential expression of ion channel transcripts in atrial muscle and sinoatrial node in rabbit. Circ Res 2006;99:1384-93.
206. Lakatta EG, DiFrancesco D. What keeps us ticking: a funny current, a calcium clock, or both? J Mol Cell Cardiol 2009;47:157-70.
207. Bogdanov Konstantin Y, Vinogradova Tatiana M, Lakatta Edward G. Sinoatrial Nodal Cell Ryanodine Receptor and Na+-Ca2+ Exchanger. Circulation Research 2001;88:1254-8.
208. Bogdanov KY, Maltsev VA, Vinogradova TM, et al. Membrane potential fluctuations resulting from submembrane Ca2+ releases in rabbit sinoatrial nodal cells impart an exponential phase to the late diastolic depolarization that controls their chronotropic state. Circ Res 2006;99:979-87.
209. Grant AO. Cardiac ion channels. Circ Arrhythm Electrophysiol 2009;2:185-94.
210. Li J, Greener ID, Inada S, et al. Computer three-dimensional reconstruction of the atrioventricular node. Circ Res 2008;102:975-85.
211. Munk AA, Adjemian RA, Zhao J, Ogbaghebriel A, Shrier A. Electrophysiological properties of morphologically distinct cells isolated from the rabbit atrioventricular node. J Physiol 1996;493 (Pt 3):801-18.
212. Greener ID, Monfredi O, Inada S, et al. Molecular architecture of the human specialised atrioventricular conduction axis. J Mol Cell Cardiol 2011;50:642-51.
213. Greener ID, Tellez JO, Dobrzynski H, et al. Ion channel transcript expression at the rabbit atrioventricular conduction axis. Circ Arrhythm Electrophysiol 2009;2:305-15.
214. Billette J. Atrioventricular nodal activation during periodic premature stimulation of the atrium. Am J Physiol 1987;252:H163-77.
215. Gaborit N, Le Bouter S, Szuts V, et al. Regional and tissue specific transcript signatures of ion channel genes in the non-diseased human heart. J Physiol 2007;582:675-93.
216. Dobrzynski H, Nikolski VP, Sambelashvili AT, et al. Site of origin and molecular substrate of atrioventricular junctional rhythm in the rabbit heart. Circ Res 2003;93:1102-10.
217. Physiology, Bundle of His. StatPearls Publishing, 2018. (Accessed 02/08/2020, 2018, at https://www.ncbi.nlm.nih.gov/books/NBK531498/.)
218. Ansari A, Yen Ho S, Anderson RH. Distribution of the Purkinje fibres in the sheep heart. The Anatomical Record 1999;254:92-7.
219. Gourdie RG, Severs NJ, Green CR, Rothery S, Germroth P, Thompson RP. The spatial distribution and relative abundance of gap-junctional connexin40 and connexin43 correlate to functional properties of components of the cardiac atrioventricular conduction system. J Cell Sci 1993;105 (Pt 4):985-91.

220. Atkinson A, Inada S, Li J, et al. Anatomical and molecular mapping of the left and right ventricular His-Purkinje conduction networks. J Mol Cell Cardiol 2011;51:689-701.
221. Robinson RB, Boyden PA, Hoffman BF, Hewett KW. Electrical restitution process in dispersed canine cardiac Purkinje and ventricular cells. Am J Physiol 1987;253:H1018-25.
222. Anumonwo JM, Tallini YN, Vetter FJ, Jalife J. Action potential characteristics and arrhythmogenic properties of the cardiac conduction system of the murine heart. Circ Res 2001;89:329-35.
223. Ono N, Yamaguchi T, Ishikawa H, et al. Morphological varieties of the Purkinje fiber network in mammalian hearts, as revealed by light and electron microscopy. Arch Histol Cytol 2009;72:139-49.
224. Demoulin JC, Kulbertus HE. Histopathological examination of concept of left hemiblock. Br Heart J 1972;34:807-14.
225. Feher J. 5.4 - The Heart as a Pump. In: Feher J, ed. Quantitative Human Physiology (Second Edition). Boston: Academic Press; 2012:516-24.
226. Grandi E, Pasqualini FS, Bers DM. A novel computational model of the human ventricular action potential and Ca transient. J Mol Cell Cardiol 2010;48:112-21.
227. Grandi E, Pandit SV, Voigt N, et al. Human atrial action potential and Ca2+ model: sinus rhythm and chronic atrial fibrillation. Circ Res 2011;109:1055-66.
228. Nerbonne JM, Kass RS. Molecular physiology of cardiac repolarization. Physiol Rev 2005;85:1205-53.
229. Bassani RA. Transient outward potassium current and Ca2+ homeostasis in the heart: beyond the action potential. Braz J Med Biol Res 2006;39:393-403.
230. Grant AO. Cardiac Ion Channels. Circulation: Arrhythmia and Electrophysiology 2009;2:185.
231. Bers DM. Cardiac excitation-contraction coupling. Nature 2002;415:198-205.
232. Lopatin AN, Nichols CG. Inward rectifiers in the heart: an update on I(K1). J Mol Cell Cardiol 2001;33:625-38.
233. Nichols CG, Lopatin AN. INWARD RECTIFIER POTASSIUM CHANNELS. Annual Review of Physiology 1997;59:171-91.
234. London B, Wang DW, Hill JA, Bennett PB. The transient outward current in mice lacking the potassium channel gene Kv1.4. J Physiol 1998;509 (Pt 1):171-82.
235. Xu H, Barry DM, Li H, Brunet S, Guo W, Nerbonne JM. Attenuation of the slow component of delayed rectification, action potential prolongation, and triggered activity in mice expressing a dominant-negative Kv2 alpha subunit. Circ Res 1999;85:623-33.
236. Sotoodehnia N, Isaacs A, de Bakker PI, et al. Common variants in 22 loci are associated with QRS duration and cardiac ventricular conduction. Nat Genet 2010;42:1068-76.
237. Kaese S, Verheule S. Cardiac electrophysiology in mice: a matter of size. Front Physiol 2012;3:345.
238. Boukens BJ, Hoogendijk MG, Verkerk AO, et al. Early repolarization in mice causes overestimation of ventricular activation time by the QRS duration. Cardiovasc Res 2013;97:182-91.
239. Opthof T. Function and structure of the mouse sinus node: nothing you can see that isn't shown. Cardiovasc Res. England2001:1-4.
240. Mangoni ME, Nargeot J. Properties of the hyperpolarization-activated current (I(f)) in isolated mouse sino-atrial cells. Cardiovasc Res 2001;52:51-64.
241. Xu H, Guo W, Nerbonne JM. Four kinetically distinct depolarization-activated K+ currents in adult mouse ventricular myocytes. J Gen Physiol 1999;113:661-78.
242. Holmqvist F, Carlson J, Platonov PG. Detailed ECG analysis of atrial repolarization in humans. Ann Noninvasive Electrocardiol 2009;14:13-8.
243. Merentie M, Lipponen JA, Hedman M, et al. Mouse ECG findings in aging, with conduction system affecting drugs and in cardiac pathologies: Development and validation of ECG analysis algorithm in mice. Physiological reports 2015;3:e12639.
244. Aanhaanen WT, Mommersteeg MT, Norden J, et al. Developmental origin, growth, and three-dimensional architecture of the atrioventricular conduction axis of the mouse heart. Circ Res 2010;107:728-36.
245. Liu G, Iden JB, Kovithavongs K, Gulamhusein R, Duff HJ, Kavanagh KM. In vivo temporal and spatial distribution of depolarization and repolarization and the illusive murine T wave. J Physiol 2004;555:267-79.
246. Brouillette J, Clark RB, Giles WR, Fiset C. Functional properties of K+ currents in adult mouse ventricular myocytes. J Physiol 2004;559:777-98.
247. Nerbonne JM. Studying cardiac arrhythmias in the mouse--a reasonable model for probing mechanisms? Trends Cardiovasc Med 2004;14:83-93.
248. Sabir IN, Killeen MJ, Grace AA, Huang CL. Ventricular arrhythmogenesis: insights from murine models. Prog Biophys Mol Biol 2008;98:208-18.

249. Zhang Y, Wu J, King JH, Huang CL, Fraser JA. Measurement and interpretation of electrocardiographic QT intervals in murine hearts. Am J Physiol Heart Circ Physiol 2014;306:H1553-7.
250. Pope CA, Muhlestein JB, May HT, Renlund DG, Anderson JL, Horne BD. Ischemic Heart Disease Events Triggered by Short-Term Exposure to Fine Particulate Air Pollution. Circulation 2006;114:2443.
251. Brook Robert D. Cardiovascular effects of air pollution. Clinical Science 2008;115:175.
252. Peters A, Dockery DW, Muller JE, Mittleman MA. Increased particulate air pollution and the triggering of myocardial infarction. Circulation 2001;103:2810-5.
253. von Klot S, Peters A, Aalto P, et al. Ambient air pollution is associated with increased risk of hospital cardiac readmissions of myocardial infarction survivors in five European cities. Circulation 2005;112:3073-9.
254. Henneberger A, Zareba W, Ibald-Mulli A, et al. Repolarization changes induced by air pollution in ischemic heart disease patients. Environ Health Perspect 2005;113:440-6.
255. Wellenius GA, Schwartz J, Mittleman MA. Air pollution and hospital admissions for ischemic and hemorrhagic stroke among medicare beneficiaries. Stroke 2005;36:2549-53.
256. Becker S, Soukup J. Coarse(PM(2.5-10)), fine(PM(2.5)), and ultrafine air pollution particles induce/increase immune costimulatory receptors on human blood-derived monocytes but not on alveolar macrophages. J Toxicol Environ Health A 2003;66:847-59.
257. Ishii H, Fujii T, Hogg JC, et al. Contribution of IL-1 beta and TNF-alpha to the initiation of the peripheral lung response to atmospheric particulates (PM10). Am J Physiol Lung Cell Mol Physiol 2004;287:L176-83.
258. Shoenfelt J, Mitkus RJ, Zeisler R, et al. Involvement of TLR2 and TLR4 in inflammatory immune responses induced by fine and coarse ambient air particulate matter. J Leukoc Biol 2009;86:303-12.
259. van Eeden SF, Tan WC, Suwa T, et al. Cytokines involved in the systemic inflammatory response induced by exposure to particulate matter air pollutants (PM(10)). Am J Respir Crit Care Med 2001;164:826-30.
260. Sigaud S, Goldsmith C-AW, Zhou H, et al. Air pollution particles diminish bacterial clearance in the primed lungs of mice. Toxicology and applied pharmacology 2007;223:1-9.
261. Gordon S. Alternative activation of macrophages. Nature Reviews Immunology 2003;3:23-35.
262. Park EJ, Roh J, Kim Y, Park K, Kim DS, Yu SD. PM 2.5 collected in a residential area induced Th1-type inflammatory responses with oxidative stress in mice. Environ Res 2011;111:348-55.
263. Yoshizaki K, Brito JM, Toledo AC, et al. Subchronic effects of nasally instilled diesel exhaust particulates on the nasal and airway epithelia in mice. Inhal Toxicol 2010;22:610-7.
264. He M, Ichinose T, Yoshida S, et al. Urban particulate matter in Beijing, China, enhances allergen-induced murine lung eosinophilia. Inhal Toxicol 2010;22:709-18.
265. Osornio-Vargas AR, Bonner JC, Alfaro-Moreno E, et al. Proinflammatory and cytotoxic effects of Mexico City air pollution particulate matter in vitro are dependent on particle size and composition. Environ Health Perspect 2003;111:1289-93.
266. Hetland R, Cassee F, Refsnes M, et al. Release of inflammatory cytokines, cell toxicity and apoptosis in epithelial lung cells after exposure to ambient air particles of different size fractions. Toxicology in vitro : an international journal published in association with BIBRA 2004;18:203-12.
267. Becker S, Mundandhara S, Devlin RB, Madden M. Regulation of cytokine production in human alveolar macrophages and airway epithelial cells in response to ambient air pollution particles: further mechanistic studies. Toxicol Appl Pharmacol 2005;207:269-75.
268. Gualtieri M, Ovrevik J, Holme JA, et al. Differences in cytotoxicity versus pro-inflammatory potency of different PM fractions in human epithelial lung cells. Toxicol In Vitro 2010;24:29-39.
269. Ovrevik J, Lag M, Holme JA, Schwarze PE, Refsnes M. Cytokine and chemokine expression patterns in lung epithelial cells exposed to components characteristic of particulate air pollution. Toxicology 2009;259:46-53.
270. Diabate S, Mulhopt S, Paur HR, Krug HF. The response of a co-culture lung model to fine and ultrafine particles of incinerator fly ash at the air-liquid interface. Altern Lab Anim 2008;36:285-98.
271. Tao F, Kobzik L. Lung macrophage-epithelial cell interactions amplify particle-mediated cytokine release. Am J Respir Cell Mol Biol 2002;26:499-505.
272. Fujii T, Hayashi S, Hogg JC, et al. Interaction of alveolar macrophages and airway epithelial cells following exposure to particulate matter produces mediators that stimulate the bone marrow. Am J Respir Cell Mol Biol 2002;27:34-41.
273. Jimenez LA, Drost EM, Gilmour PS, et al. PM(10)-exposed macrophages stimulate a proinflammatory response in lung epithelial cells via TNF-alpha. Am J Physiol Lung Cell Mol Physiol 2002;282:L237-48.
274. Boland S, Baeza-Squiban A, Fournier T, Houcine O, Gendron MC, Chevrier M. Diesel exhaust particles are taken up by human airway epithelial cells in vitro and alter cytokine production. Am J Physiol 1999;276.

275. Happo MS, Salonen RO, Halinen AI, et al. Dose and time dependency of inflammatory responses in the mouse lung to urban air coarse, fine, and ultrafine particles from six European cities. Inhal Toxicol 2007;19:227-46.
276. Nemmar A, Subramaniyan D, Ali BH. Protective effect of curcumin on pulmonary and cardiovascular effects induced by repeated exposure to diesel exhaust particles in mice. PLoS One 2012;7:e39554.
277. Dick CA, Singh P, Daniels M, Evansky P, Becker S, Gilmour MI. Murine pulmonary inflammatory responses following instillation of size-fractionated ambient particulate matter. J Toxicol Environ Health A 2003;66:2193-207.
278. Wegesser TC, Last JA. Lung response to coarse PM: bioassay in mice. Toxicol Appl Pharmacol 2008;230:159-66.
279. Mantecca P, Farina F, Moschini E, et al. Comparative acute lung inflammation induced by atmospheric PM and size-fractionated tire particles. Toxicol Lett 2010;198:244-54.
280. Roberts ES, Richards JH, Jaskot R, Dreher KL. Oxidative stress mediates air pollution particle-induced acute lung injury and molecular pathology. Inhal Toxicol 2003;15:1327-46.
281. Schins RP, Lightbody JH, Borm PJ, Shi T, Donaldson K, Stone V. Inflammatory effects of coarse and fine particulate matter in relation to chemical and biological constituents. Toxicol Appl Pharmacol 2004;195:1-11.
282. Stenfors N, Nordenhall C, Salvi SS, et al. Different airway inflammatory responses in asthmatic and healthy humans exposed to diesel. Eur Respir J 2004;23:82-6.
283. Alexis NE, Lay JC, Zeman K, et al. Biological material on inhaled coarse fraction particulate matter activates airway phagocytes in vivo in healthy volunteers. J Allergy Clin Immunol 2006;117:1396-403.
284. Behndig AF, Mudway IS, Brown JL, et al. Airway antioxidant and inflammatory responses to diesel exhaust exposure in healthy humans. Eur Respir J 2006;27:359-65.
285. Samet JM, Rappold A, Graff D, et al. Concentrated ambient ultrafine particle exposure induces cardiac changes in young healthy volunteers. Am J Respir Crit Care Med 2009;179.
286. Pope CA, Burnett RT, Thurston GD, Thun MJ, Calle EE, Krewski D. Cardiovascular Mortality and Long-Term Exposure to Particulate Air Pollution: Epidemiological Evidence of General Pathophysiological Pathways of Disease. Circulation 2003;109.
287. Pope CA, Hansen ML, Long RW, et al. Ambient particulate air pollution, heart rate variability, and blood markers of inflammation in a panel of elderly subjects. Environ Health Perspect 2004;112:339-45.
288. Ohyama M, Otake T, Adachi S, Kobayashi T, Morinaga K. A comparison of the production of reactive oxygen species by suspended particulate matter and diesel exhaust particles with macrophages. Inhalation toxicology 2007;19:157-60.
289. Donaldson K, Jimenez LA, Rahman I, Faux SP, MacNee W, Gilmour PS. Respiratory health effects of ambient air pollution particles: Role of reactive species. Oxygen/nitrogen radicals: lung injury and disease Eds Vallyathan V, Shi X Castranova V Volk 187 in Lung Biology in Health and Disease Exec Ed Lenfant C Marcel Dekker, New York2004.
290. Rahman I, MacNee W. Role of oxidants/antioxidants in smoking-induced lung diseases. Free Radic Biol Med 1996;21:669-81.
291. Donaldson K, Beswick PH, Gilmour PS. Free radical activity associated with the surface of particles: a unifying factor in determining biological activity? Toxicol Lett 1996;88:293-8.
292. Dellinger B, Pryor WA, Cueto R, Squadrito GL, Hegde V, Deutsch WA. Role of free radicals in the toxicity of airborne fine particulate matter. Chem Res Toxicol 2001;14:1371-7.
293. Li N, Hao M, Phalen RF, Hinds WC, Nel AE. Particulate air pollutants and asthma. A paradigm for the role of oxidative stress in PM-induced adverse health effects. Clin Immunol 2003;109:250-65.
294. Donaldson K, Brown DM, Mitchell C, et al. Free radical activity of PM10: iron-mediated generation of hydroxyl radicals. Environ Health Perspect 1997;105 Suppl 5:1285-9.
295. Shukla A, Timblin C, BeruBe K, et al. Inhaled particulate matter causes expression of nuclear factor (NF)-kappaB-related genes and oxidant-dependent NF-kappaB activation in vitro. Am J Respir Cell Mol Biol 2000;23:182-7.
296. Riva DR, Magalhães CB, Lopes AA, et al. Low dose of fine particulate matter (PM2.5) can induce acute oxidative stress, inflammation and pulmonary impairment in healthy mice. Inhalation Toxicology 2011;23:257-67.
297. Valavanidis A, Fiotakis K, Bakeas E, Vlahogianni T. Electron paramagnetic resonance study of the generation of reactive oxygen species catalysed by transition metals and quinoid redox cycling by inhalable ambient particulate matter. Redox Rep 2005;10:37-51.

298. Mehta M, Chen L-C, Gordon T, Rom W, Tang M-S. Particulate matter inhibits DNA repair and enhances mutagenesis. Mutation research 2008;657:116-21.
299. Han JY, Takeshita K, Utsumi H. Noninvasive detection of hydroxyl radical generation in lung by diesel exhaust particles. Free Radic Biol Med 2001;30:516-25.
300. Bosson J, Barath S, Pourazar J, et al. Diesel exhaust exposure enhances the ozone-induced airway inflammation in healthy humans. European Respiratory Journal 2008;31:1234.
301. Bouthillier L, Vincent R, Goegan P, et al. Acute effects of inhaled urban particles and ozone: lung morphology, macrophage activity, and plasma endothelin-1. The American journal of pathology 1998;153:1873-84.
302. Elder AC, Gelein R, Finkelstein JN, Cox C, Oberdorster G. Pulmonary inflammatory response to inhaled ultrafine particles is modified by age, ozone exposure, and bacterial toxin. Inhal Toxicol 2000;12.
303. Madden MC, Richards JH, Dailey LA, Hatch GE, Ghio AJ. Effect of ozone on diesel exhaust particle toxicity in rat lung. Toxicology and applied pharmacology 2000;168:140-8.
304. Wong EM, Walby WF, Wilson DW, Tablin F, Schelegle ES. Ultrafine Particulate Matter Combined With Ozone Exacerbates Lung Injury in Mature Adult Rats With Cardiovascular Disease. Toxicological Sciences 2018;163:140-51.
305. Pitts JN, Lokensgard DM, Ripley PS, et al. "Atmospheric" Epoxidation of Benzo[a]pyrene by Ozone: formation of the Metabolite Benzo[a]pyrene-4,5-Oxide. Sci (New York, NY) 1980;210.
306. Harkema J, Jackson-Humbles D, Lewandowski R, Morishita M, Arnetz B, Wagner J. Fine Particulate Matter Co-Exposure Enhances Pulmonary Neutrophilic, but Not Eosinophilic, Inflammation in a Murine Model of Ozone-Induced Non-Atopic Asthma. C103 OUTDOOR AIR POLLUTION: EPIDEMIOLOGY AND MECHANISMS: American Thoracic Society; 2017:A6841-A.
307. Kreyling WG, Semmler M, Erbe F, Mayer P, Takenaka S, Schulz H. Translocation of ultrafine insoluble iridium particles from lung epithelium to extrapulmonary organs is size dependent but very low. J Toxicol Environ Health A 2002;65.
308. Furuyama A, Kanno S, Kobayashi T, Hirano S. Extrapulmonary translocation of intratracheally instilled fine and ultrafine particles via direct and alveolar macrophage-associated routes. Arch Toxicol 2009;83.
309. Wiebert P, Sanchez-Crespo A, Falk R, et al. No significant translocation of inhaled 35-nm carbon particles to the circulation in humans. Inhal Toxicol 2006;18:741-7.
310. Wiebert P, Sanchez-Crespo A, Seitz J, et al. Negligible clearance of ultrafine particles retained in healthy and affected human lungs. Eur Respir J 2006;28:286-90.
311. Moller W, Felten K, Sommerer K, et al. Deposition, retention, and translocation of ultrafine particles from the central airways and lung periphery. Am J Respir Crit Care Med 2008;177:426-32.
312. Diez Roux AV, Auchincloss AH, Astor B, et al. Recent exposure to particulate matter and C-reactive protein concentration in the multi-ethnic study of atherosclerosis. Am J Epidemiol 2006;164:437-48.
313. Dubowsky SD, Suh H, Schwartz J, Coull BA, Gold DR. Diabetes, obesity, and hypertension may enhance associations between air pollution and markers of systemic inflammation. Environ Health Perspect 2006;114:992-8.
314. Riediker M, Cascio WE, Griggs TR, et al. Particulate matter exposure in cars is associated with cardiovascular effects in healthy young men. Am J Respir Crit Care Med 2004;169:934-40.
315. Schwartz J. Air pollution and blood markers of cardiovascular risk. Environ Health Perspect 2001;109 Suppl 3:405-9.
316. Pekkanen J, Brunner EJ, Anderson HR, Tiittanen P, Atkinson RW. Daily concentrations of air pollution and plasma fibrinogen in London. Occup Environ Med 2000;57:818-22.
317. Hoffmann B, Moebus S, Dragano N, et al. Chronic residential exposure to particulate matter air pollution and systemic inflammatory markers. Environ Health Perspect 2009;117:1302-8.
318. Chen JC, Schwartz J. Metabolic syndrome and inflammatory responses to long-term particulate air pollutants. Environ Health Perspect 2008;116:612-7.
319. Calderon-Garciduenas L, Villarreal-Calderon R, Valencia-Salazar G, et al. Systemic inflammation, endothelial dysfunction, and activation in clinically healthy children exposed to air pollutants. Inhal Toxicol 2008;20:499-506.
320. Kampfrath T, Maiseyeu A, Ying Z, et al. Chronic fine particulate matter exposure induces systemic vascular dysfunction via NADPH oxidase and TLR4 pathways. Circ Res 2011;108:716-26.
321. Mukae H, Vincent R, Quinlan K, et al. The effect of repeated exposure to particulate air pollution (PM10) on the bone marrow. Am J Respir Crit Care Med 2001;163:201-9.

322. Goto Y, Ishii H, Hogg JC, et al. Particulate matter air pollution stimulates monocyte release from the bone marrow. Am J Respir Crit Care Med 2004;170:891-7.
323. Terashima T, Wiggs B, English D, Hogg JC, van Eeden SF. Phagocytosis of small carbon particles (PM10) by alveolar macrophages stimulates the release of polymorphonuclear leukocytes from bone marrow. Am J Respir Crit Care Med 1997;155:1441-7.
324. Mukae H, Hogg JC, English D, Vincent R, van Eeden SF. Phagocytosis of particulate air pollutants by human alveolar macrophages stimulates the bone marrow. Am J Physiol Lung Cell Mol Physiol 2000;279:L924-31.
325. Harrison D, Griendling KK, Landmesser U, Hornig B, Drexler H. Role of oxidative stress in atherosclerosis. Am J Cardiol 2003;91:7A-11A.
326. Chuang KJ, Chan CC, Su TC, Lee CT, Tang CS. The effect of urban air pollution on inflammation, oxidative stress, coagulation, and autonomic dysfunction in young adults. Am J Respir Crit Care Med 2007;176:370-6.
327. Baccarelli A, Zanobetti A, Martinelli I, et al. Air Pollution, Smoking, and Plasma Homocysteine. Environmental Health Perspectives 2007;115:176-81.
328. Park SK, O'Neill MS, Vokonas PS, et al. Traffic-related particles are associated with elevated homocysteine: the VA normative aging study. Am J Respir Crit Care Med 2008;178:283-9.
329. Romieu I, Garcia-Esteban R, Sunyer J, et al. The effect of supplementation with omega-3 polyunsaturated fatty acids on markers of oxidative stress in elderly exposed to PM(2.5). Environ Health Perspect 2008;116:1237-42.
330. Sun Q, Yue P, Ying Z, et al. Air pollution exposure potentiates hypertension through reactive oxygen species-mediated activation of Rho/ROCK. Arterioscler Thromb Vasc Biol 2008;28:1760-6.
331. Coogan PF, White LF, Jerrett M, et al. Air pollution and incidence of hypertension and diabetes mellitus in black women living in Los Angeles. Circulation 2012;125:767-72.
332. Zanobetti A, Canner MJ, Stone PH, et al. Ambient pollution and blood pressure in cardiac rehabilitation patients. Circulation 2004;110:2184-9.
333. Dvonch JT, Kannan S, Schulz AJ, et al. Acute effects of ambient particulate matter on blood pressure: differential effects across urban communities. Hypertension 2009;53:853-9.
334. Choi JH, Xu QS, Park SY, et al. Seasonal variation of effect of air pollution on blood pressure. J Epidemiol Community Health 2007;61:314-8.
335. Ibald-Mulli A, Stieber J, Wichmann HE, Koenig W, Peters A. Effects of air pollution on blood pressure: a population-based approach. Am J Public Health 2001;91:571-7.
336. Auchincloss AH, Diez Roux AV, Dvonch JT, et al. Associations between recent exposure to ambient fine particulate matter and blood pressure in the Multi-ethnic Study of Atherosclerosis (MESA). Environ Health Perspect 2008;116:486-91.
337. Baumgartner J, Zhang Y, Schauer JJ, Huang W, Wang Y, Ezzati M. Highway proximity and black carbon from cookstoves as a risk factor for higher blood pressure in rural China. Proc Natl Acad Sci U S A 2014;111:13229-34.
338. van den Hooven EH, de Kluizenaar Y, Pierik FH, et al. Air pollution, blood pressure, and the risk of hypertensive complications during pregnancy: the generation R study. Hypertension 2011;57:406-12.
339. Delfino RJ, Tjoa T, Gillen DL, et al. Traffic-related air pollution and blood pressure in elderly subjects with coronary artery disease. Epidemiology 2010;21:396-404.
340. Calderon-Garciduenas L, Vincent R, Mora-Tiscareno A, et al. Elevated plasma endothelin-1 and pulmonary arterial pressure in children exposed to air pollution. Environ Health Perspect 2007;115:1248-53.
341. Ibald-Mulli A, Timonen KL, Peters A, et al. Effects of particulate air pollution on blood pressure and heart rate in subjects with cardiovascular disease: a multicenter approach. Environ Health Perspect 2004;112:369-77.
342. Madsen C, Nafstad P. Associations between environmental exposure and blood pressure among participants in the Oslo Health Study (HUBRO). Eur J Epidemiol 2006;21:485-91.
343. Zhang Z, Dong B, Li S, et al. Exposure to ambient particulate matter air pollution, blood pressure and hypertension in children and adolescents: A national cross-sectional study in China. Environment International 2019;128:103-8.
344. Liu L, Ruddy TD, Dalipaj M, et al. Influence of personal exposure to particulate air pollution on cardiovascular physiology and biomarkers of inflammation and oxidative stress in subjects with diabetes. J Occup Environ Med 2007;49:258-65.
345. Baumgartner J, Schauer JJ, Ezzati M, et al. Indoor air pollution and blood pressure in adult women living in rural China. Environ Health Perspect 2011;119:1390-5.

346. Chuang KJ, Chan CC, Shiao GM, Su TC. Associations between submicrometer particles exposures and blood pressure and heart rate in patients with lung function impairments. J Occup Environ Med 2005;47:1093-8.
347. Cosselman KE, Krishnan RM, Oron AP, et al. Blood pressure response to controlled diesel exhaust exposure in human subjects. Hypertension 2012;59:943-8.
348. Langrish JP, Mills NL, Chan JK, et al. Beneficial cardiovascular effects of reducing exposure to particulate air pollution with a simple facemask. Part Fibre Toxicol 2009;6:8.
349. McCracken JP, Smith KR, Diaz A, Mittleman MA, Schwartz J. Chimney stove intervention to reduce long-term wood smoke exposure lowers blood pressure among Guatemalan women. Environ Health Perspect 2007;115:996-1001.
350. Adar SD, Sheppard L, Vedal S, et al. Fine particulate air pollution and the progression of carotid intima-medial thickness: a prospective cohort study from the multi-ethnic study of atherosclerosis and air pollution. PLoS Med 2013;10:e1001430.
351. Diez Roux AV, Auchincloss AH, Franklin TG, et al. Long-term exposure to ambient particulate matter and prevalence of subclinical atherosclerosis in the Multi-Ethnic Study of Atherosclerosis. Am J Epidemiol 2008;167:667-75.
352. Künzli N, Jerrett M, Mack WJ, et al. Ambient air pollution and atherosclerosis in Los Angeles. Environ Health Perspect 2005;113:201-6.
353. O'Neill MS, Veves A, Zanobetti A, et al. Diabetes enhances vulnerability to particulate air pollution-associated impairment in vascular reactivity and endothelial function. Circulation 2005;111:2913-20.
354. Suwa T, Hogg JC, Quinlan KB, Ohgami A, Vincent R, van Eeden SF. Particulate air pollution induces progression of atherosclerosis. J Am Coll Cardiol 2002;39.
355. Sun Q, Wang A, Jin X, et al. Long-term air pollution exposure and acceleration of atherosclerosis and vascular inflammation in an animal model. JAMA 2005;294:3003-10.
356. Araujo JA, Barajas B, Kleinman M, et al. Ambient particulate pollutants in the ultrafine range promote early atherosclerosis and systemic oxidative stress. Circ Res 2008;102:589-96.
357. Brook RD, Brook JR, Urch B, Vincent R, Rajagopalan S, Silverman F. Inhalation of fine particulate air pollution and ozone causes acute arterial vasoconstriction in healthy adults. Circulation 2002;105.
358. Levin ER. Endothelins. New England Journal of Medicine 1995;333:356-63.
359. Kodavanti UP, Thomas R, Ledbetter AD, et al. Vascular and cardiac impairments in rats inhaling ozone and diesel exhaust particles. Environ Health Perspect 2011;119.
360. Fakhri AA, Ilic LM, Wellenius GA, et al. Autonomic effects of controlled fine particulate exposure in young healthy adults: effect modification by ozone. Environ Health Perspect 2009;117.
361. Wang G, Jiang R, Zhao Z, Song W. Effects of ozone and fine particulate matter (PM(2.5)) on rat system inflammation and cardiac function. Toxicol Lett 2013;217.
362. Wagner JG, Allen K, Yang HY, Nan B, Morishita M, Mukherjee B. Cardiovascular depression in rats exposed to inhaled particulate matter and ozone: effects of diet-induced metabolic syndrome. Environ Health Perspect 2014;122.
363. Baccarelli A, Cassano PA, Litonjua A, et al. Cardiac autonomic dysfunction: effects from particulate air pollution and protection by dietary methyl nutrients and metabolic polymorphisms. Circulation 2008;117:1802-9.
364. Wheeler A, Zanobetti A, Gold DR, Schwartz J, Stone P, Suh HH. The relationship between ambient air pollution and heart rate variability differs for individuals with heart and pulmonary disease. Environ Health Perspect 2006;114:560-6.
365. Chang CC, Hwang JS, Chan CC, Wang PY, Hu TH, Cheng TJ. Effects of concentrated ambient particles on heart rate variability in spontaneously hypertensive rats. J Occup Health 2005;47:471-80.
366. Anselme F, Loriot S, Henry JP, et al. Inhalation of diluted diesel engine emission impacts heart rate variability and arrhythmia occurrence in a rat model of chronic ischemic heart failure. Arch Toxicol 2007;81:299-307.
367. Corey LM, Baker C, Luchtel DL. Heart-rate variability in the apolipoprotein E knockout transgenic mouse following exposure to Seattle particulate matter. J Toxicol Environ Health A 2006;69:953-65.
368. Bautista DM, Jordt SE, Nikai T, et al. TRPA1 mediates the inflammatory actions of environmental irritants and proalgesic agents. Cell 2006;124:1269-82.
369. Bessac BF, Jordt SE. Breathtaking TRP channels: TRPA1 and TRPV1 in airway chemosensation and reflex control. Physiology (Bethesda) 2008;23:360-70.

370. Middlekauff HR, Park J, Moheimani RS. Adverse effects of cigarette and noncigarette smoke exposure on the autonomic nervous system: mechanisms and implications for cardiovascular risk. J Am Coll Cardiol 2014;64:1740-50.
371. Lin YS, Hsu CC, Bien MY, Hsu HC, Weng HT, Kou YR. Activations of TRPA1 and P2X receptors are important in ROS-mediated stimulation of capsaicin-sensitive lung vagal afferents by cigarette smoke in rats. J Appl Physiol (1985) 2010;108:1293-303.
372. Tobaldini E, Bollati V, Prado M, et al. Acute particulate matter affects cardiovascular autonomic modulation and IFN-γ methylation in healthy volunteers. Environmental Research 2018;161:97-103.
373. Simula S, Laitinen T, Vanninen E, et al. Baroreflex sensitivity in asymptomatic coronary atherosclerosis. Clin Physiol Funct Imaging 2013;33:70-4.
374. Pham H, Bonham AC, Pinkerton KE, Chen CY. Central neuroplasticity and decreased heart rate variability after particulate matter exposure in mice. Environ Health Perspect 2009;117:1448-53.
375. Yang X, Feng L, Zhang Y, et al. Cytotoxicity induced by fine particulate matter (PM2.5) via mitochondria-mediated apoptosis pathway in human cardiomyocytes. Ecotoxicology and Environmental Safety 2018;161:198-207.
376. Wang Q, Gan X, Li F, et al. PM(2.5) Exposure Induces More Serious Apoptosis of Cardiomyocytes Mediated by Caspase3 through JNK/ P53 Pathway in Hyperlipidemic Rats. International journal of biological sciences 2019;15:24-33.
377. Wittkopp S, Staimer N, Tjoa T, et al. Nrf2-related gene expression and exposure to traffic-related air pollution in elderly subjects with cardiovascular disease: An exploratory panel study. Journal of Exposure Science & Environmental Epidemiology 2016;26:141-9.
378. Gorr MW, Youtz DJ, Eichenseer CM, et al. In vitro particulate matter exposure causes direct and lung-mediated indirect effects on cardiomyocyte function. American Journal of Physiology-Heart and Circulatory Physiology 2015;309:H53-H62.
379. Zhang S, Breitner S, Cascio WE, et al. Short-term effects of fine particulate matter and ozone on the cardiac conduction system in patients undergoing cardiac catheterization. Particle and fibre toxicology 2018;15:38-.
380. Dianat M, Radmanesh E, Badavi M, Goudarzi G, Mard SA. The effects of PM10 on electrocardiogram parameters, blood pressure and oxidative stress in healthy rats: the protective effects of vanillic acid. Environmental Science and Pollution Research 2016;23:19551-60.
381. Ghelfi E, Rhoden CR, Wellenius GA, Lawrence J, Gonzalez-Flecha B. Cardiac oxidative stress and electrophysiological changes in rats exposed to concentrated ambient particles are mediated by TRP-dependent pulmonary reflexes. Toxicol Sci 2008;102:328-36.
382. Zhang ZM, Whitsel EA, Quibrera PM, et al. Ambient fine particulate matter exposure and myocardial ischemia in the Environmental Epidemiology of Arrhythmogenesis in the Women's Health Initiative (EEAWHI) study. Environ Health Perspect 2009;117:751-6.
383. Campen MJ, McDonald JD, Reed MD, Seagrave J. Fresh gasoline emissions, not paved road dust, alter cardiac repolarization in ApoE-/- mice. Cardiovasc Toxicol 2006;6:199-210.
384. Pelter MM, Adams MG. Non-conducted P waves. Am J Crit Care: Off Pub Am Assoc Crit-Care Nurses 2003;12.